Spring 2004

Mathematical and empirical modeling of chemical reactions in a microreactor

Jing Hu
Louisiana Tech University

MATHEMATICAL AND EMPIRICAL MODELING OF CHEMICAL REACTIONS IN A MICROREACTOR

by

Jing Hu, B.S.

A Dissertation Presented in Partial Fulfillment
of the Requirements for the Degree
Doctor of Philosophy

COLLEGE OF ENGINEERING AND SCIENCE
LOUISIANA TECH UNIVERSITY

May 2004

LOUISIANA TECH UNIVERSITY

THE GRADUATE SCHOOL

April 22, 2004
Date

We hereby recommend that the dissertation prepared under our supervision by Jing Hu

entitled Mathematical and Empirical Modeling of Chemical Reactions in a Microreactor

be accepted in partial fulfillment of the requirements for the Degree of Ph.D. in Computational Analysis and Modeling

Raja Hassan 4/22/04
Supervisor of Dissertation Research

Richard A. Greene 4/22/04
Head of Department

Department

Recommendation concurred in:

Raja Hassan 4/22/04

4/22/04

Advisory Committee

Weizhong Dai 4/22/04

Approved:

Director of Graduate Studies

Approved:

Dean of the Graduate School

Dean of the College

GS Form 13
(5/03)

ABSTRACT

This dissertation is concerned with mathematical and empirical modeling to simulate three important chemical reactions (cyclohexene hydrogenation and dehydrogenation, preferential oxidation of carbon monoxide, and the Fischer-Tropsch (F-T) synthesis in a microreaction system.

Empirical modeling and optimization techniques based on experimental design (Central Composite Design (CCD)) and response surface methodology were applied to these three chemical reactions. Regression models were built, and the operating conditions (such as temperature, the ratio of the reactants, and total flow rate) which maximize reactant conversion and product selectivity were determined for each reaction.

A probability model for predicting the probability that a certain species undergoing reaction inside a microreactor exits the reactor by a certain time T was applied to cyclohexene hydrogenation and dehydrogenation reaction and the F-T synthesis reaction. The probability is estimated by the partial pressure of the reactant in the exit stream divided by the base partial pressure without the reaction (pp/base). Parameters of the residence time distribution and the reaction rate were estimated for these chemical reactions. Lastly, the activation energy of these reactions was estimated, and the flow behavior of the reactant gas inside the microreactor was characterized from the residence time distribution.

A stochastic Markov chain approach was used to simulate cyclohexene hydrogenation and dehydrogenation reaction, and preferential oxidation of carbon monoxide reaction in a fuel cell. Simulation results from the stochastic approach were presented. Simulation results were in qualitative agreement with experimental results.

APPROVAL FOR SCHOLARLY DISSEMINATION

The author grants to the Prescott Memorial Library of Louisiana Tech University the right to reproduce, by appropriate methods, upon request, any or all portions of this Dissertation. It is understood that "proper request" consists of the agreement, on the part of the requesting party, that said reproduction is for his personal use and that subsequent reproduction will not occur without written approval of the author of this Dissertation. Further, any portions of the Dissertation used in books, papers, and other works must be appropriately referenced to this Dissertation.

Finally, the author of this Dissertation reserves the right to publish freely, in the literature, at any time, any or all portions of this Dissertation.

Author 

Date April 22, 2004

GS Form 14
(5/03)

I dedicate this work to my grandma, my parents, my brother, and my husband Peng.

TABLE OF CONTENTS

LIST OF TABLES

LIST OF FIGURES

NOMENCLATURE

η_x mean response

Y_x response surface

ε_x random error

σ^2 variance

$Y_{x,t}$ the t th observation

$\varepsilon_{x,t}$ random error

β_i the partial effect of the i th factor

β_{ii} the partial quadratic effect of the i th factor

β_{ij} the partial interaction effect between the i th and j th factors

$N(0,\sigma^2)$ standard normal distribution

n_f the number of factorial points

n_0 the number of center points

n the number of all points

n_a the number of axial points

$\overline{Y_f}$ the average of the n_f factorial points

$\overline{Y_0}$ the average of the n_0 center points

α confidence level?

ssQ sum of squares

$msPE$ the mean squares for pure error

$F_{1,n_0-1,\alpha}$ F distribution

p number of factors

t time

t, t+δt time interval

$\lambda e^{-\lambda t}(\lambda t)^{n-1}/\Gamma(n)$ Gamma distribution

$\lambda e^{-\lambda t}$ PDF of exponential distribution

T time

τ time

λ parameter of the residence time distribution

κ_S the ratio of the forward reaction constant (k_S) to the backward reaction constant (k_{-S})

$C_{c.s}$ the concentration of cyclohexene on the surface of the catalyst

$C_{A.S}$ the concentration of the adsorbed benzene reaction product

P_H the partial pressure of hydrogen

$C_{B.S}$ the concentration of cyclohexane adsorbed on the catalyst

Pr probability

E_i the outcome at the m th trial

E_j the outcome at the m+1th trial

p_{ij} the transition probabilities

π the unique limiting probability vector of a Markov chain

$n_i(0)$ initial molecules of type $A_i (i = 1, 2, ..., l)$

D an absorbing state

$x_1(m+1)$ the number of molecules of types A_1 fed in the reactor during the time interval $(m, m+1)$

$x_2(m+1)$ the number of molecules of types A_2 fed in the reactor during the time interval $(m, m+1)$

A_j chemical species

Pt Platinum

n_A the temperature

n_B the mole flow rates of hydrogen

n_C the mole flow rates of helium

n_{D1} the mole flow rates of cyclohexene

n_{D2} the mole flow rates of cyclohexane

n_{D3} the mole flow rates of benzene

$\hat{y}_{h_2}$ partial pressure of hydrogen

$\hat{y}_{h_e}$ the partial pressure of helium

$\hat{y}_{C_6h_{10}}$ the partial pressure of cyclohexene

$\hat{y}_{C_6h_{12}}$ the partial pressure of cyclohexane

$\hat{y}_{C_6h_6}$ the partial pressure of benzene

$Conv_{C_6H_{10}}$ the conversion of cyclohexene

$Sele_{C_6H_{12}}$ the selectivity of cyclohexane

$Sele_{C_6H_6}$ the selectivity of benzene

μ the reaction rate

E_a the activation energy of the reaction

C_{i0} the initial molar concentration of chemical species A_i in the microreactor

C_{if} molar concentration of chemical species A_i in the feed stream

q the volumetric flow rate

V the volume of the reacting mixture in the microreactor

N_0 Avogadro number

ACKNOWLEDGEMENTS

I would like to express my sincere appreciation to my advisor Dr. Raja Nassar and committee member Dr. Weizhong Dai for their professional guidance and help during the course of this work. Their patience, insight, and encouragement have greatly enhanced my knowledge in applied mathematical modeling.

I would also like to thank my other committee members, Dr. James Palmer and Dr. Ben Choi, for their help on my dissertation work.

Special thanks to Dr. Ronald Besser, who helped me in understanding chemical reactions in microreactors and to Ouyang Xun and Shihuai Zhao, for their help in running the experiments.

I wish to express my thanks to the IfM staff members, Mr. Scott Williams, Mr. John McDonald, and others who facilitated the use of the IfM laboratory facility for running experiments.

I would also like to thank my husband, Peng Zhen, for his support and help.

Last, I would like to thank the CAM program and Louisiana Tech University for providing the financial support for conducting this study.

CHAPTER ONE

INTRODUCTION

1.1 General Overview

Microreactors are devices that behave as continuous flow systems whose dimensions are in the sub-millimeter range. Microreactors are well suited as laboratory reactors because of the many advantages they possess, mostly because of their small size [Besser 2001].

There are several advantages of microreactors, including high surface-to-volume ratio, better heat transfer, flexibility over wide operation range, minimum inventory, and on-site production. The most important advantages of chemical process miniaturization (CPM) are the safety and environmental benefits of handling smaller quantities of materials, especially hazardous chemicals. All these advantages give rise to research interests in this area. As a result, the "Lab-on-a-Chip" concept has been successfully applied to many problems in biochemistry and in biomedicine.

Several reaction systems have been extensively explored recently in microreactors. One such system is cyclohexene hydrogenation and dehydrogenation, a popular model for many chemical reaction systems in the petroleum refining industries

[Segal 1978] [Davis 1980] [Xu 1994] [Chen 1996] [Su 1999]. In this research, the hydrogenation and dehydrogenation of cyclohexene over a platinum catalyst was studied.

Fuel cells have emerged as alternatives to combustion engines because of their potential in reducing adverse environmental effects as well as the dependence on fossil fuels [Sossina 2003]. Fuel cells will play an essential role in any future hydrogen fuel economy, and they are attractive for their modular and distributed nature, zero noise pollution, and high efficiency and low emissions [Sossina 2003]. Therefore, preferential oxidation for carbon monoxide amelioration in hydrogen fuel cells with platinum as a catalyst was explored.

As the global reserves of oil are being consumed, Fischer-Tropsch (F-T) synthesis becomes an important route for the production of fuels and chemicals. F-T synthesis involves the conversion of carbon monoxide and hydrogen to higher molecular weight hydrocarbons [Liu 2001]. In this study, combined catalysts of iron/cobalt supported by aluminum oxide for syn-gas reactions were investigated.

1.2 Research Objectives

Silicon microreactors have been shown to be a useful tool for fast catalyst discovery and chemical process optimization. Accurate and precise quantitative analysis of the chemical information is particularly important for both of these purposes. A mass spectrometer (MS) is used as the chemical information analyzer because of its fast response and economy. However, as MS sensitivity changes with different gas species and with different gas compositions, especially in the presence of hydrogen gas, statistical analysis methods were introduced for calibration. Therefore, one of the

objectives is to develop a statistical model for the MS measurements depending on different known gas compositions.

The second objective of this research is to develop an empirical model, based on experimental design and response surface methodology, for optimizing the cyclohexene hydrogenation and dehydrogenation reaction scheme. From this empirical model, one can determine the factor combination which gives the maximum yield/selectivity of cyclohexane or benzene, and the maximum conversion of cyclohexene.

The third objective of this research is to apply empirical modeling and optimization, based on experimental design and response surface methodology techniques, to fuel cell experiments for building a numerical model to maximize conversion of CO and selectivity of CO_2.

The fourth objective of this research is to apply empirical modeling and optimization, based on experimental design and response surface methodology techniques, to F-T synthesis experiment in order to maximize conversion of CO and selectivity of higher alkanes (C_3H_8).

The residence time distribution (RTD) of a reactor is a reflection of the mixing that occurs inside the reactor; hence, the residence time exhibited by a certain chemical reactor is one of the most informative characterizations concerning its performance and efficiency. Therefore, the fifth objective of this research is to build a continuous time and discrete state compartmental model, utilizing residence time distribution coupled with cyclohexene hydrogenation and dehydrogenation reactions and preferential F-T synthesis reaction, for predicting conversion and selectivity of the chemical reaction under consideration.

The last objective of this research is to use Markov chain techniques to characterize a catalytic reaction scheme in order to predict conversion and selectivity.

1.3 Organization of this Dissertation

Chapter One, as an introduction, generally describes a microreactor, introduces the reactions that have been modeled, and states the goals of this dissertation. Chapter Two provides a literature review of the three chemical reactions utilized in the microreactor experiments. Chapter Three describes the theories behind the mathematical and empirical modeling, including optimization based on experimental design and response surface methodology, and continuous time and discrete state compartmental modeling utilizing residence time distribution coupled with chemical reactions. Chapter Four introduces the experimental equipment and procedure, including the structure of the microreactor and the whole microreaction system. Chapter Five describes the calibration of the mass spectrometer (MS), the experimental design, experimental results, and the empirical model for each of the hydrogenation and dehydrogenation of cyclohexene reaction, preferential oxidation of carbon monoxide reaction, and the Fischer-Tropsch synthesis reaction. Chapter Six presents mathematical modeling and a stochastic Markov chain approach to cyclohexene hydrogenation and dehydrogenation reactions and to preferential oxidation of carbon monoxide amelioration in a hydrogenation fuel cell reaction. Conclusions and future studies are addressed in Chapter Seven.

CHAPTER TWO

LITERATURE REVIEW

2.1 Chemical Microreactors

Microreactors used in this study are chip-scale microfabricated reactors, comprised of channels etched in the silicon substrate using the well-known silicon bulk micromachining techniques involving photolithography and etching techniques [Low 1999] [Kovacs 1998]. There are many materials, such as metal, glass, or silicon, that could be used as substrates of the microreactors; however, silicon is chosen as the substrate for this research since there are well-developed photolithography and etching techniques for it in the microelectronic industry.

Microreactors, because of their small dimensions (in the order of micrometers), have many advantages over the conventional lab-scaled reactors. They consume less space, materials, and energy; have shorter response times; and have more information gained per unit and space. They have exceedingly low volumes of reaction and high aspect ratios, which allow reactions in extreme temperature and pressure regimes with little or no danger of explosion [Ehrfeld 2000] [Jensen 2000]. Microreactors have very good heat and mass transfer properties, which include uniform flow and temperature distributions, no dead zones, and fast response times caused by low volume. Microreactors offer great potential when used in large numbers for on-site and on-

demand synthesis of chemicals and also for studies in heterogeneous catalysis for rapid catalyst evaluation and development [Srinivasan 1997] [Senkan 1999]. Microreactors also produce negligible chemical waste and allow easy integration with other devices and easy control of reaction parameters because of small volume. All these performance benefits of microreactors make them very important in the biochemistry and biomedicine fields.

2.2 Chemical Reactions

The chemical reactions under consideration in this study are cyclohexene hydrogenation and dehydrogenation, preferential oxidation for carbon monoxide amelioration in hydrogen fuel cells, and the Fischer-Tropsch synthesis.

2.2.1 Cyclohexene Hydrogenation and Dehydrogenation Reactions

The reaction of cyclohexene (C_6H_{10}) and hydrogen over a platinum catalyst has been investigated in recent years by a number of groups using a variety of surface analytical techniques [Segal 1978] [Davis 1980] [Xu 1994] [Chen 1996] [Su 1999]. Study of this reaction at the micro scale was conducted by a number of research groups [Roberts 1990] [Hassan 1995] [Hunka 1997] [Surangalikar 2003] including the Institute of Manufacturing (IfM) at Louisiana Tech University [Ouyang 2003]. This reaction system is a popular model for many similar systems ubiquitous in the chemical process and petroleum refining industries, including (a) hydrotreating [Rase 2000] for aromatics reduction, desulfurization, and denitrogenation; (b) reforming for aromatics reduction and

dehydrocyclization [Gary 2001] [Weissermel 1997]; and (c) fuel processing of liquid hydrocarbons for the generation of hydrogen feed for fuel cells [Sandestede 2000]. Previous results on Pt (111) revealed that cyclohexene underwent selective dehydrogenation to form benzene, with the selectivity to gas-phase benzene being approximately 75% [Chen 1996] [Henn 1992].

Cyclohexene could react selectively, with the help of a platinum catalyst, to give two products, cyclohexane (C_6H_{12}) or benzene (C_6H_6). The reactions are given as

$$C_6H_{10} + H_2 \xrightarrow{Pt} C_6H_{12} \tag{2.1}$$

$$C_6H_{10} \xrightarrow{Pt} C_6H_6 + 2H_2. \tag{2.2}$$

The hydrogenation reaction (Eq. (2.1)) gives cyclohexane as a product and is favored at low temperatures. On the other hand, the dehydrogenation reaction (Eq. (2.2)) produces benzene and is favored at high temperatures.

2.2.2 Preferential Oxidation of Carbon Monoxide Reaction

During the last decade, worldwide concern regarding both the release of greenhouse gases into the atmosphere and poor air quality in many of the world's metropolitan areas has significantly increased [Cowan 1996] [Lloyd 2000]. The internal combustion engine is known as a major source of noxious gaseous emissions. Against such a backdrop of environmental and health concerns, fuel cells have emerged as alternatives to combustion engines because of their potential in reducing the environmental impact and in reducing the dependence on fossil fuels [Sossina 2003]. A fuel cell is a battery in which a fuel, usually hydrogen or methanol, reacts at the anode

and oxygen reacts at the cathode. However, unlike a normal battery, fuel cell electrodes are not consumed, but only the fuel is consumed [Burstein 1998]. The choice of fuel for the fuel cell stacks is the key issue. Pure hydrogen is the ideal fuel used in the present generation of fuel cells because it simplifies system integration, maximizes system efficiency, and provides zero emissions [Dicks 1996].

The liberation of hydrogen from natural gas, methane, or methanol produces carbon dioxide and carbon monoxide. The presence of carbon monoxide in the hydrogen-rich feed gas to fuel cells can poison the platinum anode electrode and dramatically reduce the power output [Manasilp 2002]. Many other studies also showed the negative effect of *CO* on the performance of fuel cells [Rohland 1999] [Gotz 1998]. Therefore, carbon monoxide clean-up and amelioration is very important for fuel cell technology. Palladium-based membrane purification, catalytic methanation, and selective catalytic *CO* oxidation are methods of reducing the *CO* in the feed to 10 *ppm* or less, necessary for operation of the fuel cell, with minimal loss of hydrogen. Of these three methods, selective *CO* oxidation is the most promising and lowest cost approach.

Many catalysts were investigated for removal of *CO* contained in hydrogen. Oxidative removal of a small quantity of *CO* from a hydrogen atmosphere was examined by using catalysts containing 3d transition metal oxides. The oxidation of *CO* takes place in preference to that of H_2 on catalysts containing *Co* or *Mn* in a temperature range from 323-423 K. Best performance was achieved by the catalyst with the ratio of *Pt/Ru* =1 for both H_2 and $H_2 + CO$ in the oxidation kinetics investigation of H_2 and H_2+ 100 ppm *CO* in Italy. Denis in 1999 showed that a 2% Pt/alumina sol-gel catalyst can selectively

oxidize *CO* down to a few ppm with constant selectivity and high space velocity [Denis 1999]. In this regard, the preferred catalyst is platinum.

Research at Louisiana Tech University has focused on preferential oxidation of *CO* using a microreactor with platinum as the catalyst. The two competitive reactions that take place are shown below:

$$2CO + O_2 \xrightarrow{Pt} 2CO_2 \tag{2.3}$$

$$2H_2 + O_2 \xrightarrow{Pt} 2H_2O \tag{2.4}$$

High conversion of *CO* is required to reduce the *CO* concentration to a level that is not detrimental to a PEM-based fuel cell. However, hydrogen oxidation competes with *CO* oxidation leading to a loss of fuel efficiency. Therefore, in the conversion of *CO*, high selectivity of CO_2 is desired.

2.2.3 Fischer-Tropsch Synthesis Reaction

Fischer-Tropsch (F-T) synthesis, being the technology for conversion of natural gas to liquid and an attractive alternative for bringing static gas resources to market, becomes an important route for the production of fuels and chemicals. The conversion of *CO* and H_2 to methane was first investigated by Sabatier and Senderens in 1902. More than two decades later, Fischer and Tropsch described their catalyst development efforts, which included the synthesis of higher hydrocarbons over nickel- and cobalt-based catalysts.

F-T synthesis involves the conversion of carbon monoxide and hydrogen to higher molecular weight hydrocarbons. The reaction mechanism of F-T synthesis remains uncertain despite tremendous efforts devoted to this process in the last 70 years. With

extensive Density Functional Theory (DFT) studies on F-T reactions, Liu obtained relative stabilities of many key intermediates and compared quantitatively several C/C coupling mechanisms as shown below [Liu 2001]:

$$C + H \rightarrow CH, \quad CH + H \rightarrow CH_2, \quad CH_2 + H \rightarrow CH_3 \ldots\ldots, \tag{2.5}$$

wherein the first step of the F-T synthesis is the CO and H_2 dissociations, followed by the hydrogenation process. Then, the CH_x species (x=0, 1, 2) couple with each other (C/C coupling) to form higher-weight hydrocarbons.

F-T synthesis has been re-visited by several corporations, including Exxon, Mobil, Rentech, Sasol, Shell, Synthroleum, and commercialized by Shell, and Sasol. Among these companies and other research groups, extensive interest has been focused on finding a better catalyst to increase productivity, control hydrocarbon product distribution, and lengthen the catalyst life [Roberts 1990] [Hunka 1997]. Cobalt-based catalysts and iron-based catalysts have been investigated in F-T synthesis reaction by some research groups [Hassan 1996] [Linda 1993]. Linda shows that cobalt-based catalysts have lower water-gas shift activity than iron-based ones [Linda 1993].

In on-going research at Louisiana Tech University, combined catalysts of iron/cobalt supported by aluminum oxide for syn-gas reactions are being used.

A relationship between the physical parameters of a reaction and yield is important for optimizing the reaction, and one common engineering approach in optimization is to change one parameter at a time while keeping the others fixed. This procedure is repeated until all the parameters are changed. This method is, of course, time consuming and costly. To make the process efficient, experimental design and response surface methodology were introduced to determine the relation between several

independent variables (such as temperature, reactants ratio, and total flow rate) and the dependent variables (such as yield or selectivity), and to optimize the reaction yield and product selectivity.

Response surface methodology was developed by Box and Wilson in 1951 [Box and Wilson 1951] to aid the improvement of manufacturing processes in the chemical industry. The purpose was to optimize chemical reactions to obtain high yield and purity at low cost. This optimization was accomplished through the use of sequential experimentation involving factors such as temperature, pressure, duration of reaction, and proportion of reactants. The same methodology can be used to optimize any response that is affected by the levels of one or more quantitative factors [Angela 1999]. The Central Composite Design (CCD) [Box and Draper 1987] is widely used in response surface methodology for process optimization. Details of response surface methodology and central composite design are shown in Chapter Three.

2.3 Markov Chain Approach

Chou et al. [Chou 1988] presented a Markov chain approach to simulate complex chemical reactions. Because the states of the Markov chain need to be properly identified, two ways to identify these states in order to simulate the dynamics of a chemical reaction system were identified. One is the number of molecules of the chemical species participating in the reactions, and the other is to appropriately select the chemical species participating in the reactions. The selection of these species needs to be subject to the stoichiometric constraint based on atomic balance.

A molecule of type A_j was regarded as the "entity" at level j, and any reaction involving it was viewed as a transition of this "entity" from this level to another. The collection of all transitions involving the "entity" forms a Markov chain. $P_{ij}(m, m+1)$ is the one-step transition probability that the "entity" at level i at time $m\Delta t$ will be at level j at time $(m+1)\Delta t$ inside the reactor. The one-step transition probabilities of the Markov chain are given by Eq. (3) in the article. The $P_{id}(m, m+1)$ is the transition probability that the "entity" at level i at time $m\Delta t$ will be discharged to the surrounding environment (dead or absorbing state) from the reactor at time $(m+1)\Delta t$. In this article, Eqs. (4)-(10) gave the probability distributions of the "entity" among the selected l levels and the dead state after m-step transitions. The mean number of molecules of any type A_i in the well mixed reactor at time $(m+1)\Delta t$ is obtained by applying the chemical reaction to Eq. (2.6).

$$\begin{aligned} & E[N_j(m+1) \mid N_i(m) = n_i(m), X_i(m) = x_i(m), i = 1,2,...,J] \\ & = E[\sum_{i=1}^{l} N_{ij}(m, m+1)] + E[X_j(m)] \\ & = \sum_{i=1}^{l} E[N_{ij}(m, m+1)] + x_j(m) \\ & = \sum_{i=1}^{l} n_i(m) p_{ij}(m, m+1) + x_j(m), j = 1,2,...,l \end{aligned} \tag{2.6}$$

In Too et al. [Too 1983] a stochastic approach, namely a Markov chain, was used to simulate numerically the dynamics of complex reactions in a flow chemical reactor without either solving directly the deterministic differential equations governing the performance of the reactor or obtaining a closed form solution to such equations. A basic reason for formulating classical chemical kinetics in a stochastic framework is that a chemical reaction is probabilistic in nature.

Results of the simulation using a Markov chain were in good agreement with the known deterministic solutions which shows the Markov chain as an effective tool for simulating the dynamics of complex chemical reactions in a reactor, flow, or batch. The Markov chain technique used in Too et al. [Too 1983] can be applied to a variety of flow reactors with complex chemical reactions whose governing equation cannot be easily solved by a deterministic approach.

In this study, the stochastic modeling approaches used by Too et al. [Too 1983] and Chou et al. [Chou 1988] are extended to model catalytic chemical reactions in a microreactor.

CHAPTER THREE

MATHEMATICAL AND EMPIRICAL MODELING

In this study, the microreactor modeling approach employs empirical modeling and optimization based on experimental design and response surface methodology and continuous time and discrete state compartmental modeling utilizing residence time distribution coupled with chemical reactions. The methodology behind these two approaches will be described in detail in this chapter.

3.1 Response Surface Methodology

Response surface methodology, developed by Box and Wilson [1951], is widely used for modeling or optimizing any response affected by the levels of one or more quantitative factors. The purpose in this study is to optimize the microreactor chemical reaction process in order to obtain high yield and selectivity. For the reaction scheme under consideration, the quantitative continuous variable (e.g., yield or selectivity) is called the response, and a smooth but unknown function of the levels of the three factors (e.g., temperature, mole flow rate, and $CO: O_2$ ratio), is the expected response. Plotting the expected response as a function of the factor combinations, one obtains the response surface in four dimensions.

The objectives of a response surface are (1) to locate a feasible factor combination for which the mean response is optimum (e.g., maximum, minimum, or equal to a specific target value); and (2) to estimate the response surface in the vicinity of this factor combination (or location) in order to better understand the effects of the factors on the mean response.

Figure 3.1 shows a response surface for two factors, temperature and CO: O_2 ratio for 0.2 sccm total flow rate for preferential oxidation of a carbon monoxide experiment. The response surface is generated from fitting a second order regression model to the experimental data. The levels at which the observations were taken are marked on the plot. It is seen from this figure that the response surface is more sensitive to changes in the CO: O_2 ratio (stoichiometry) than to changes in temperature. Also, the CO response is maximum for a temperature of about 175.9 °C and a CO: O_2 ratio of about 1.31.

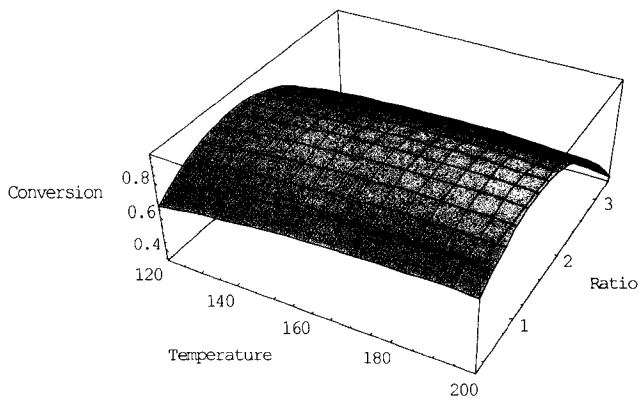

Figure 3.1: Response surface (conversion of CO) for two factors, temperature and CO: O_2 ratio for 0.2 sccm total flow rate.

Let x_1 denote the temperature level, and x_2 denote the ratio level. Let $x = (x_1, x_2)$ denote a treatment (or factor) combination, and $\eta_x = E[Y_x]$ denote the mean response at x. The response surface model is expressed as

$$Y_x = \eta_x + \varepsilon_x \tag{3.1}$$

where ε_x is a random error variable, normally distributed with zero mean and variance σ^2.

In order to attain the two aforementioned objectives, data collection from experiments is needed. However, collecting all observations at each location on a grid of treatment combinations spanning the entire experimental region of interest can be time consuming and costly. A more efficient approach is to conduct a sequence of small, local experiments in order to locate the region of optimum mean response (maximum response, in this case) and then to study this region for locating the factor combination where the mean response is optimum.

In order to search for the location of the peak (or maximum) mean response on a response surface, a local experiment will be run first, utilizing a first-order design, and a first-order model will be fitted to the data collected on this local experiment.

For p factors in general, the standard first-order model is a first-order polynomial regression model expressed as

$$Y_{x,t} = \beta_0 + \beta_1 x_1 + \beta_2 x_2 + ... + \beta_p x_p + \varepsilon_{x,t} \ , \tag{3.2}$$

where $Y_{x,t}$ indicates the tth observation at treatment combination $\mathbf{x}=(x_1, x_2, ...x_p)$, and $\varepsilon_{x,t}$ is random error. The random errors are assumed to be independent with a normal distribution of mean zero and variance σ^2. The parameter β_i denotes a measure of the local partial effect of the ith factor when the other factors are held constant ($i = 1, 2, ...p$).

If still far from the peak, this first-order model is often adequate. The fitted first-order model is a plane from which the direction or path of steepest ascent is easily determined. The path is followed as long as the response continues to increase. When the response stops increasing, another local experiment can be conducted to determine a new path of steepest ascent. This procedure can be iterated until the first-order model no longer adequately describes the local true surface. At that point, a large number of observations are needed to fit a higher-order model with which to locate the peak or optimum. Normally, a second-order model is satisfactory.

For p factors, the standard second-order model is

$$Y_{x,t} = \beta_0 + \sum_{i=1}^{p} \beta_i x_i + \sum_{i=1}^{p} \beta_{ii} x_i^2 + \sum_{i<j} \beta_{ij} x_i x_j + \varepsilon_{x,t} \ , \tag{3.3}$$

where $Y_{x,t}$ denotes the t th response observed at treatment combination $\mathbf{x}=(x_1, x_2, \ldots x_p)$, and $\varepsilon_{x,t}$ are assumed to be independent random errors with a $N(0,\sigma^2)$ distribution. The parameter β_i denotes the partial effect of the i th factor , β_{ii} represents the partial quadratic effect of the i th factor, and β_{ij} represents the partial interaction effect between the i th and j th factors.

3.2 Test for Lack-Of-Fit

Lack-of-fit of the linear model in Eq. (3.2) to response data can occur when the local response surface is no longer a plane, but exhibits curvature caused by quadratic effects. In this case, a second-order model would provide an adequate approximation to the local response surface. An effective way to test for lack-of-fit caused by quadratic

effects is to compare the mean response at the center of the design region with the mean response at the factorial points by including multiple center points $\mathbf{z}_0 = (0, \ldots, 0)$ in the first-order design. With respect to the coded factor levels, the standard second-order model for p factors is

$$Y_{z,l} = \gamma_0 + \sum_i \gamma_i z_i + \sum_i \gamma_{ii} z_i^2 + \sum_{i<j} \gamma_{ij} z_i z_j + \varepsilon_{z,l}, \tag{3.4}$$

The quadratic-effect parameters are aliased with one another, and their sum can be estimated as in Eq. (3.5).

$$E[\overline{Y_f} - \overline{Y_0}] = \sum_{i=1}^{P} \gamma_{ii} \tag{3.5}$$

with

$$Var(\overline{Y_f} - \overline{Y_0}) = (\frac{1}{n_0} + \frac{1}{n_f})\sigma^2 = \frac{n}{n_f n_0}\sigma^2 \tag{3.6}$$

where $\overline{Y_f}$ and $\overline{Y_0}$ denote the average of the n_f factorial points and the average of the n_0 center points, respectively. Equation (3.7) gives the sum of squares with one degree of freedom for testing whether or not the sum of the quadratic parameters in Eq. (3.5) is zero.

$$ssQ = \frac{n_f n_0}{n}(\overline{Y_f} - \overline{Y_0})^2 \tag{3.7}$$

The mean squares for pure error, with $n_0 - 1$ degrees of freedom, can be calculated based on the n_0 center points responses, Y_{i0} $(i = 1, 2, \ldots n_0)$. This mean squares for pure error can be expressed as

$$msPE = \frac{\sum_{i=1}^{n_0} Y_{i0}^2 - \frac{(\sum_{i=1}^{n_0} Y_{i0})^2}{n_0}}{n_0 - 1} \tag{3.8}$$

The ratio $ssQ/msPE$ is used to test the null hypothesis of no quadratic effects. The null hypothesis is rejected at level α if this ratio exceeds $F_{1,n_0-1,\alpha}$.

3.3 Central Composite Design

The Central Composite Design, CCD [Box and Draper 1987], is widely used in response surface methodology for process optimization. The design contains a standard first-order design with n_f orthogonal factorial points and n_0 center points, augmented by n_a "axial points." Here, if there are p factors, then there are $n_f = 2^p$ factorial points, which have coded levels ± 1 for each factor and $2p$ distinct axial points. The axial points (α's) are points located at a specified distance from the design center in each direction on each axis defined by the coded factor levels. The choice of α depends on the properties required of the design. A popular choice of α which gives a rotatable design (a design with equal variance of prediction at equal distances from the center point) is $\alpha = (n_f)^{1/4}$. Figure 3.2 shows the central composite designs for $p = 3$ factors.

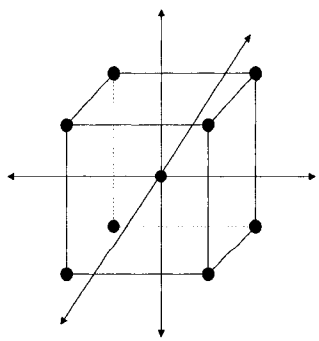

Figure 3.2: The central composite designs for $p = 3$ factors.

3.4 Residence Time Distribution

A simple, yet realistic first approach to modeling the residence time distribution is to divide the reactor in the flow direction into n arbitrary compartments where each compartment is perfectly mixed as in a continuous stirred tank reactor (CSTR). Using cyclohexene hydrogenation and dehydrogenation reaction (as an example in the following sections), consider a cyclohexene molecule which enters the reactor in compartment 1 and exits from compartment n. Because of the ideal mixing in a compartment, the probability that a molecule in compartment j-1 exits to compartment j (j=2,3,..., n+1, where n+1 is the exit stream) during the infinitesimal time interval t, t+δt is equal to $\lambda t + o(t)$.

As such, it can be readily seen that the residence time distribution in any compartment is exponential with probability density function (PDF) $\lambda e^{-\lambda t}$. Considering that a molecule enters compartment 1 and exits compartment n, the time it takes the molecule to exit the reactor is the sum of n exponential random variables and is given by the Gamma distribution

$$\lambda e^{-\lambda t}(\lambda t)^{n-1}/\Gamma(n) \tag{3.9}$$

The Gamma distribution (Eq. (3.9)) can be used to characterize the RTD of a chemical reactor by running experiments where the input is either pulse or continuous feed. In this research, continuous feed cyclohexene hydrogenation and dehydrogenation experiments and Fischer-Tropsch (F-T) synthesis experiments were run, and the partial pressure of cyclohexene or carbon monoxide (PP) in the exit stream was measured. The ratio PP/PP_{base} at time T is an estimate of the probability that a cyclohexene molecule, entering the reactor at time τ, exits the reactor by time $T-\tau$, where PP_{base} is the partial

pressure of the reactant (in this study, it is cyclohexene or carbon monoxide) in the exit stream when there is no reaction. This probability is given by the integral of

$$\lambda e^{-\lambda(T-\tau)}(\lambda(T-\tau))^{n-1}/\Gamma(n) \tag{3.10}$$

between zero and T.

Fitting the model to the experimental observations PP/PP_{base} over time, one can estimate λ and n for a given microreactor and flow system.

3.5 Chemical Kinetics

When a reaction occurs, it is assumed that in the infinitesimal time interval t, t+δt the probability that a cyclohexene molecule in compartment j-1 reacts is μt +0(t), (a reasonable assumption in that with a microreactor, one can safely ignore the mass transfer effect or the diffusion effect when considering the catalytic reaction occurring on the walls of the reactor). On the other hand, the probability that the cyclohexene molecule exits to compartment j is λt +o(t). Under continuous feed, the probability that a cyclohexene molecule (C_6H_{10}) entering the reactor at time τ exits by time T (T ≥ τ) is given by

P [C_6H_{10} exits the reactor at time T]

= P [C_6H_{10} exiting at time T| C_6H_{10} did not react by time T] *P[C_6H_{10} did not react by time T] =

$$\int_0^T e^{-\mu(T-\tau)}\frac{\lambda e^{-\lambda(T-\tau)}(\lambda(T-\tau))^{n-1}}{\Gamma(n)}d\tau \tag{3.11}$$

The probability of exiting the reactor by time T can be evaluated from Eq. (3.11) to give

$$\left[-\frac{\lambda^n T^{(n-1)}}{\Gamma(n)(\lambda+\mu)}-\frac{\lambda^n T^{(n-2)}}{\Gamma(n-1)(\lambda+\mu)^2}-\ldots-\frac{\lambda^n T}{(\lambda+\mu)^{(n-1)}}\right]e^{-(\lambda+\mu)T}+(1-e^{-(\lambda+\mu)T})\frac{\lambda^n}{(\lambda+\mu)^n} \quad (3.12)$$

As T approaches infinity, Eq. (3.12) reduces to

$$\frac{\lambda^n}{(\lambda+\mu)^n} \quad (3.12a)$$

For characterizing the microreactor, we fitted the above model to cyclohexene PP/PP_{base} data over time and to F-T synthesis data over time in the exit stream in order to estimate λ and μ and n. Note that the rate of the reactant conversion is $1-(PP/PP_{base})$.

For a heterogeneous catalytic reaction at equilibrium (such as the cyclohexene or F-T reactions), it can be shown [Fogler 1999] that the rates of each of the three reaction steps (adsorption, surface reaction, and desorption) are equal. For instance, considering the surface reaction rate of the dehydrogenation reaction in Eq. (2.2), one may show that the parameter μ in Eq. (3.12) can be expressed as

$$\mu=k_S(C_{C.S}-(C_{A.S}P_H/\kappa_S)) \quad (3.13)$$

where κ_S is the ratio of the forward reaction constant (k_S) to the backward reaction constant (k_{-S}) in Eq. (2.2). $C_{c.s}$ is the concentration of cyclohexene on the surface of the catalyst, $C_{A.S}$ is the concentration of the adsorbed benzene reaction product, and P_H is the partial pressure of hydrogen. Similarly, for the hydrogenation reaction in Eq. (2.1), one may show, assuming that the reaction is between the adsorbed cyclohexene molecule and hydrogen in the gas phase, that

$$\mu = k_S(C_{C.S}P_H-(C_{B.S}/\kappa_S)) \quad (3.14)$$

where $C_{B,S}$ is the concentration of cyclohexane adsorbed on the catalyst. On the other hand, if adsorbed cyclohexene reacts with adsorbed hydrogen, then P_H in Eq. (3.14) is replaced by $C_{H,S}$, the concentration of hydrogen on the catalyst.

Since, the concentrations on the catalyst of cyclohexene, cyclohexane, benzene, and hydrogen are proportional to the surface area of the catalyst, μ is also proportional to the surface area of the catalyst.

The model in Eq. (3.12) can be used to characterize a flow chemical reactor with regard to yield or conversion concerning the different reaction schemes being investigated. When μ and λ are not necessarily constant over compartments, the above model can be readily generalized, using continuous time and discrete state (compartments) Markov chains techniques to obtain the cumulative probability of exiting the microreactor.

3.6 Markov Chain Approach

The theory of Markov chains, which is a special case of Markov processes, is named after A. A. Markov who, in 1906, introduced the concept of chains with a discrete parameter and finite number of states [Chiang 1975].

A formal definition of Markov chains is presented as follows: a sequence of random variables $\{X_n, n = 0,1,...\}$ is called a Markov chain if, for every collection of integers (n=0,1,…), the conditional distribution of X_{n+1} satisfies the relation

$$\Pr\{X_{n+1} = i \mid X_0, X_1..., X_n\} = \Pr\{X_{n+1} = i \mid X_n\}. \qquad (3.15)$$

Where $\Pr\{X_{n+1}=i \mid X_0, X_1, ..., X_n\}$ represents the probability of the future state $X_{n+1}=i$ given all states $(X_0, X_1, ..., X_n)$ before state (X_{n+1}), and $\Pr\{X_{n+1}=i \mid X_n\}$ represents the probability of the future state $X_{n+1}=i$ given the previous state (X_n). Thus, given the knowledge of a present state (X_n), the outcome in the future ($X_{n+1}=i$) is no longer dependent upon the past $(X_0, X_1, ..., X_{n-1})$ [Chiang 1975].

Therefore, a Markov chain is a sequence of random variables such that for a given X_m, X_{m+1} is conditionally independent of $X_1, X_2, ..., X_{m-1}$.

In a Markov chain, if the outcome at the mth trial is E_i, and the outcome at the m+1th trial is E_j, this indicates that the chain has made a transition from E_i to E_j at the mth trial or step. The one-step transition probability of this event is expressed as

$$\Pr[X_{m+1}=E_j \mid X_m=E_i]=p_{ij}(m+1) \tag{3.16}$$

where the direction of the transition is denoted by the order of the subscripts in $P_{ij}(m+1)$. A Markov chain is characterized by its stochastic matrix (transition probability matrix) with the transition probabilities p_{ij} as its elements. In matrix form, the transition probabilities of a Markov chain are expressed as

$$\mathrm{P}(m+1)=P_{ij}(m+1)=\begin{pmatrix} p_{11}(m+1) & p_{12}(m+1) & \cdots & p_{1l}(m+1) \\ p_{21}(m+1) & p_{22}(m+1) & \cdots & p_{2l}(m+1) \\ \vdots & \vdots & \ddots & \vdots \\ p_{l1}(m+1) & p_{l2}(m+1) & \cdots & p_{ll}(m+1) \end{pmatrix}. \tag{3.17}$$

Note that all the elements in the transition matrix are non-negative, and the elements in each row sum to unity, i.e.,

$$\sum_{j=1}^{l} p_{ij}(m+1)=1, \qquad i=1,2,...,l. \tag{3.18}$$

Let P(0) denote the initial distribution vector,

$$\mathrm{P}(0) = [p_1(0)p_2(0)...p_l(0)]. \tag{3.19}$$

The distribution after one transition is given by

$$p_j(1) = \sum_{i=1}^{l} p_i(0)p_{ij}(1) \tag{3.20}$$

Since the probability that the chain is in state E_i is $p_i(0)$ initially and the probability of a transition from state E_i to state E_j is $p_{ij}(1)$, $p_j(1)$ is the result of all transitions leading to state E_j. Thus, in matrix form, Eq. (3.21) can be expressed as

$$\mathrm{P}(1) = \mathrm{P}(0)\,\mathrm{P}(1) \tag{3.21}$$

Similarly,

$$\mathrm{P}(2) = \mathrm{P}(1)\,\mathrm{P}(2) = \mathrm{P}(0)\,\mathrm{P}(1)\,\mathrm{P}(2) \tag{3.22}$$

and in general,

$$\mathrm{P}(m) = \mathrm{P}(0)\prod_{k=1}^{m}\mathrm{P}(k) \tag{3.23}$$

Equation (3.23) indicates that the process is completely determined once the initial distribution and the transition probability matrix for each step are specified.

In this study, a time homogeneous finite Markov chain was used in which the transition probabilities

$$\Pr\{X_{m+1} = E_j \mid X_m = E_i\} = p_{ij} \tag{3.24}$$

are independent of time (m) and there are a finite number of states. The transition probability matrix for the time homogeneous Markov chain can then be written as

$$\mathrm{P} = \begin{pmatrix} p_{11} & p_{12} & \cdots & p_{1l} \\ p_{21} & p_{22} & \cdots & p_{2l} \\ \vdots & \vdots & \ddots & \vdots \\ p_{l1} & p_{l2} & \cdots & p_{ll} \end{pmatrix} \tag{3.25}$$

The corresponding probability vector at any time stage m, P(m), in Eq. (3.23) reduces to

$$\mathrm{P}(m) = \mathrm{P}(0)\,\mathrm{P}^m . \tag{3.26}$$

There are many ways to classify the states of a Markov chain. State X_j is accessible from state X_i if state X_j can be reached from state X_i in a finite number of transitions. Two states are said to communicate if they are accessible to each other. Further, a Markov chain is irreducible if all states communicate with each other. A non-empty set of states is said to be closed if no states outside the set are accessible from any state inside the set. A single state forming a closed set is an absorbing state. A Markov chain that has one or more absorbing states is said to be an absorbing Markov chain, and, once the chain enters any of the absorbing states (a closed set), it will remain there. There are absorbing Markov chains, regular Markov chains, and ergodic Markov chains. In this study, an absorbing Markov chain was used.

In an irreducible Markov chain, all states belong to the same class; therefore, they are all recurrent states. The following theorem exists for this special class.

Theorem: If a Markov chain with finitely many states is irreducible and aperiodic, then

$$\pi_j = \lim_{m\to\infty} p_j(m); \qquad j = 1,2,...l, \tag{3.27}$$

and the unique limiting probability vector, π, of the Markov chain is given by solving the system of linear equations

$$\pi = \pi\,\mathrm{P} \quad , \tag{3.28}$$

where

$$\sum_{j=1}^{l} \pi_j = 1. \tag{3.29}$$

A Markov chain approach [Too 1983] was used to model the dynamics of chemical reactions. Consider a flow chemical reactor initially containing $n_i(0)$ molecules of type $A_i (i = 1,2,...,l)$. Molecules of this type enter the reactor at a rate of $x_i(m)$ molecules per unit time. Each molecule of any type will reside in the flow reactor for a random length of time before it reacts in it or exits from it. The type of molecules, $A_1, A_2, ..., A_l$, are considered as different transient states of the system. The exit stream is considered as an absorbing state (state of death); it is designed as state D. Once a molecule enters state D, it will never return to any of the transient states. Then, $P_{ij}(m+1)$ represents the probability that a molecule in state A_i at time m will be in state A_j at time (m+1). The probability that a molecule in state A_i will remain unchanged at time (m+1) is then $P_{ii}(m+1)$. Let $P_{id}(m+1)$ denote the probability that a molecule will exit from the reactor during this transition. As such,

$$\sum_{j=1}^{l} p_{ij}(m+1) + p_{id}(m+1) = 1. \tag{3.30}$$

As an example, consider a very simple chemical reaction

$$A_1 \xrightarrow{k_1} A_2 \tag{3.31}$$

and let $n_1(m)$ and $n_2(m)$ be the numbers of molecules of type A_1 and A_2 in the reactor at time m, respectively. The transition matrix for this reaction is

$$\mathrm{P}(m+1) = \begin{array}{c} \\ A1 \\ A2 \\ D \end{array} \begin{array}{c} \begin{array}{ccc} A1 & A2 & D \end{array} \\ \begin{pmatrix} p_{11} & p_{12} & p_{13} \\ p_{21} & p_{22} & p_{23} \\ p_{31} & p_{32} & p_{33} \end{pmatrix} \end{array} \tag{3.32}$$

With the aid of a computer, the number of molecules of each type, n_1 or n_2, in the reactor at any moment can be estimated by iterating over the following equations:

$$n_1(m+1) = n_1(m)p_{11}(m+1) + n_2(m)p_{21}(m+1) + x_1(m+1) \tag{3.33}$$

and

$$n_2(m+1) = n_1(m)p_{12}(m+1) + n_2(m)p_{22}(m+1) + x_2(m+1), \quad m = 0,1,2,... \tag{3.34}$$

where $x_1(m+1)$ and $x_2(m+1)$ are the number of molecules of types A_1 and A_2, respectively, fed in the reactor during the time interval $(m, m+1)$.

A Markov chain approach to simulate complex chemical reactions was presented by Chou et al. [Chou 1988]. By presenting a method to properly identify the states of the chain, Chou rendered the Markov chain approach in Too's method more specific to complex chemical reactions. In Chou's approach, a molecule is viewed as an "object," "entity," or system. The transformation of the molecule from one species to another is visualized as the transition of this "entity" from one form to another. The selection of such species is subject to the stoichiometric constraint based on atomic balance.

Consider a chemical reaction system containing a mixture of chemical species, A_j, $j = 1,2,...,J$. A chemical reaction involving A_j induces a change in the state of the mixture of the system. A molecule of type A_j is regarded as the "entity" at level j, and any reaction involving it is viewed as a transition of this "entity" from this level to

another, or vice versa. Thus, the collection of all transitions involving the "entity" forms a Markov chain.

Let the level of the "entity" of the state of the system at time $m\Delta t$ be the random variable $Y(m)$, and $p_{ij}(m,m+1)$ be the one-step transition probability that the "entity" at level i at time $m\Delta t$ will be at level j at time $(m+1)\Delta t$ inside the reactor. Furthermore, let $p_{id}(m,m+1)$ denote the transition probability that the "entity" at level i at time $m\Delta t$ will be discharged to the surrounding environment (dead or absorbing state) from the reactor at time $(m+1)\Delta t$. Thus, the one-step transition probabilities of this Markov chain in the form of a matrix are shown below:

$$\mathrm{P}(m,m+1)=\begin{pmatrix} p_{11}(m,m+1) & p_{12}(m,m+1) & \cdots & p_{1l}(m,m+1) & p_{1d}(m,m+1) \\ p_{21}(m,m+1) & p_{22}(m,m+1) & \cdots & p_{2l}(m,m+1) & p_{2d}(m,m+1) \\ \vdots & \vdots & \ddots & \vdots & \vdots \\ p_{l1}(m,m+1) & p_{l2}(m,m+1) & \cdots & p_{ll}(m,m+1) & p_{ld}(m,m+1) \\ 0 & 0 & \cdots & 0 & 1 \end{pmatrix} \tag{3.35}$$

where $l(l \le J)$ is the total number of the entity levels serving as the states of the Markov chain. Note that all elements in this matrix are non-negative and elements of each row sum to unity.

According to the properties of a Markov chain shown in Eqs. (3.20)- (3.23), the corresponding probability vector at any time stage $m+1$, $\mathrm{P}^*(m+1)$, in matrix form, is shown as

$$\mathrm{P}^*(m+1)=\mathrm{P}^*(m)\,\mathrm{P}(m,m+1). \tag{3.36}$$

or

$$P_j(m+1)=\sum_{i=1}^{l} p_i(m)\,p_{ij}(m,m+1), \qquad j=1,2,...l,d \tag{3.37}$$

Assume that $n_i(0)$ molecules of type A_i are initially in the reactor. Moreover, let the random variable $X_i(m)$ be the number of molecules of type A_i entering the reactor during the time interval $[m\Delta t,(m+1)\Delta t]$, and let the random variable $N_i(m)$ denote the number of molecules of type A_i in the reactor at time $m\Delta t$; $x_i(m)$ and $n_i(m)$ are the realizations of $X_i(m)$ and $N_i(m)$, respectively. Furthermore, let the random variable $N_{ij}(m,m+1)$ represent the number of "entities" at level j inside the reactor at time $(m+1)\Delta t$, which have come from the $n_i(m)$ "entities" at level i at time $m\Delta t$, resulting from the transition of these "entities" from level i to level j. Also, let the random variable $N_{id}(m,m+1)$ represent the number of these $n_i(m)$ "entities" discharged into the surrounding environment (dead state) from the reactor during the time interval $[m\Delta t,(m+1)\Delta t]$. If these $n_i(m)$ "entities" transform among the selected l levels or exit from the reactor independently during the time interval $[m\Delta t,(m+1)\Delta t]$, then each of these "entities" must be at one of the l levels, e.g., level j, inside the reactor with a probability $p_{ij}(m,m+1)$ or outside the reactor with probability $p_{id}(m,m+1)$ at time $(m+1)\Delta t$. Therefore, these $n_i(m)$ "entities" will have a multinomial distribution over the states 1,2,...l and d, with parameters $n_i(m)$, $p_{i1}(m,m+1)$, $p_{i2}(m,m+1)$, ..., $p_{il}(m,m+1)$, $p_{id}(m,m+1)$ at time $(m+1)\Delta t$ [Rohatgi 1976]. As such, we have

$$n_i(m)=\sum_{i=1}^{l} n_{ij}+n_{id},\ j=1,2,...,l \tag{3.38}$$

and

$$E[N_{ij}(m,m+1)]=n_i(m)p_{ij}(m,m+1),\qquad i=1,2,...,l;\quad j=1,2,...,l,d \tag{3.39}$$

Note that

$$N_j(m+1) = \sum_{i=1}^{l} N_{ij}(m, m+1) + X_j(m), \qquad j = 1,2,...l \tag{3.40}$$

and the random variables $N_{ij}(m, m+1), N_{kj}(m, m+1)$ and $X_j(m), i \neq k$, are independent. Thus, the conditional mean of $N_j(m+1)$, given that $N_i(m) = n_i(m)$ and $X_i(m) = x_i(m), i = 1,2,..., j$, are expressed as [Rohatgi 1976]

$$\begin{aligned} & E[N_j(m+1) \mid N_i(m) = n_i(m), X_i(m) = x_i(m), i = 1,2,...,J] \\ &= E[\sum_{i=1}^{l} N_{ij}(m, m+1)] + E[X_j(m)] \\ &= \sum_{i=1}^{l} E[N_{ij}(m, m+1)] + x_j(m) \\ &= \sum_{i=1}^{l} n_i(m) p_{ij}(m, m+1) + x_j(m), j = 1,2,...,l \end{aligned} \tag{3.41}$$

In this present study, we extend these two modeling approaches to model catalytic reactions by considering the microreactor as composed of two phases, the solid phase and the flow or gas phase. Details are shown in Chapter Seven.

CHAPTER FOUR

EXPERIMENTAL EQUIPMENT AND PROCEDURE

In this chapter, the structure of the microreactor and the design of the microreaction system used for the experiments are described.

4.1 The Microreactor

In this study, a microreactor made from a double-sided polished, (101) - silicon orientation wafer (four-inch in diameter, and 500 μm thick) was used. As shown in Fig 4.1, the microreactor is 1.6cm×3.1cm in size, with 1.2cm×1.34cm for the micro channels. It is composed of an inlet-via (a hole through the wafer) to allow gas to flow into the microreactor, inlet channel, manifold, reaction zone, outlet channel, and a outlet-via to allow gas to flow out of the reactor. The reaction zone is made of 599, 5 μ m wide and 100 μ m high, waved channels deposited with a catalyst.

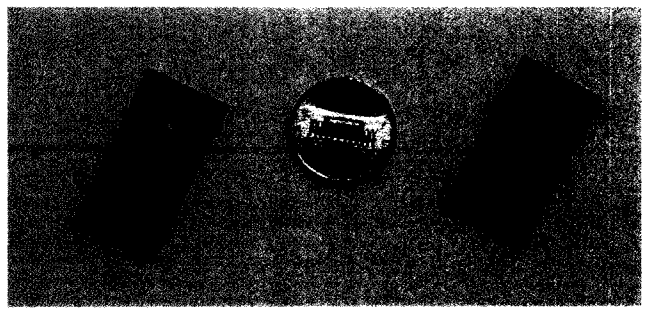

Figure 4.1 Microreactor and inside structure.

To increase the residence time of the reactant in the reaction area, the structures of the microchannels are designed to be zigzagged (see Figure 4.2). The reactant gas flows through the inlet-via into the microreactor and into the inlet channels. After entering the inlet channel, the chemical species mix in the manifold area and then flow into the reaction zone which is composed of 599 microchannels. Once the reaction is complete, the effluent of the microreactor moves out of the reactor through the outlet channel and outlet-via. Then, the effluent is sent to a mass spectrometer for chemical information analysis.

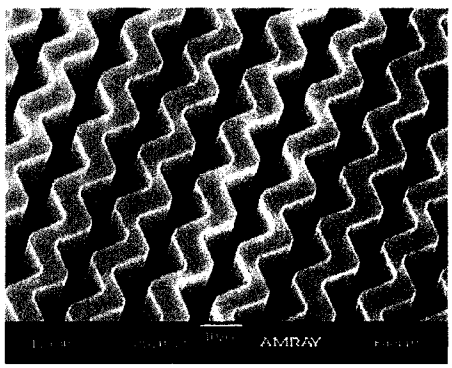

Figure 4.2 The structure of the microchannels of the microreactor.

The microreactor is fabricated using a lithography-based process and dry etching method. The lithography process used to make the microreactor is much like the one used in the integrated circuit (IC) industry [Okuzaki 2000]. After the microreactor is fabricated, the catalyst needs to be deposited on the walls and bottom of the microchannels. Two methods are used to deposit the catalyst in the reaction zone: physical, chemical. The physical method is sputtering deposition to coat the platinum, cobalt, or iron into the microreactor channels, which includes channel sidewall, and bottom. The chemical method is the sol-gel method, ion impregnation, or a combination of both.

After the microreactor fabrication and catalyst coating, the reactor is covered on top with the same size, 500 μm thick, Pyrex glass 7740 using anodic bonding [Zhao 2003].

4.2 Experimental Setup

In this work, the microreaction system is a gas-phase system (Figure 4.3). It consists of the following three subsystems: reaction system, data acquisition interface system, and Quadrupole Mass Spectrometer (QMS) [Lichtman 1984] [Dawson 1995]. The reaction system is composed of a mounting (heating) block, integrated with an air-tight tubing system, a gas source cylinder, mass flow controllers, pressure transducers, and a vacuum pump. The data acquisition system consists of a computer with the control software LabView for computerized control of temperature, gas flows, and pressure of the chemical reactions. As the chemical information analyzer, the QMS is used for qualitative and quantitative analysis of the reaction products.

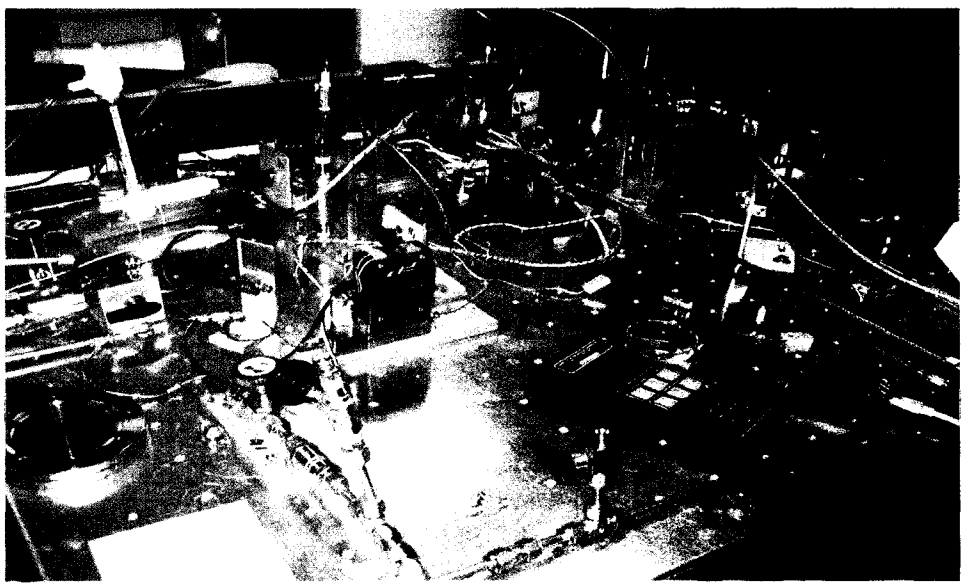

Figure 4.3 Experimental setup for the microreaction system.

The microreactor was mounted on a specially designed steel heating block, which has the inlet and outlet connections to the outer 1/16 in (1.59 mm)-diameter stainless steel tubing with the help of Swagelok fitting. The block has resistive heating elements and a thermocouple for temperature control. The inlet and outlet vias of the microreactor were connected to the corresponding holes in the block and compression-sealed using O-rings. The seal was checked by evacuating the tubing system using a vacuum pump. The reactor temperature was controlled with the help of solid-state-relay driven cartridges and a thermocouple. The reactant gases that come from a source gas cylinder are fed to the block by mass flow controllers, used to monitor the flow of the reactant gases. Digital pressure sensors are situated in the inlet and outlet streams to monitor pressure drop. The instantaneous values of the reaction temperature, flows, and pressure are monitored and controlled by the data acquisition software interface system, a PC running LabView software. Figure 4.4 shows the LabView data control interface. The reactant gas reacts in the microchannels of the microreactor. The outlet stream for the experiments was at atmospheric pressure. The microreactor effluents were continuously sampled and monitored for composition using a Stanford Research Systems mass spectrometer having its own PC for acquisition and control. The partial pressures of all the species present in the effluent stream were measured. The effluent stream in these experiments varied between approximately 0.2 *sccm* (standard cubic centimeter per minute) and 5 *sccm*. Since very low flow rates are involved in these experiments, the effluent stream was diluted with helium gas to ensure a minimum required flow rate of the effluent sample for the QMS and to prevent the pumping system in the QMS from adversely affecting the operating pressure in the experimental setup at the same time. For the experiments, argon

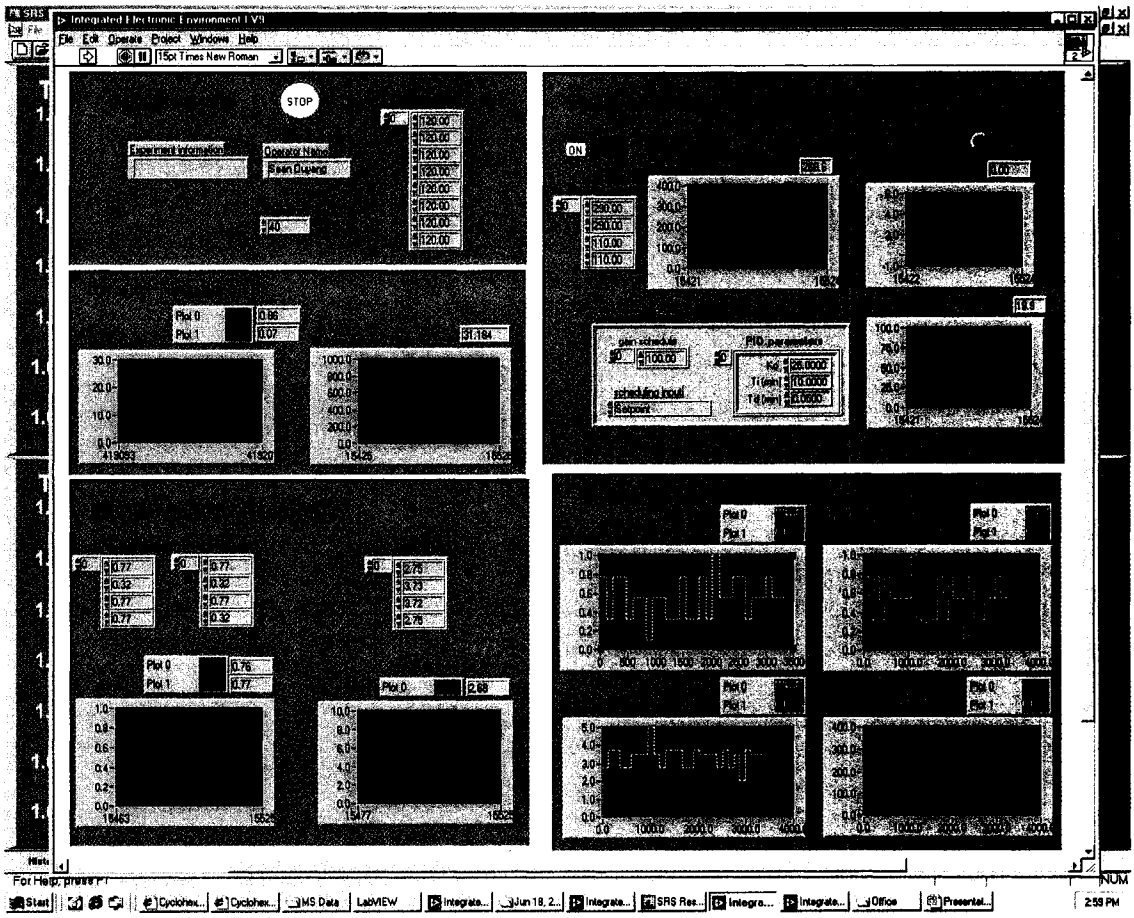

Figure 4.4 LabView data control interface.

as a carrier gas was bubbled into the reactant reservoir which contained liquid cyclohexene at ambient conditions, so that the carrier gas was saturated with the reactant vapor which formed the feed gas to the microreator. Gas lines downstream of the bubbler were heated to a few degrees above room temperature to prevent condensation of reactants or products.

For quantitative analysis of the effluents, the mass spectrometer, with ambient air as a standard, was calibrated first for establishing its sensitivity to nitrogen. Then, pure reactant and products were fed in the reactor in combination with nitrogen in order to determine their sensitivity factors. Finally, the calibrated mass spectrometer was used to

record continuous partial-pressure-data during the course of the experiments where conditions of temperature and reactant flow rates varied.

For each of the three experiments presented in this dissertation, a new microreactor was prepared for reaction by mounting it onto a heating block and by positioning it precisely on the o-rings to make an air-tight seal for the reactor. In order to eliminate leaks, testing involving evacuating the reactor, isolating the pumping system, and determining the rate of pressure increase was done. The system was then evacuated for an extended period (30 min or more) to remove any traces of gaseous impurities so that a standard background could be established in the QMS before the start of the actual reaction. With the system still isolated, hydrogen was introduced into the system. Once the pressure reached 1 *atm*, the outlet was opened to the atmosphere.

For the cyclohexene hydrogenation and dehydrogenation experiments, hydrogen flow continued at room temperature for at least one hour as a method of pre-treatment of the Pt catalyst. Because of liquid cylohexene under ambient condition, argon as a carrier gas equilibrated the cylohexene and was fed to the microreactor. Pure hydrogen was the other reactant gas used for this reaction. Platinum (Pt) was used as the catalyst, and sputtering deposition was the method used for a uniform Pt coating inside the microchannels of the microreactor.

For preferential oxidation of carbon monoxide amelioration in a hydrogen fuel cell experiment, mixed gas ordered from Nextair was used. The concentration of the mixed gas was 70% hydrogen, 2% carbon monoxide, and 28% argon as a balance gas. This composition is the same as in the fuel cell feed-in gas in the industry. Pure oxygen from Nextair was used to oxidize carbon monoxide. The existence of water and carbon

dioxide will affect the conversion of carbon monoxide and selectivity of carbon monoxide to carbon dioxide or water. Platinum (Pt) was used as the catalyst in this reaction, and the so-gel method was used to deposit Pt on the walls and bottom of the microchannels of the microreactor.

For the Fischer-Tropsch experiments, pure hydrogen from Nextair and carbon monoxide from Aldrich were the reactants mixed together before being fed into the microreactor. Iron was used as the catalyst in this reaction, and the so-gel method was used to deposit iron/cobalt on the walls and bottom of the microchannels of the microreactor.

CHAPTER FIVE

EXPERIMENTAL DESIGN AND CALIBRATION RESULTS

5.1 Mass Spectrometer Calibration for the Cyclohexene Hydrogenation and Dehydrogenation Experiments

In our chemical microsystem, a mass spectrometer (MS) was applied as the main gas analyzer because of its fast response time and ease of use. Qualitative analysis becomes possible with the basic knowledge in analytical mass spectrometry. Precise quantitative analysis, however, had been difficult in that MS sensitivity changes with different gas species and different concentrations. It has been popular to use GC/MS for precise quantitative analysis, but not much literature explored precise quantitative analysis with MS. The common MS quantitative analysis involves only calibration of different gas species. We have developed a calibration method to compensate for both gas species and concentration variations by using statistical analysis methods.

The type of MS we used is the Residual Gas Analyzer (RGA), which is very compact with the state-of-the-art pumps and electronics and is, thereby, ideal for on-line analysis because of its continuous sampling from the gas system. RGA can be operated under different modes, including continuous spectrum scan and partial pressures vs. time. After understanding the reaction mechanism, the most commonly used mode is the partial

pressures vs. time mode. Partial pressures were given according to the initial calibration and basic recalibration from the response current in the ion detector, stated below.

Initial calibration was performed to build up a rough relationship between the ion current and gas pressure. It is done by introducing air to RGA, and a partial pressure sensitivity factor was calculated according to the concentration and the fragmentation pattern of nitrogen in air. In the basic recalibration, with the initial calibration completed, each gas species of interest was then introduced with nitrogen at a 1:1 molar ratio. As such, the partial pressure sensitivity factor for this specific gas species was established. Details of the initial calibration and basic recalibration can be found in the literature [QMS 100] [Mao 1987].

Further calibration is crucial for quantitative analysis because the overall sensitivity of MS is influenced by different gas concentrations. For example, the existence of species (such as hydrogen) with low ionization energy in the gas mixture will enhance sensitivities for all gases at different levels, resulting in inaccurate partial pressure readings. The source of the enhancements is believed to stem from hydrogen addition which increases the kinetic energy of the ions and enhances transmission through the ion lenses [Venable 2000]. In order to obtain accurate molar flow rates in a flow system for the purpose of calculating conversion and selectivity in a chemical reaction, a complete calibration of the MS with all gases of interest at different concentrations is necessary. The ultimate goal is then to be able to calculate the true molar flow rates at the microreactor outlet from the partial pressure data recorded by a calibrated MS instrument. By knowing both inlet and outlet molar flow rates for all gas components, quantitative analysis (conversion, selectivity, etc.) can be achieved.

In our chemical microsystem, mass flow controllers (MFC 1, 2, 3) are used for precise flow control of different gas components (Fig. 5.1) so that both inlet and outlet

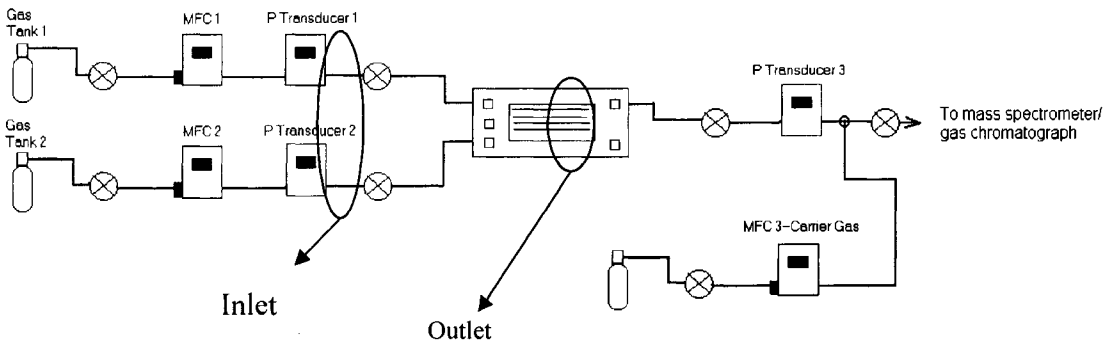

Figure 5.1. Microreaction setup.

flow rates are known when there is no reaction in the system. This inlet or outlet flow rate is attained by using a microreactor without a catalyst at low temperature hence equaling the inlet and outlet composition in the system. With known flow rates, we recorded the partial pressure signals for all gas species. A functional relationship between molar flow rates of all gas species and partial pressure signals in the mass spectrometer was then developed as follows:

Consider the function

$$PP_i = f_i(n_1, n_2, n_3 \ldots),$$

where PP_i is the measured partial pressure for gas species i from the mass spectrometer after initial and basic calibration, n_j is the molar flow rate for gas species j, and $i\,(i \neq j)$ is a gas species in the effluent.

By varying the molar ratios of all gas species and using statistical methods, a mathematical model was developed for the gas components of interest. The model comprises i nonlinear equations. In a catalytic reaction experiment with partial pressures

and only inlet flow rates known ($Flow_{inlet} \neq Flow_{outlet}$), a backward iteration using these equations can be used to calculate the true outlet flow rates for the different species in the experiment from the partial pressure data. With both inlet and outlet flow rates of all species known, conversions and selectivities can be accurately calculated.

In order to calibrate the mass spectrometer used in measuring partial pressures of different gases in the exit stream, factorial experiments (without a catalyst) were run using the second order central composite design [Box and Draper 1987]. Temperature, mole flow rates of hydrogen (H_2), helium (He), and cyclohexene (C_6H_{10}) were used as regressors or independent variables and the base partial pressure of cyclohexene in the exit stream as the dependent variable. The second-order regression model developed for predicting the base partial pressure of cyclohexene (C_6H_{10}) without a catalytic reaction is given by

$$\begin{aligned}\hat{y}_{c_6h_{10}} = {} & 2.928 + 0.001n_A + 4426.169n_B - 33137n_C + 464150n_{D1} + 0.000002n_A^2 \\ & -338049791n_B^2 + 90027466n_C^2 + 14311798856n_{D1}^2 - 20.507365n_An_B \\ & -16.368n_An_C + 448.68n_An_{D1} + 195329649n_Bn_C - 1183919728n_Bn_{D1} \\ & -1821459351n_Cn_{D1}\end{aligned} \qquad (5.1)$$

where $n_A, n_B, n_C,$ and n_{D1} are the temperature and the mole flow rates of hydrogen, helium, and cyclohexene (or argon as carrier gas), respectively. This model, when applied to an independent data set, predicted the cyclohexene base partial pressure (PP_{base}) with high accuracy ($R^2 = 0.95$) and was used for measuring base pressure and conversion of cyclohexene in the presence of the catalyst. Conversion is measured as (PP_{base} −PP)/ PP_{base} , where PP is the partial pressure of cyclohexene in the exit stream under catalytic reactions.

Similarly, base level experiments for cyclohexane (C_6H_{12}) and benzene (C_6H_6) were run. The second-order regression model developed for predicting the base partial pressure of cyclohexane (C_6H_{12}) without a catalytic reaction is given by

$$\begin{aligned}\hat{y}_{c_6h_{12}} = {} & 0.378 + 0.000774n_A + 735.761n_B - 4146n_C + 81102n_{D2} - 0.0000001n_A^2 \\ & - 55466466n_B^2 + 13598517n_C^2 + 3005106895n_{D2}^2 - 0.561n_An_B - 4.989n_An_C \\ & - 23.123n_An_{D2} - 662734n_Bn_C + 1031882048n_Bn_{D2} - 308411116n_Cn_{D2}\end{aligned} \quad (5.2)$$

where n_{D2} represents the mole flow rate of cyclohexane.

The second-order regression model developed for predicting the base partial pressure of benzene (C_6H_6) without a catalytic reaction is given by

$$\begin{aligned}\hat{y}_{c_6h_6} = {} & 2.373 - 0.001n_A - 19376n_B - 26304n_C + 487940n_{D3} + 0.000003n_A^2 \\ & - 1503465n_B^2 + 80433971n_C^2 + 10826606095n_{D3}^2 + 7.693n_An_B - 9.746n_An_C \\ & + 480.43n_An_{D3} + 211474634n_Bn_C - 2127211448n_Bn_{D3} - 2560095855n_Cn_{D3}\end{aligned} \quad (5.3)$$

where n_{D3} represents the mole flow rate of benzene.

Figure 5.2 presents partial pressure measurements plotted against experiment run number. A total of nine different lines are in this plot. The first three lines at the top are the partial pressures of helium measured in the cyclohexene, cyclohexane, and benzene experiments, respectively. These three lines are almost the same and seem to coincide. The three lines between 1.00E+02 and 1.00E+03 are the partial pressures of hydrogen obtained from the cyclohexene, cyclohexane, and benzene experiments, respectively. These three lines are also the same. The measurements of partial pressure of cyclohexene, benzene, and cyclohexane are shown in the three lines at the bottom of Fig. 5.2. Since the partial pressures of hydrogen and helium in these three different hydrocarbon base level

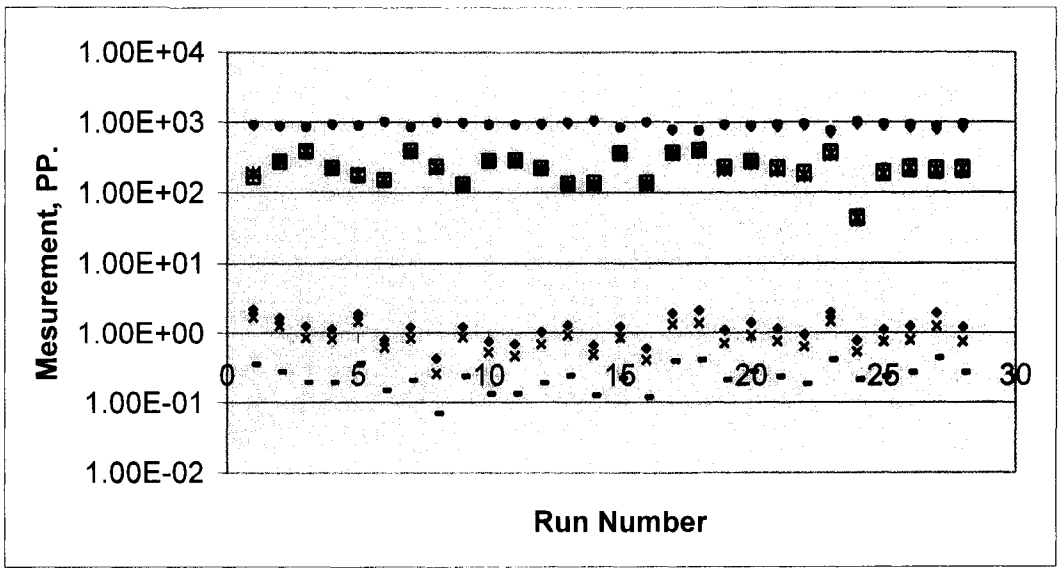

Figure 5.2 Experimental results of base level partial pressures (PP) for C_6H_{10}, C_6H_{12}, and C_6H_6.

experiments are almost the same, this indicates that the effect of the hydrocarbons (C_6H_{10}, C_6H_{12}, and C_6H_6) on the sensitivity of the MS is very small. Hence, for predicting the partial pressure for hydrogen and helium, we used only results from the cyclohexene experiment to obtain the regression models.

Therefore, a full second-order regression model to predict the partial pressure of hydrogen is given by

$$\begin{aligned}\hat{y}_{h_2} = {} & 308.901+0.052n_A+20439923n_B-3732279n_C-18691374n_{D1}-0.000129n_A^2 \\ & -66770120872n_B^2+10772892951n_C^2-468017400000n_{D1}^2+1583.811n_An_B \\ & -210.575n_An_C+1879.23n_An_{D1}-62218940289n_Bn_C-118558800000n_Bn_{D1} \\ & +140364161224n_Cn_{D1}.\end{aligned} \quad (5.4)$$

Also, a full second-order regression model to predict the partial pressure of helium is given by

$$\hat{y}_{he} = 769.983+0.051n_A-8706225n_B+4226627n_C-68984875n_{D1}-0.000223n_A^2 +60171320245n_B^2-11663066160n_C^2+4289545500000n_{D1}^2-1295.855n_An_B -227.877n_An_C+13269n_An_{D1}+15829571415n_Bn_C-114106000000n_Bn_{D1} +167731110378n_Cn_{D1}. \quad (5.5)$$

For a given experiment, temperature (n_A) is constant, the partial pressure of hydrogen ($\hat{y}_{h_2}$), the partial pressure of helium ($\hat{y}_{h_e}$), the partial pressure of cyclohexene ($\hat{y}_{C_6h_{10}}$), the partial pressure of cyclohexane ($\hat{y}_{C_6h_{12}}$), and the partial pressure of benzene ($\hat{y}_{C_6h_6}$) can be read from the MS. By solving the inverse equation system Eqs. (5.1)- (5.5), one can calculate the mole flow rate of hydrogen (n_B), the mole flow rate of helium (n_C), the mole flow rate of cyclohexene (n_{D1}), the mole flow rate of cyclohexane (n_{D2}),and the mole flow rate of benzene (n_{D3}) in the outlet stream of the microreactor. Then, the conversion of cyclohexene ($Conv_{C_6H_{10}}$) can be easily calculated as

$$Conv_{C_6H_{10}} = \frac{n_{D1inlet} - n_{D1outlet}}{n_{D1inlet}}. \quad (5.6)$$

Also, the selectivity of cyclohexane ($Sele_{C_6H_{12}}$) is given by

$$Sele_{C_6H_{12}} = \frac{n_{D2outlet}}{n_{D2outlet} + n_{D3outlet}}, \quad (5.7)$$

and the selectivity of benzene ($Sele_{C_6H_6}$) can be expressed as

$$Sele_{C_6H_6} = 1 - Sele_{C_6H_{12}} = \frac{n_{D3outlet}}{n_{D2outlet} + n_{D3outlet}}. \quad (5.8)$$

5.2 Cyclohexene Hydrogenation and Dehydrogenation Experiments

With cyclohexene base pressure measurement in place, the central composite design was used to run experiments in the presence of the catalyst in order to optimize or maximize the conversion rate of cyclohexene. In developing the experimental design for cyclohexene hydrogenation and dehydrogenation experiments, three factors were used: temperature (x_1), the flow rate of hydrogen (x_2), and the flow rate of argon (x_3). The conversion of C_6H_{10} (Y) is considered as the dependent variable or response. The purpose of using experimental design is to find the treatment combination $\mathbf{x}=(x_1, x_2, x_3)$ for which the conversion of C_6H_{10} is maximized.

Because the hydrogenation reaction gives cyclohexane as a product and is favored at low temperatures, and the dehydrogenation reaction produces benzene and is favored at high temperatures, two experimental designs were performed, one at a low temperature and the other at a high temperature.

The first-order, cube plus center points, part of the central composite design was run first using the temperature range 25~180°C, the flow rate of hydrogen range 0.1~1, and the flow rate of argon range 0.1~1 sccm. This design involved 8 factorial points (n_f=8) of a single-replicate, augmented by n_0 = 4 center points. Here, the center points are needed to provide error degrees of freedom for testing model lack-of-fit. Table 5.1 presents the design for coded and real values of the three factors (temperature x_1, the flow rate of hydrogen, x_2, and the flow rate of cyclohexene, x_3, as measured by the flow rate of argon (*Ar*) used as a carrier gas) with a center point (x_1=102.5°C, x_2=0.55sccm, and

x_3=0.55sccm). At this low temperature range, cyclohexene hydrogenation is the favored reaction.

Table 5.1 Central composite design used to study the conversion rate of C_6H_{10} in the cyclohexene hydrogenation reaction with three factors (temperature: x_1, flow rate of H_2: x_2,and flow rate of Ar: x_3) with a center point (x_1= 102.5°C, x_2= 0.55 sccm, and x_3= 0.55 sccm).

Run order	Design Num	Temperature x_1 (°C)	Flow Rate of H_2 x_2 (sccm)	Flow Rate of Ar x_3 (sccm)	Coded Value x_1 (°C)	Coded Value x_2 (sccm)	Coded Value x_3 (sccm)	C_6h_{10} Conversion Y (%)
3	1	56.37	0.28	0.28	-1	-1	-1	0.9072
7	2	56.37	0.28	0.82	-1	-1	1	0.7453
1	3	56.37	0.82	0.28	-1	1	-1	0.8854
9	4	56.37	0.82	0.82	-1	1	1	0.7472
5	5	148.63	0.28	0.28	1	-1	-1	0.9229
2	6	148.63	0.28	0.82	1	-1	1	0.8706
8	7	148.63	0.82	0.28	1	1	-1	0.8559
11	8	148.63	0.82	0.82	1	1	1	0.8263
6	9	102.5	0.55	0.55	0	0	0	0.8603
10	10	102.5	0.55	0.55	0	0	0	0.8208
4	11	102.5	0.55	0.55	0	0	0	0.8600
12	12	102.5	0.55	0.55	0	0	0	0.8237

Table 5.2 First-order cyclohexene hydrogenation model for C_6H_{10} conversion with parameter estimates for the three factors, temperature (x_1), the flow rate of H_2 (x_2), and the flow rate of Ar (x_3) with a center point (x_1= 102.5°C, x_2= 0.55 sccm, and x_3= 0.55 sccm).

Variable	DF	Parameter Estimate	Standard Error	t Value	Pr >]t]
Intercept	1	0.922	0.044	21.06	<.0001
x_1	1	0.000517	0.000253	2.04	0.076
x_2	1	-0.061	0.044	-1.40	0.198
x_3	1	-0.178	0.044	-4.08	0.004

In applying the central composite design and response surface methodology, experiments are first run utilizing the linear or first-order part of the design with center points (Table 5.1). Fitting a linear regression model to the first-order design, using SAS, gave the model in Table 5.2

$$Y = 0.922+0.000517x_1-0.061x_2-0.178x_3 \ , \tag{5.9}$$

where, x_1 represents temperature, x_2 the hydrogen flow rate, and x_3 the argon flow rate. Results of the analysis using the F-test in Eq. (3.8) did not show any significant lack-of-fit which indicated that the linear model was adequate for describing the conversion rate in the experimental region. In order to determine if improvements can still be made, we pursued the path of steepest ascent in order to determine a new center point around which another first-order experiment will be run. The path of steepest ascent was determined by increasing temperature (x_1) and decreasing the flow rate of hydrogen (x_2) and the flow rate of argon (x_3) proportional to their partial regression coefficients with constraints on the maximum or minimum values that can be attained.

Along this path, experiments will be run to determine the temperature and flow rates combination that gives maximum conversion. Table 5.3 presents the design for coded and real values of the three factors (temperature, x_1, the flow rate of hydrogen, x_2, and the flow rate of cyclohexene, x_3, as measured by the flow rate of argon (*Ar*) used as a carrier gas) at a new center point (x_1=150°C, x_2=0.28sccm, and x_3=0.28sccm). This design used the temperature range 116.4~183.6°C, the flow rate of hydrogen range 0.1~0.46 sccm, and the flow rate of argon range 0.1~0.46 sccm.

Table 5.3 Central composite design used to study the conversion rate of C_6H_{10} in the cyclohexene hydrogenation reaction with three factors (temperature: x_1, flow rate of H_2 : x_2,and flow rate of Ar: x_3) with a new center point (x_1 = 150°C, x_2 = 0.28 sccm, and x_3 = 0.28 sccm).

		Ture Value			Coded Value			Observed
Design Num	Run Num	Temp x_1 (^{0}C)	flowrate of H_2 x_2 (sccm)	flowrate of Ar x_3 (sccm)	x_1	x_2	x_3	Conversion (C6h10) Y (%)
1	1	170	0.39	0.39	-1	-1	-1	0.9263
2	12	170	0.39	0.17	-1	-1	1	0.9230
3	2	170	0.17	0.39	-1	1	-1	0.9296
4	10	170	0.17	0.17	-1	1	1	0.9180
5	9	130	0.39	0.39	1	-1	-1	0.9331
6	7	130	0.39	0.17	1	-1	1	0.9265
7	11	130	0.17	0.39	1	1	-1	0.9343
8	4	130	0.17	0.17	1	1	1	0.9310
9	6	150	0.28	0.28	0	0	0	0.9120
10	5	150	0.28	0.28	0	0	0	0.9107
11	3	150	0.28	0.28	0	0	0	0.9111
12	8	150	0.28	0.28	0	0	0	0.9355

In applying the central composite design and response surface methodology, experiments were first run utilizing the linear or first-order part of the design with center points (Table 5.3). Fitting a linear regression model to the first-order design gave the model in Table 5.4.

$$y = 0.944 - 0.000175x_1 - 0.005x_2 + 0.028x_3 \quad , \tag{5.10}$$

where, x_1 represents temperature, x_2 is the hydrogen flow rate, and x_3 is the argon flow rate. Results of the analysis using the F-test in Eq. (3.8) did not show any significant lack of fit which indicates that the linear model was adequate for describing the conversion rate in the experimental region. The conversion rate of C_6H_{10} did increase in this new

range. All the above analyses show that within the limit of the physical parameters in the microsystem, the conversion rate of C_6H_{10} is planar in the cyclohexene hydrogenation reaction and can be described by a linear model (Eq. (5.10)).

Table 5.4 First-order cyclohexene hydrogenation model for C_6H_{10} conversion with parameter estimates for the three factors, temperature (x_1), the flow rate of H_2 (x_2), and the flow rate of Ar (x_3) with a center point (x_1= 150°C, x_2= 0.28 sccm, and x_3= 0.28 sccm).

Variable	DF	Parameter Estimate	Standard Error	t Value	Pr > |t|
Intercept	1	0.944	0.029	32.85	<.0001
T	1	-0.000175	0.000172	-1.02	0.338
F1	1	-0.005	0.031	-0.15	0.887
F2	1	0.028	0.031	0.90	0.393

We have conducted similar experiments at higher temperatures for optimizing the conversion rate of cyclohexene where the dehydrogenation reaction is favored. Table 5.5 presents the design for coded and real values of the three factors (temperature x_1, the flow rate of hydrogen, x_2, and the flow rate of cyclohexene, x_3, as measured by the flow rate of argon (*Ar*) used as a carrier gas) with a center point (x_1=270°C, x_2= 0.55 sccm, and x_3= 0.55 sccm). This design was in the temperature range 130~410°C, the flow rate of hydrogen range 0.1~1 sccm, and the flow rate of argon range 0.1~1 sccm.

Fitting a linear regression model to the first order design, using SAS, gave the model in Table 5.6

$$Y = 0.92152+0.00005x_1-0.0132x_2+0.03848x_3 \quad , \tag{5.11}$$

where, x_1 represents temperature, x_2 is the hydrogen flow rate, and x_3 is the argon flow

Table 5.5 Central composite design used to study the conversion rate of C_6H_{10} in the cyclohexene dehydrogenation reaction with three factors (temperature: x_1, flow rate of H_2: x_2, and flow rate of Ar: x_3) with a center point (x_1 = 270°C, x_2 = 0.55 sccm, and x_3 = 0.55 sccm).

	True Value			Coded Value			Observed conversion of C_6H_{10}
Design Num	Temp x_1 (°C)	Flow Rate of H_2 x_2 (sccm)	Flow Rate of Ar x_3 (sccm)	x_1 (°C)	x_2 (sccm)	x_3 (sccm)	Y (%)
1	186.7	0.282	0.282	-1	-1	-1	0.93693
2	186.7	0.282	0.818	-1	-1	1	0.96213
3	186.7	0.818	0.282	-1	1	-1	0.93045
4	186.7	0.818	0.818	-1	1	1	0.94257
5	353.3	0.282	0.282	1	-1	-1	0.94171
6	353.3	0.282	0.818	1	-1	1	0.96365
7	353.3	0.818	0.282	1	1	-1	0.93996
8	353.3	0.818	0.818	1	1	1	0.96316
9	270	0.55	0.55	0	0	0	0.95301
10	270	0.55	0.55	0	0	0	0.95703
11	270	0.55	0.55	0	0	0	0.95493
12	270	0.55	0.55	0	0	0	0.95649

Table 5.6 First-order cyclohexene dehydrogenation model for C_6H_{10} conversion with parameter estimates for the three factors, temperature (x_1), the flow rate of H_2 (x_2), and the flow rate of Ar (x_3) with a center point (x_1 = 270°C, x_2 = 0.55 sccm, and x_3 = 0.55 sccm).

Variable	DF	Parameter Estimate	Standard Error	t Value	Pr > |t|
Intercept	1	0.922	0.009	97.21	<.0001
x_1	1	0.000055	0.000026	2.12	0.066
x_2	1	-0.013	0.008	-1.65	0.137
x_3	1	0.038	0.008	4.81	0.001

rate. Results of the analysis using the F-test in Eq. (3.8) did not show any significant lack-of-fit which indicated that the linear model was adequate for describing the conversion rate in the experimental region. C_6H_{10} conversion was up to 96% in this region of the experiments, which is quite high, This analysis result indicates that, within the limit of the physical parameters in the microsystem, the conversion rate of C_6H_{10} is planar for cyclohexene dehydrogenation reaction and can be described by a linear model (Eq. (5.11)). One reason for that may be the fact that the experiment was already at or close to the peak of the response surface.

In designing the experiment for cyclohexene hydrogenation and dehydrogenation reaction, we did not consider residence time and stoichiometry which are important factors that affect the yield or selectivity of a chemical reaction. Therefore, in the following fuel cell and syn-gas experiments, residence time and stoichimetry will be considered in the design.

5.3 Preferential Oxidation for Carbon Monoxide Amelioration in Hydrogen Fuel Cell

5.3.1 Experimental Design and Procedure

In running fuel cell experiments, the three factors that were considered were temperature, flow rate of CO, and flow rate of O_2. It would seem natural, at first, to use these factors in setting up the design. To have done so, however, would have ignored two important factors with regard to conversion and selectivity, namely the ratio of CO to O_2

(which affect the stoichiometry of the reaction) and the total flow rate (which determine the residence time).

Hence, in developing the experimental design for the preferential oxidation of CO in fuel cells, the three factors that were used were temperature (x_1), $CO:O_2$ ratio (x_2), and the total flow rate (x_3). The conversion of CO (Y_1) and the selectivity of CO_2(Y_2) are considered as the dependent variables or response. The purpose of using experimental design is to find the treatment combination $\mathbf{x}=(x_1, x_2, x_3)$ for which the conversion of CO and the selectivity of CO_2 are maximized.

The first-order, cube plus center points, part of the central composite design was run first in the temperature range 120~220°C, the $CO:O_2$ ratio range 0.25~4, and the total flow rate range 0.2~1 sccm. This design involved 8 factorial points (n_f =8) of a single-replicate, augmented by n_0 = 4 center points. Here, the center points are needed to provide error degrees of freedom for testing model lack-of-fit. The first 12 runs in Table 5.7 represent the first-order design for coded and real values of the three factors (temperature, $CO:O_2$ ratio, and the total flow rate). A linear multiple regression (Eq. (3.2) with p =3) was fitted to the first-order design. Results of the analysis using the F-test in Eq. (3.8) showed a quadratic lack-of-fit of the linear model. This indicated that the surface in that region of the experiment was not planer, but showed curvature. As a result, a second-order regression (Eq. (3.3) for p = 3) was fitted to the second-order central composite design in Table 5.7, obtained by augmenting the cube by the six axial points (a=±1.68).

Table 5.7 Central composite design used to study the conversion rate of CO and the selectivity of CO_2 in the preferential oxidation of CO in fuel cells with three factors (temperature, $CO:O_2$ ratio, and total flow rate).

Design	Run	Temperature	$CO:O_2$ Ratio	TotalFlow Rate	Coded Values			Conversion	Selectivity
Num	Order	$x_1(^0C)$	x_2	x_3(sccm)	x_1	x_2	x_3	of CO, Y_1	of CO_2, Y_2
1	13	140.24	1.01	0.36	-1	-1	-1	0.596	0.727
2	18	140.24	1.01	0.84	-1	-1	1	0.375	0.338
3	7	140.24	3.24	0.36	-1	1	-1	0.535	0.857
4	2	140.24	3.24	0.84	-1	1	1	0.371	0.511
5	14	199.76	1.01	0.36	1	-1	-1	0.577	0.748
6	8	199.76	1.01	0.84	1	-1	1	0.319	0.327
7	5	199.76	3.24	0.36	1	1	-1	0.507	0.635
8	11	199.76	3.24	0.84	1	1	1	0.367	0.441
9	1	170.00	2.13	0.60	0	0	0	0.401	0.534
10	16	170.00	2.13	0.60	0	0	0	0.390	0.386
11	6	170.00	2.13	0.60	0	0	0	0.392	0.559
12	9	170.00	2.13	0.60	0	0	0	0.441	0.468
13	12	120.00	2.13	0.60	-1.68	0	0	0.474	0.584
14	3	220.00	2.13	0.60	1.68	0	0	0.423	0.599
15	4	170.00	0.25	0.60	0	-1.68	0	0.423	0.539
16	10	170.00	4.00	0.60	0	1.68	0	0.451	0.543
17	15	170.00	2.13	0.20	0	0	-1.68	0.702	0.874
18	17	170.00	2.13	1.00	0	0	1.68	0.338	0.261

5.3.2 Results and Discussion

Data analysis was performed using SAS (1990). Tables 5.8 and 5.9 present the second-order regression model obtained by fitting to data from the second-order central composite design (Table 5.4) for the cases of yield and selectivity. Tables 5.10 and 5.11 give the predicted responses for yield and selectivity obtained from the quadratic regression models in Tables 5.8 and 5.9.

From Table 5.8, it is seen that the second-order regression model for CO conversion based on the true values of the factors is

$$Y_1 = 1.508 - 0.005x_1 - 0.104x_2 - 1.331x_3 + 0.000013x_1^2 + 0.000162x_1x_2 + 0.006x_2^2 - 0.000243x_1x_3 + 0.082x_2x_3 + 0.643x_3^2 \quad (5.12)$$

The second regression model for CO conversion based on the coded factor values is

$$Y_1 = 0.407 - 0.014x_1 - 0.003x_2 - 0.102x_3 + 0.011x_1^2 + 0.007x_2^2 + 0.037x_3^2 + 0.005x_1x_2 - 0.002x_1x_3 + 0.022x_2x_3 \quad (5.12a)$$

Also, from Table 5.9, the second-order regression model for the selectivity of CO_2 based on the true values of the factors is given by

$$Y_2 = 2.419 - 0.014x_1 + 0.073x_2 - 1.959x_3 + 0.000042x_1^2 - 0.001x_1x_2 + 0.016x_2^2 + 0.002x_1x_3 + 0.126x_2x_3 + 0.507x_3^2 \quad (5.13)$$

The second regression model for CO_2 selectivity based on the coded factor values is

$$Y_2 = 0.487 - 0.019x_1 + 0.023x_2 - 0.174x_3 + 0.037x_1^2 + 0.019x_2^2 + 0.029x_3^2 - 0.038x_1x_2 + 0.015x_1x_3 + 0.034x_2x_3 \quad (5.13a)$$

The coefficients in Eq. (5.12a) and Eq. (5.13a) show that total flow rate (x_3) has the largest and dominant effect on the conversion of CO and selectivity of CO_2. It is seen that the partial regression coefficient for x_3 is negative implying that smaller flow rate or larger residence time increases both CO conversion and CO_2 selectivity. Predicted responses, Table 5.10, from the second-order model of CO conversion in Eq. (5.12) show that temperature, $CO:O_2$ ratio, and total flow rate combination at the point (166.67, 1.77, 0.21) gave maximum conversion of CO (68.77%). From Table 5.11, the second-order model for selectivity of CO_2 (Eq. (5.13)) shows that temperature, $CO:O_2$ ratio, and total flow rate combination at the point (158.14, 1.99, 0.21) gave maximum selectivity of CO_2 (87.06%). The Spearman correlation coefficient between the conversion of CO and

Table 5.8 Second-order fuel cell model on *CO* conversion with parameter estimates for the three factors, temperature (x_1), ratio (x_2), and total flow rate(x_3).

Parameter	DF	Estimate	Standard Errort Value		Pr > |t|
Intercept	1	1.508	0.288	5.240	0.001
x_1	1	-0.005	0.003	-1.770	0.115
x_2	1	-0.104	0.054	-1.920	0.091
x_3	1	-1.331	0.262	-5.080	0.001
x_1^2	1	0.000013	0.000008	1.620	0.143
x_1x_2	1	0.000162	0.000260	0.620	0.550
x_2^2	1	0.006	0.006	1.050	0.325
x_1x_3	1	-0.000243	0.001	-0.200	0.845
x_2x_3	1	0.082	0.032	2.540	0.035
x_3^2	1	0.643	0.121	5.330	0.001

Table 5.9 Second-order fuel cell model on CO_2 selectivity with parameter estimates for the three factors, temperature (x_1), ratio (x_2), and total flow rate (x_3).

Parameter	DF	Estimate	Standard Error	t Value	Pr > |t|
Intercept	1	2.419	0.754	3.210	0.013
x_1	1	-0.014	0.007	-1.880	0.097
x_2	1	0.073	0.141	0.510	0.621
x_3	1	-1.959	0.686	-2.850	0.021
x_1^2	1	0.000042	0.000020	2.070	0.072
x_1x_2	1	-0.001	0.001	-1.670	0.133
x_2^2	1	0.016	0.014	1.080	0.311
x_1x_3	1	0.002	0.003	0.660	0.529
x_2x_3	1	0.126	0.084	1.490	0.176
x_3^2	1	0.507	0.316	1.600	0.147

selectivity of CO_2 is 0.90299. Because of this high positive correlation, it would seem possible to locate a factor combination that would optimize both conversion and selectivity simultaneously. In fact, the three factor combination at the point (158.13, 1.77, 0.21) used in the second-order model for *CO* conversion (Eq. (5.12)) and the second-

order model for CO_2 selectivity (Eq. (5.13)), predicted a CO conversion of 69.31% and a CO_2 selectivity of 88.08%.

Table 5.10 Predicted response for the conversion of CO for three factors, temperature (x_1), ratio (x_2), and total flow rate (x_3).

Factor Values			Predicted	Standard
x1	x2	x3	Response	Error
170.000	2.125	0.600	0.407	0.012
169.374	2.114	0.560	0.425	0.012
168.856	2.094	0.521	0.446	0.012
168.423	2.066	0.481	0.468	0.012
168.056	2.034	0.442	0.493	0.011
167.742	1.997	0.403	0.520	0.011
167.469	1.956	0.364	0.549	0.012
167.231	1.913	0.325	0.580	0.013
167.021	1.868	0.286	0.614	0.014
166.834	1.822	0.247	0.650	0.016
166.667	1.774	0.208	0.688	0.019

Table 5.11 Predicted response for the selectivity of CO_2 for three factors, temperature (x_1), ratio (x_2), and total flow rate (x_3).

Factor Values			Predicted	Standard
x1	x2	x3	Response	Error
170.000	2.125	0.600	0.487	0.032
169.365	2.144	0.561	0.517	0.032
168.548	2.153	0.521	0.549	0.031
167.574	2.153	0.482	0.583	0.031
166.469	2.146	0.443	0.618	0.030
165.255	2.132	0.404	0.655	0.030
163.950	2.111	0.365	0.694	0.031
162.573	2.086	0.327	0.735	0.033
161.137	2.057	0.288	0.779	0.037
159.655	2.023	0.250	0.824	0.042
158.137	1.986	0.213	0.871	0.050

It is clear from the results in Tables 5.10 and 5.11 that the predicted response for conversion and selectivity was maximum when the total flow rate was set at a minimum value of about 0.2 sccm. As a result, we ran a new round of experiments setting the total flow rate at 0.2 sccm (the minimum flow rate the microreactor setup can accommodate)

and varying the temperature and CO: O_2 ratio first according to a two-level factorial design with center points, later augmented to a second-order central composite design (CCD). The design (first-order, 8 cube points plus 4 center points, with augmentation, ± 1.414 points, to second-order) and experimental results on selectivity and conversion are shown in Table 5.12.

Table 5.12 Central composite design used to study the conversion rate of CO and the selectivity of CO_2 in the preferential oxidation of CO in fuel cells with two factors (temperature and $CO:O_2$ ratio).

RunNum	DesNum	True Value Temp x_1	True Value $CO:O_2$ x_2	Coded Value x_1	Coded Value x_2	Conversion of CO Y_1	Selectivity to CO2 Y_2
2	1	131.71	0.70	-1	-1	0.794	0.653
8	2	131.71	2.90	-1	1	0.525	0.597
10	3	188.29	0.70	1	-1	0.901	0.865
16	4	188.29	2.90	1	1	0.586	0.576
9	5	160.00	1.80	0	0	0.921	0.896
1	6	160.00	1.80	0	0	0.915	0.888
7	7	160.00	1.80	0	0	0.909	0.867
12	8	160.00	1.80	0	0	0.926	0.898
13	9	160.00	1.80	0	0	0.914	0.859
15	10	160.00	1.80	0	0	0.901	0.865
11	11	160.00	1.80	0	0	0.922	0.834
6	12	160.00	1.80	0	0	0.902	0.851
5	13	120.00	1.80	-1.414	0	0.895	0.877
3	14	200.00	1.80	1.414	0	0.903	0.823
4	15	160.00	0.25	0	-1.414	0.764	0.763
14	16	160.00	3.35	0	1.414	0.453	0.643

Analysis based on a linear regression model fit to the data corresponding to the first-order design in Table 5.12 using the F-test in Eq. (2.8) showed a quadratic lack of fit for the linear regression model. This result led to fitting a second-order or quadratic regression model to the data for the second-order design in Table 5.12. From the analysis in Table 5.13, it is seen that the second-order regression model for CO conversion based on the true values of the factors is given by

$$Y_1 = -0.2 + 0.01x_1 + 0.438x_2 - 0.000025x_1^2 - 0.138x_2^2 - 0.00037x_1x_2 \quad (5.14)$$

The second regression model for CO conversion based on the coded factor values is

$$Y_1 = 0.914 + 0.022x_1 - 0.128x_2 - 0.02x_1^2 - 0.166x_2^2 - 0.012x_1x_2 \quad (5.14a)$$

Table 5.13 Second-order regression model on CO conversion with parameter estimates for the two factors, temperature (x_1) and $CO:O_2$ ratio (x_2).

Parameter	DF	Estimate	Standard Error	t Value	Pr > |t|
Intercept	1	-0.2	0.414	-0.48	0.639
x_1	1	0.010	0.005	1.940	0.081
x_2	1	0.438	0.095	4.640	0.001
x_1^2	1	-0.000025	0.000015	-1.690	0.123
x_2^2	1	-0.138	0.010	-13.880	<.0001
x_1x_2	1	-0.000370	0.001	-0.680	0.511

Table 5.14 Second-order regression model on CO_2 selectivity with parameter estimates for the two factors, temperature (x_1) and $CO:O_2$ ratio (x_2).

Parameter	DF	Estimate	Standard Error	t Value	Pr > |t|
Intercept	1	-1.079	0.751	-1.440	0.181
x_1	1	0.018	0.009	2.040	0.068
x_2	1	0.568	0.171	3.320	0.008
x_1^2	1	-0.000045	0.000027	-1.640	0.131
x_2^2	1	-0.091	0.018	-5.060	0.001
x_1x_2	1	-0.002	0.001	-1.900	0.086

A similar analysis for CO_2 selectivity (Table 5.14) gave the second-order model based on the true values of the factors

$$Y_2 = -1.079 + 0.018x_1 + 0.568x_2 - 0.000045x_1^2 - 0.091x_2^2 - 0.002x_1x_2. \quad (5.15)$$

The second regression model for CO_2 selectivity based on the coded factor values is

$$Y_2=0.87+0.014x_1-0.064x_2-0.036x_1^2 \\ -0.109x_2^2-0.058x_1x_2 \quad (5.15a)$$

With the total flow rate fixed, the coefficients in Eq. (5.14a) and Eq. (5.15a) show that $CO:O_2$ ratio (stoichiometry) has more effect than temperature on the conversion of CO and CO_2 selectivity. From results in Table 5.15, the second-order model for CO conversion shows that temperature, $CO:O_2$ ratio combination at the point (179.03, 1.35) gave maximum conversion of CO (94.75%). Also from Table 5.16, the second-order model for the selectivity of CO_2 shows that temperature, $CO:O_2$ ratio combination at the point (175.9, 1.31) gave maximum selectivity of CO_2 (88.81%). These results indicate that practically the same factor combination gave both maximum conversion and maximum selectivity. This indication can be explained by the conversion and selectivity being highly positively correlated.

Table 5.15 Statistical analysis of the predicted response for the conversion of CO for two factors, temperature (x_1) and $CO:O_2$ ratio (x_2).

Factor Values		Predicted	Standard
Temperature	$CO:O_2$ ratio	Response	Error
160.000	1.800	0.914	0.012
161.046	1.650	0.929	0.012
163.370	1.519	0.938	0.012
167.388	1.434	0.944	0.012
171.981	1.390	0.946	0.013
176.510	1.363	0.947	0.013
180.916	1.344	0.947	0.015
185.228	1.329	0.947	0.017
189.472	1.317	0.945	0.019
193.669	1.306	0.942	0.023
197.829	1.296	0.939	0.027

Table 5.16 Statistical analysis of the predicted response for the selectivity of CO_2 for two factors, temperature (x_1) and $CO:O_2$ ratio (x_2).

Factor Values		Predicted	Standard
Temperature	$CO:O_2$ ratio	Response	Error
160.000	1.800	0.870	0.022
161.638	1.657	0.877	0.022
164.595	1.546	0.882	0.022
168.145	1.459	0.886	0.022
171.878	1.385	0.887	0.023
175.665	1.312	0.888	0.024
179.469	1.256	0.888	0.027
183.276	1.197	0.886	0.030
187.083	1.140	0.883	0.035
190.888	1.083	0.880	0.041
194.690	1.028	0.875	0.048

To verify the predicted maxima from the quadratic models for conversion and selectivity, experiments were run for these two treatment or factor combinations. Results from these experiments, presented in Table 5.17, gave close agreement between predicted

Table 5.17 Experimental results verifying the predicted results on CO conversion and CO_2 selectivity.

Temperature	$CO:O_2$	experimental Run	Predicted Values: CO conv	Experimental result : CO conv	Experimental result: selec of CO_2
179	1.35	1	94.70%	94.34%	87.53%
		2	94.70%	95.17%	87.94%
		3	94.70%	94.27%	88.32%
Temperature	$CO:O_2$	experimental Run	CO_2Selec	Experimental result: CO conv	Experimental result: selec of CO_2
175.9	1.31	1	88.80%	94.29%	89.13%
		2	88.80%	93.91%	89.32%
		3	88.80%	92.65%	88.54%

and observed conversion and selectivity. Further, it is shown that, in fact, one factor combination of temperature, $CO:O_2$ ratio, and total flow at the point (175.9, 1.31 and 0.2) can be used to maximize CO conversion and CO_2 selectivity.

5.4 Fischer-Tropsch Synthesis

5.4.1 Experimental Design and Procedure

In this study, the Fischer-Tropsch (F-T) synthesis experiment focused on the reaction of carbon monoxide and hydrogen to produce propane. Therefore, the purpose in this study was to optimize the microreactor chemical reaction process in order to obtain high CO conversion and propane (C_3H_8) selectivity.

Three independent variables or factors were considered important for this reaction process, the total flow rate (x_1), $H_2:CO$ ratio (x_2), and temperature (x_3). The conversion of CO (Y_1), and the selectivity of C_3H_8(Y_2) were considered as the dependent variables. The purpose of using experimental design was to find the treatment combination $\mathbf{x}=(x_1,x_2,x_3)$ for which the conversion of CO and the selectivity of C_3H_8 are maximized.

The first-order, cube plus center points, part of the central composite design was run first in the total flow rate range 0.5~1.1 sccm, the $H_2:CO$ ratio range 2~4, and the temperature range 180~260^{0}C. This design involved 8 factorial points (n_f = 8) of a single-replicate, augmented by n_0 = 6 center points. Here, the center points are needed to provide error degrees of freedom for testing model lack of fit. Because of the limitation

resulting from the length of time the catalyst remain active, a first-order design was run in two days using two different microreactors as two blocks. The first 14 runs in Table 5.18 represent the first-order design for coded and real values of the three factors (total flow rate, $H_2 : CO$ ratio, and temperature). Linear multiple regressions (Eq. (5.16) and (5.17)

Table 5.18 Central composite design used to study the conversion rate of CO and the selectivity of C_3H_8 in the Fischer-Tropsch (F-T) synthesis experiment with three factors (total flow rate: x_1, $H_2 : CO$ ratio: x_2, and temperature: x_3).

		Coded Value			True Value				Selectivity	
De Num	Block	x_1	x_2	x_3	Total Flow Rate x_1 (sccm)	H_2:CO Ratio x_2	Temp x_3 (^{0}C)	Conc.Of CO Y_1 (%)	Methane Y_2 (%)	Ethane Y_3 (%)	Propane Y_4 .(%)
1	1	-1	-1	-1	0.5	2	180	59.75%	10.36%	11.49%	78.15%
2	2	-1	-1	1	0.5	2	260	54.54%	5.06%	17.52%	77.42%
3	2	-1	1	-1	0.5	4	180	65.28%	5.71%	12.72%	81.57%
4	1	-1	1	1	0.5	4	260	70.97%	0.50%	7.55%	91.95%
5	2	1	-1	-1	1.1	2	180	67.10%	10.52%	22.73%	66.75%
6	1	1	-1	1	1.1	2	260	61.32%	0.25%	20.32%	79.43%
7	1	1	1	-1	1.1	4	180	61.28%	3.99%	8.62%	87.39%
8	2	1	1	1	1.1	4	260	61.39%	7.91%	11.99%	80.10%
9	1	0	0	0	0.8	3	220	61.78%	7.04%	8.35%	84.61%
10	1	0	0	0	0.8	3	220	62.64%	4.01%	9.00%	86.99%
11	1	0	0	0	0.8	3	220	62.64%	5.24%	7.99%	86.77%
12	2	0	0	0	0.8	3	220	61.21%	6.49%	10.00%	83.51%
13	2	0	0	0	0.8	3	220	62.36%	5.82%	7.87%	86.31%
14	2	0	0	0	0.8	3	220	62.64%	6.24%	8.14%	85.62%
15	3	-1.69	0	0	0.293	3	220	71.48%	6.45%	9.50%	84.05%
16	3	1.69	0	0	1.307	3	220	55.39%	8.57%	9.43%	82.00%
17	3	0	-1.69	0	0.8	1.3	220	53.30%	13.34%	10.34%	76.32%
18	3	0	1.69	0	0.8	4.7	220	58.34%	5.68%	8.64%	85.68%
19	3	0	0	-1.69	0.8	3	152.4	61.48%	7.45%	15.79%	76.76%
20	3	0	0	1.69	0.8	3	287.6	59.72%	6.79%	16.68%	76.53%
21	3	0	0	0	0.8	3	220	63.53%	6.34%	9.11%	84.55%
22	3	0	0	0	0.8	3	220	61.95%	5.93%	8.34%	85.73%
23	3	0	0	0	0.8	3	220	63.23%	6.49%	12.20%	81.31%
24	3	0	0	0	0.8	3	220	62.45%	7.34%	10.23%	82.43%

with p =3) were fitted to the first-order design. Results of the analysis showed no quadratic lack-of-fit for the linear model in Eq. (5.16), but did show a quadratic lack-of-fit for the linear model in Eq. (5.17). This analysis result indicated that the surface of *CO* conversion is planar, but the surface of selectivity of propane (C_3H_8) in that region of the experiment was not planer. As a result, a second-order regression (Eq. (5.18) for p = 3) was fitted to the second-order central composite design in Table5.18, obtained by augmenting the cube by the six axial points ($\alpha = \pm 1.69$) with four center points.

5.4.2 Experimental Results and Statistical Analysis

From Table 5.19, the first-order regression model for *CO* conversion based on the true values of the factors is given by

$$Y_1 = 0.598 + 0.002x_1 + 0.02x_2 - 0.00162x_3 \tag{5.16}$$

From Table 5.20, the first-order regression model for propane selectivity based on the true factor values is given by

$$Y_4 = 0.651\text{-}0.049\text{Bl}\text{-}0.064x_1 + 0.049x_2 + 0.00047x_3. \tag{5.17}$$

and from Table 5.21, the second-order regression model for propane selectivity based on the true values of the factors is given by

$$\begin{aligned} Y_4 = {} & \text{-}0.52 + 0.035\text{BL}_1 - 0.014\text{BL}_2 + 0.106x_1 + 0.165x_2 \\ & + 0.01x_3 - 0.06x_1^2 - 0.013x_2^2 - 0.000017x_3^2 \\ & + 0.014x_1x_2 - 0.000444x_1x_3 - 0.000277x_2x_3. \end{aligned} \tag{5.18}$$

The second-order regression model for propane selectivity based on the coded values of the factors is

$$Y_4 = 0.841 + 0.035BL_1 - 0.014BL_2 - 0.014x_1 + 0.04x_2 + 0.011x_3 - 0.005x_1^2 - 0.013x_2^2 - 0.028x_3^2 + 0.004x_1x_2 - 0.005x_1x_3 - 0.011x_2x_3 \quad (5.18a)$$

The coefficients in Eq. (5.18a) show that $H_2:CO$ ratio (stoichiometry) has the largest effect on propane selectivity. From Table 5.22, canonical analysis, using SAS, the second-order model of propane selectivity shows that the total flow rate, $H_2:CO$ ratio, and temperature combination at the point (0.60, 4.51, and 218.16) gave a maximum selectivity of propane (C_3H_8) equal to 88.25%.

Table 5.19 First-order F-T synthesis model on CO conversion with parameter estimates for the three factors, total flow rate (x_1), $H_2:CO$ ratio (x_2), and temperature (x_3).

Variable	DF	Parameter Estimate	Standard Error	t Value	Pr > |t|
Intercept	1	0.598	0.091	6.56	<.0001
x_1	1	0.002	0.044	0.05	0.960
x_2	1	0.020	0.013	1.52	0.159
x_3	1	-0.000162	0.000333	-0.49	0.636

Table 5.20 First-order F-T synthesis model on C_3H_8 selectivity with parameter estimates for the three factors, total flow rate (x_1), $H_2:CO$ ratio (x_2), and temperature (x_3).

Variable	DF	Parameter Estimate	Standard Error	t Value	Pr > |t|
Intercept	1	0.651	0.102	6.40	0.0001
block	1	-0.049	0.022	-2.18	0.057
x_1	1	-0.064	0.049	-1.31	0.224
x_2	1	0.049	0.015	3.33	0.009
x_3	1	0.00047	0.00037	1.27	0.235

Table 5.21 Second-order F-T synthesis model on C_3H_8 selectivity with parameter estimates for the three factors, total flow rate (x_1), $H_2:CO$ ratio (x_2), and temperature (x_3).

Variable	DF	Parameter Estimate	Standard Error	t Value	Pr > |t|
Intercept	1	-0.520	0.328	-1.59	0.139
b_1	1	0.035	0.014	2.50	0.028
b_2	1	-0.014	0.014	-0.96	0.355
x_1	1	0.106	0.246	0.43	0.673
x_2	1	0.165	0.075	2.20	0.048
x_3	1	0.010	0.002	4.15	0.001
x_1^2	1	-0.060	0.078	-0.77	0.454
x_2^2	1	-0.013	0.007	-1.78	0.010
x_3^2	1	-0.000017	0.0000044	-3.96	0.002
x_1x_2	1	0.014	0.034	0.42	0.684
x_1x_3	1	-0.000444	0.000840	-0.53	0.607
x_2x_3	1	-0.000277	0.000252	-1.10	0.293

Table5.22: Canonical analysis of response surface selectivity of propane based on coded data.

	Critical Value	
Factor	Coded	Uncoded
x_1	-0.390178	0.602180
x_2	0.895127	4.512765
x_3	-0.027242	218.15843

Predicted selectivity: 88.25%

CHAPTER SIX

PROBABILITY AND STOCHASTIC MODELING

6.1 Probabilistic Modeling

In Chapter Three, we presented the methodology of a mathematical model for predicting the probability that a certain species undergoing reaction inside a microreactor exits the reactor by a certain time T. From the model, we can show that the probability (P) of exiting the reactor by time T is

$$P = \int_0^T e^{-\mu(T-\tau)} \frac{\lambda e^{-\lambda(T-\tau)} (\lambda(T-\tau))^{n-1}}{\Gamma(n)} d\tau \tag{6.1}$$

In deriving Eq. (6.1), it was assumed, in general, that the microchannel is composed of n compartments in series. In order to fit the model to experimental data, one may evaluate Eq. (6.1), for different n values. This is given below for n = 1, 2,..., 6.

n = 1,

$$P = \frac{\lambda}{\lambda+\mu}\left[1 - e^{-(\lambda+\mu)T}\right], \tag{6.2}$$

n = 2,

$$P = -\frac{T\lambda^2}{\lambda+\mu} e^{-(\lambda+\mu)T} + (1 - e^{-(\lambda+\mu)T}) \frac{\lambda^2}{(\lambda+\mu)^2}, \tag{6.3}$$

n = 3,

$$P=\left[-\frac{\lambda^3T^2}{2(\lambda+\mu)}-\frac{\lambda^3T}{(\lambda+\mu)^2}\right]e^{-(\lambda+\mu)T}+(1-e^{-(\lambda+\mu)T})\frac{\lambda^3}{(\lambda+\mu)^3}, \tag{6.4}$$

n = 4,

$$P=\left[-\frac{\lambda^4T^3}{6(\lambda+\mu)}-\frac{\lambda^4T^2}{2(\lambda+\mu)^2}-\frac{\lambda^4T}{(\lambda+\mu)^3}\right]e^{-(\lambda+\mu)T}+(1-e^{-(\lambda+\mu)T})\frac{\lambda^4}{(\lambda+\mu)^4}, \tag{6.5}$$

n = 5,

$$P=\left[-\frac{\lambda^5T^4}{24(\lambda+\mu)}-\frac{\lambda^5T^3}{6(\lambda+\mu)^2}-\frac{\lambda^5T^2}{2(\lambda+\mu)^3}-\frac{\lambda^5T}{(\lambda+\mu)^4}\right]e^{-(\lambda+\mu)T}+(1-e^{-(\lambda+\mu)T})\frac{\lambda^5}{(\lambda+\mu)^5}, \tag{6.6}$$

and n = 6,

$$P=\left[-\frac{\lambda^6T^5}{120(\lambda+\mu)}-\frac{\lambda^6T^4}{24(\lambda+\mu)^2}-\frac{\lambda^6T^3}{6(\lambda+\mu)^3}-\frac{\lambda^6T^2}{2(\lambda+\mu)^4}-\frac{\lambda^6T}{(\lambda+\mu)^5}\right]e^{-(\lambda+\mu)T}+(1-e^{-(\lambda+\mu)T})\frac{\lambda^6}{(\lambda+\mu)^6}. \tag{6.7}$$

The probability of exiting the reactor by time T is estimated by the partial pressure of the reactant in the exit stream divided by the base partial pressure without the reaction (pp/base). Here, n and λ are parameters of the residence time distribution, and μ (the reaction rate) is proportional to the surface area of the catalyst.

The model for different n values was fitted to data on pp/base over time in order to estimate λ, and μ. In the following section, this mathematical modeling approach was applied to the cyclohexene hydrogenation and dehydrogenation experiments and to the Fischer-Tropsch synthesis experiment.

6.1.1 Cyclohexene Hydrogenation Reaction

In the case of the cyclohexene hydrogenation experiment, the probability in Eq. (3.11) is the conversion rate of C_6H_{10} at time T for the case of an open flow involving C_6H_{10} and H_2. This probability as a function of time was compared to the observed C_6H_{10} conversion from cyclohexene hydrogenation experiments in order to estimate model parameters. From these parameters, we estimated the reaction rate (and hence the activation energy of the reaction, E_a) and characterized the flow behavior from the residence time distribution.

The data in Table 6.1 were used for estimating λ, μ, and n for a cyclohexene hydrogenation experiment under the operating condition, temperature = 56.37°C, flow rate of hydrogen = 0.28 sccm, and flow rate of Argon = 0.82 sccm.

The SAS software was used to fit the data in Table 6.1 to the model Eqs. (6.2)-(6.4) for different n values. Figures 6.1 to 6.4 show the observed values of PP/Base vs time for C_6H_{10} in the exit stream and the predicted values from Eqs. (6.2) to (6.4). It is clear that the predicted values give the best fit to the observed values when n = 1 (Fig. 6.1). The SSE (sum of squared errors) of 0.0657 is minimal for n = 1. The lack-of-fit was even worse for higher n values. This result indicates that the microchannel behaves as one compartment, implying that the flow is well mixed and is time homogeneous, in which case, each molecule in the reactor has the same exit intensity (or rate) λ. The estimated values for λ and μ were 0.0252/min and $0.0793 / M \cdot \text{min}$, respectively.

Table 6.1: Cyclohexene hydrogenation experimental data, under the operating condition (temp = 56.37°C, flow rate of H_2 = 0.28 sccm, and flow rate of Ar = 0.82 sccm), used to estimate λ, μ, and n.

Time(min)	C_6H_{10}:p.p/base	Time(min)	C_6H_{10}:p.p/base	Time(min)	C_6H_{10}:p.p/base
0.0000	0.1010	28.0053	0.2004	56.0107	0.2395
0.6668	0.0971	28.6721	0.2052	56.6774	0.2355
1.3336	0.1124	29.3389	0.2162	57.3442	0.2612
2.0007	0.1069	30.0057	0.2028	58.0113	0.2553
2.6673	0.1207	30.6728	0.2170	58.6781	0.2501
3.3340	0.1140	31.3397	0.2182	59.3447	0.2545
4.0009	0.1168	32.0065	0.2134	60.0115	0.2359
4.6681	0.1262	32.6732	0.2229	60.6781	0.2521
5.3345	0.1416	33.3398	0.2217	61.3449	0.2493
6.0015	0.1452	34.0064	0.2099	62.0119	0.2497
6.6681	0.1401	34.6732	0.2115	62.6788	0.2584
7.3347	0.1586	35.3403	0.2059	63.3456	0.2533
8.0017	0.1641	36.0071	0.2225	64.0121	0.2351
8.6686	0.1479	36.6738	0.2249	64.6790	0.2387
9.3353	0.1547	37.3404	0.2178	65.3457	0.2564
10.0022	0.1558	38.0073	0.2044	66.0125	0.2631
10.6689	0.1649	38.6740	0.2288	66.6792	0.2545
11.3357	0.1767	39.3408	0.2182	67.3460	0.2442
12.0024	0.1732	40.0076	0.2328	68.0133	0.2643
12.6692	0.1720	40.6745	0.2237	68.6798	0.2414
13.3359	0.1602	41.3416	0.2304	69.3464	0.2608
14.0027	0.1795	42.0081	0.2367	70.0132	0.2635
14.6696	0.1685	42.6747	0.2355	70.6800	0.2647
15.3366	0.1791	43.3415	0.2395	71.3470	0.2422
16.0032	0.1965	44.0083	0.2253	72.0138	0.2620
16.6698	0.1886	44.6751	0.2340	72.6804	0.2442
17.3366	0.1945	45.3419	0.2355	73.3472	0.2533
18.0037	0.1819	46.0088	0.2249	74.0139	0.2549
18.6702	0.1842	46.6757	0.2363	74.6807	0.2474
19.3372	0.1969	47.3423	0.2324	75.3477	0.2588
20.0040	0.2024	48.0091	0.2422	76.0150	0.2517
20.6707	0.1973	48.6762	0.2501	76.6815	0.2584
21.3374	0.1988	49.3431	0.2418	77.3481	0.2568
22.0045	0.2036	50.0098	0.2383	78.0149	0.2533
22.6714	0.2012	50.6764	0.2399	78.6817	0.2624
23.3382	0.2075	51.3431	0.2430	79.3485	0.2411
24.0049	0.1945	52.0098	0.2418	80.0153	0.2596
24.6715	0.1981	52.6766	0.2371	80.6820	0.2572
25.3381	0.2016	53.3434	0.2466	81.3486	0.2545
26.0049	0.2067	54.0102	0.2347	82.0154	0.2572
26.6717	0.1969	54.6771	0.2462	82.6822	0.2466
27.3385	0.2099	55.3438	0.2545	83.3490	0.2829

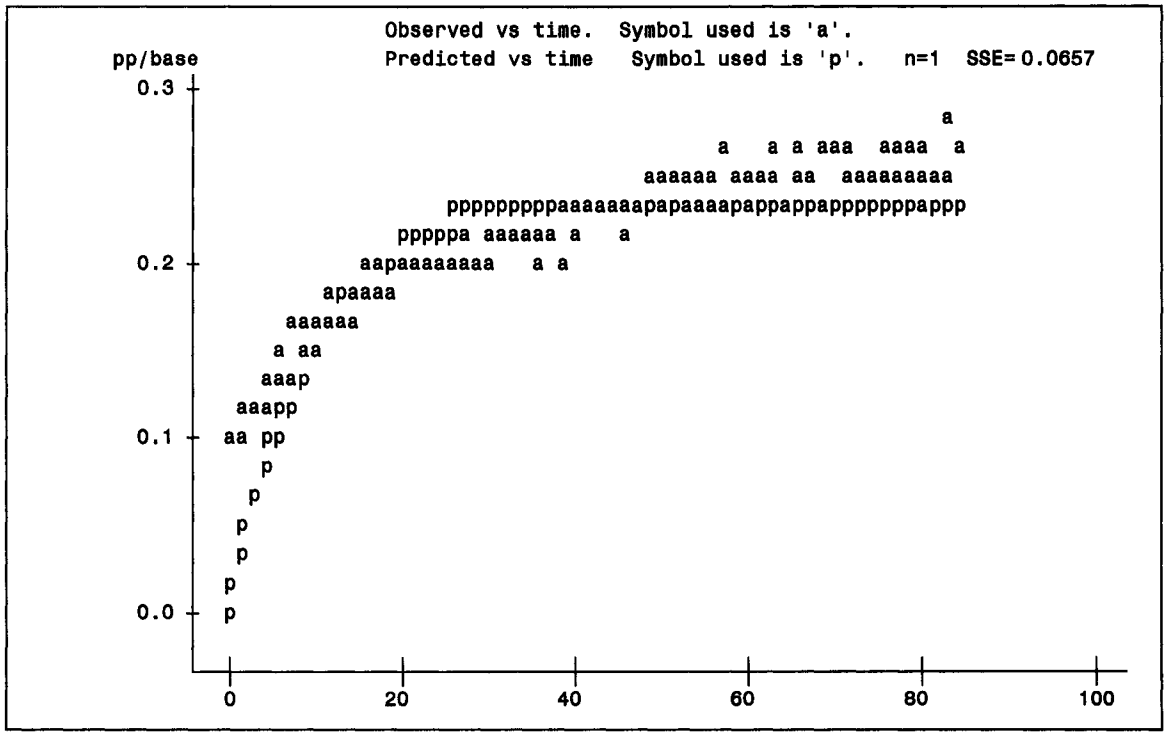

Figure 6.1 Plot of the observed PP/Base (for C_6H_{10}) and predicted value by fitting the data in Table 6.1 to Eq. (6.2).

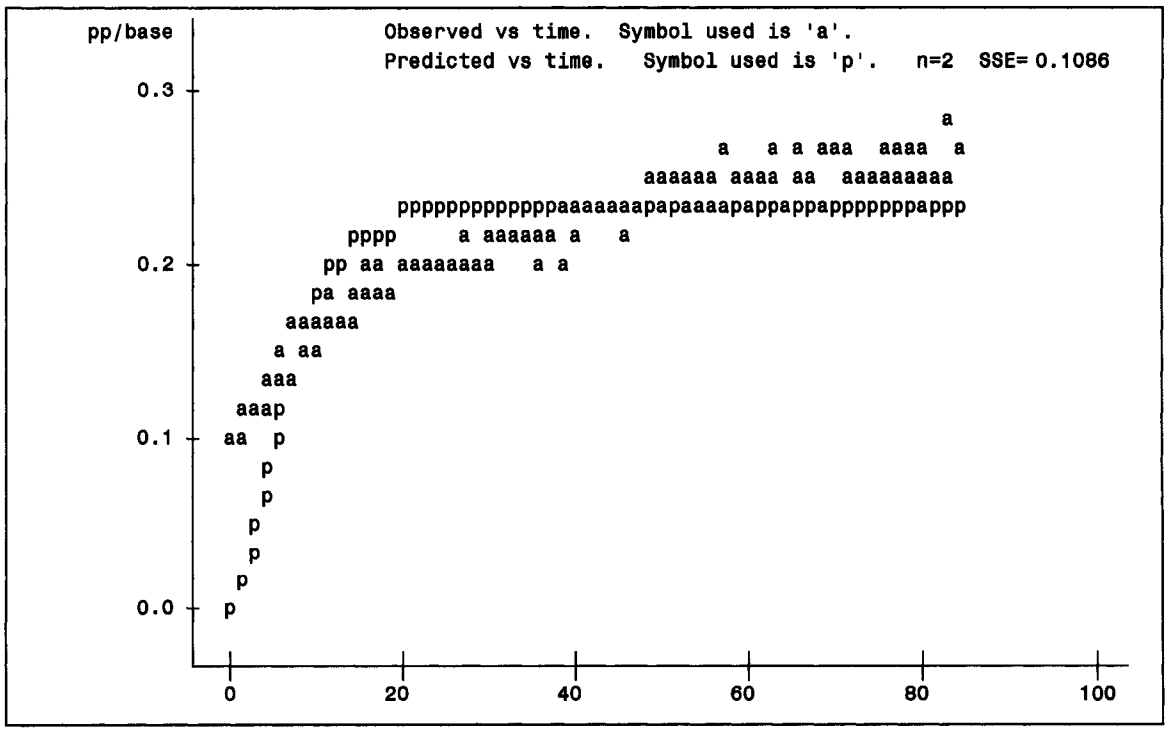

Figure 6.2 Plot of the observed PP/Base (for C_6H_{10}) and predicted value by fitting the data in Table 6.1 to Eq. (6.3).

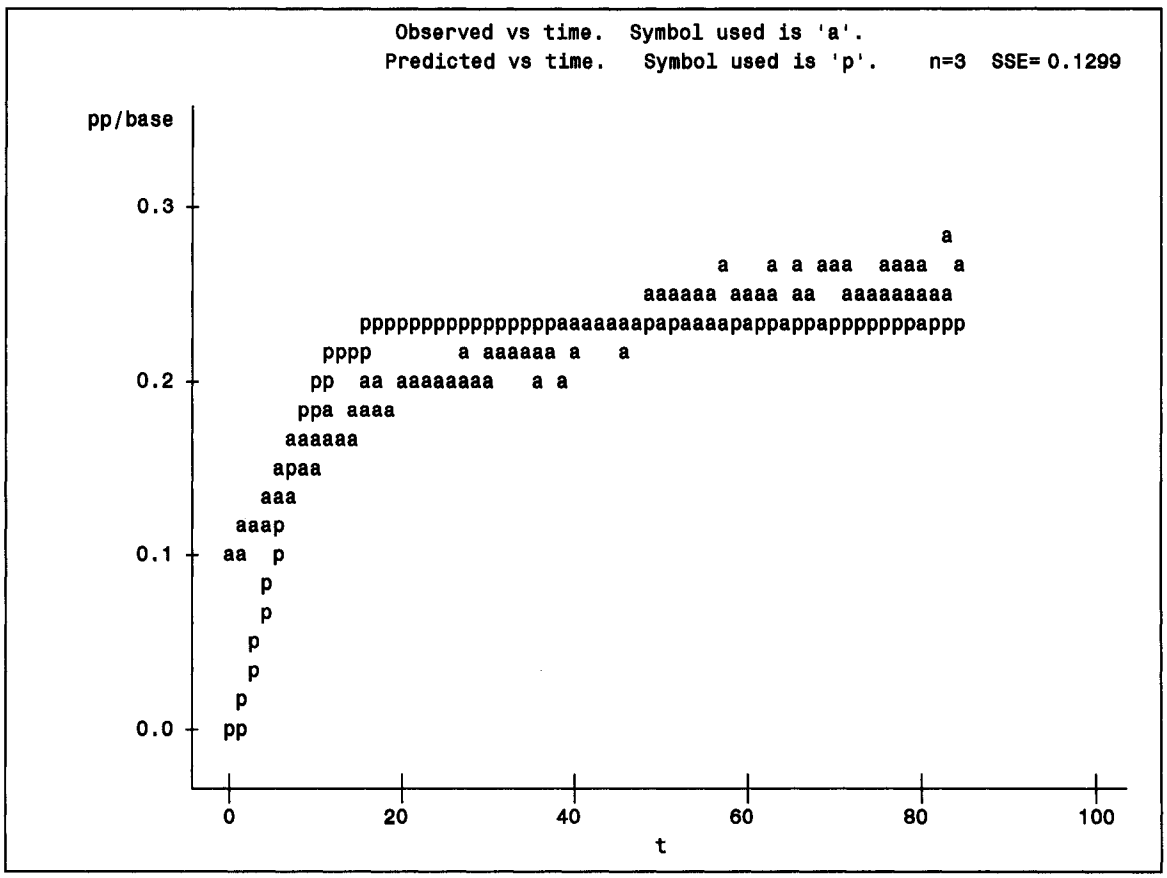

Figure 6.3 Plot of the observed PP/Base (for C_6H_{10}) and predicted value by fitting the data in Table 6.1 to Eq. (6.4).

The data in Table 6.2 were used for estimating λ, μ, and n for a cyclohexene hydrogenation experiment under the operating condition, temperature = 102.5°C, flow rate of hydrogen = 0.55 sccm, and flow rate of Argon = 0.55 sccm.

The SAS software was again used to fit the data in Table 6.2 to the model Eqs. (6.2)-(6.4) for different n values. Figures 6.4 to 6.6 show the observed values of PPc/Base for C_6H_{10} over time and the predicted values from Eqs. (6.2) to (6.4). It is clear that the predicted values give the best fit to the observed values when n = 1 (Fig. 6.4). The SSE (sum of squared errors) of 0.0162 is minimal for n = 1. The lack-of-fit was once more worse for higher n values. This result indicates that the microchannel behaves as one

compartment, implying that the flow is well mixed and is time homogeneous. The estimated values for λ and μ were 0.0454/min and 0.2935 / M•min, respectively.

Table 6.2: Cyclohexene hydrogenation experimental data, under the operating condition (temp = 102.5°C, flow rate of H_2 = 0.55 sccm, and flow rate of Ar = 0.55 sccm), used to estimate λ, μ, and n.

Time(min)	C_6H_{10}:p.p/base	Time(min)	C_6H_{10}:p.p/base	Time(min)	C_6H_{10}:p.p/base
0.0000	0.0626	21.3375	0.1296	42.6749	0.1393
0.6673	0.0404	22.0042	0.1242	43.3417	0.1417
1.3338	0.0699	22.6711	0.1368	44.0088	0.1320
2.0004	0.0903	23.3377	0.1276	44.6754	0.1378
2.6672	0.0859	24.0047	0.1271	45.3419	0.1364
3.3340	0.0903	24.6715	0.1378	46.0088	0.1252
4.0008	0.0815	25.3381	0.1504	46.6756	0.1533
4.6676	0.0985	26.0049	0.1368	47.3424	0.1475
5.3344	0.0951	26.6719	0.1378	48.0092	0.1349
6.0012	0.0815	27.3387	0.1334	48.6759	0.1291
6.6681	0.1019	28.0056	0.1368	49.3426	0.1364
7.3351	0.1136	28.6722	0.1402	50.0094	0.1451
8.0020	0.0888	29.3390	0.1271	50.6764	0.1301
8.6690	0.1126	30.0057	0.1388	51.3432	0.1339
9.3355	0.1145	30.6724	0.1252	52.0098	0.1446
10.0021	0.1068	31.3392	0.1354	52.6766	0.1344
10.6687	0.1087	32.0062	0.1368	53.3437	0.1281
11.3355	0.1136	32.6730	0.1305	54.0105	0.1475
12.0025	0.1140	33.3396	0.1470	54.6771	0.1655
12.6692	0.1242	34.0066	0.1325	55.3438	0.1422
13.3359	0.1228	34.6737	0.1301	56.0106	0.1334
14.0026	0.1296	35.3407	0.1334	56.6774	0.1301
14.6694	0.1121	36.0068	0.1398	57.3445	0.1529
15.3364	0.1315	36.6739	0.1354	58.0111	0.1373
16.0032	0.1432	37.3405	0.1291	58.6779	0.1461
16.6698	0.1368	38.0073	0.1373	59.3447	0.1373
17.3368	0.1368	38.6740	0.1325	60.0115	0.1432
18.0036	0.1368	39.3407	0.1548	60.6783	0.1393
18.6704	0.1271	40.0076	0.1291	61.3454	0.1364
19.3370	0.1237	40.6743	0.1490	62.0122	0.1373
20.0040	0.1063	41.3411	0.1436	62.6787	0.1378
20.6707	0.1179	42.0079	0.1339	63.3454	0.1291
				64.0122	0.1213

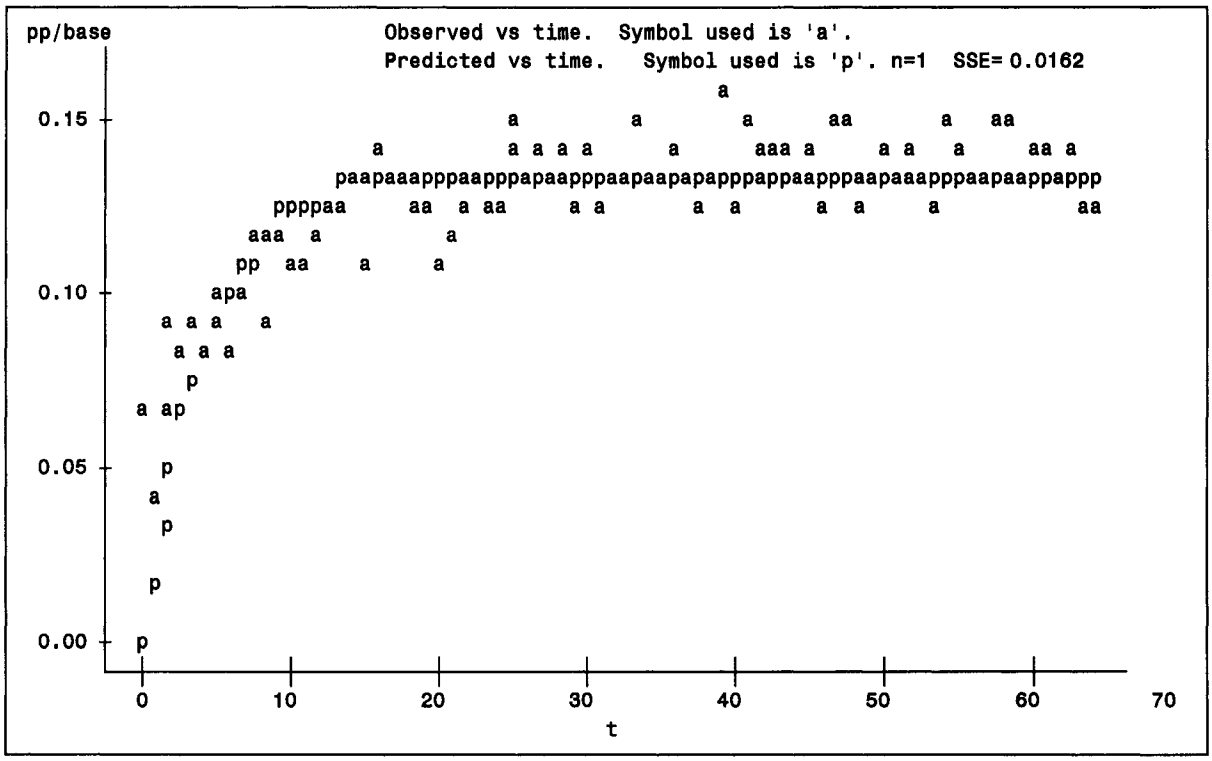

Figure 6.4 Plot of the observed PP/Base (for C_6H_{10}) and predicted value by fitting the data in Table 6.2 to Eq. (6.2).

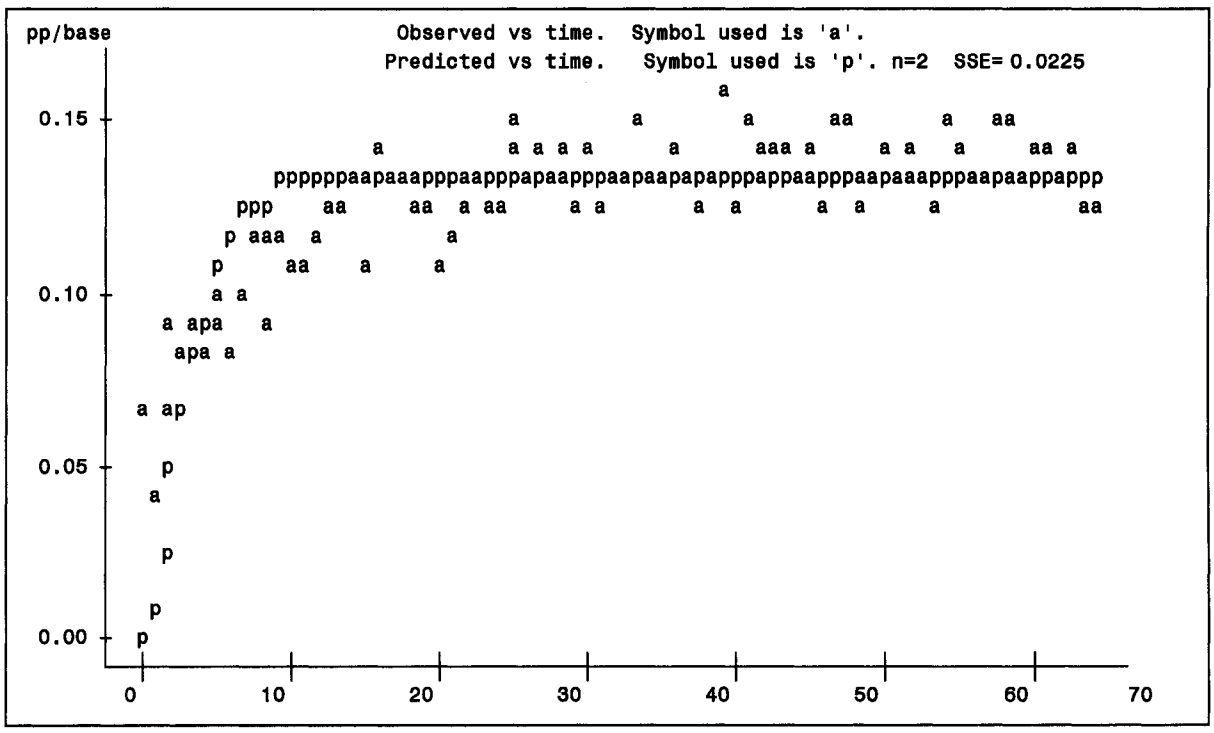

Figure 6.5 Plot of the observed PP/Base (for C_6H_{10}) and predicted value by fitting the data in Table 6.2 to Eq. (6.3).

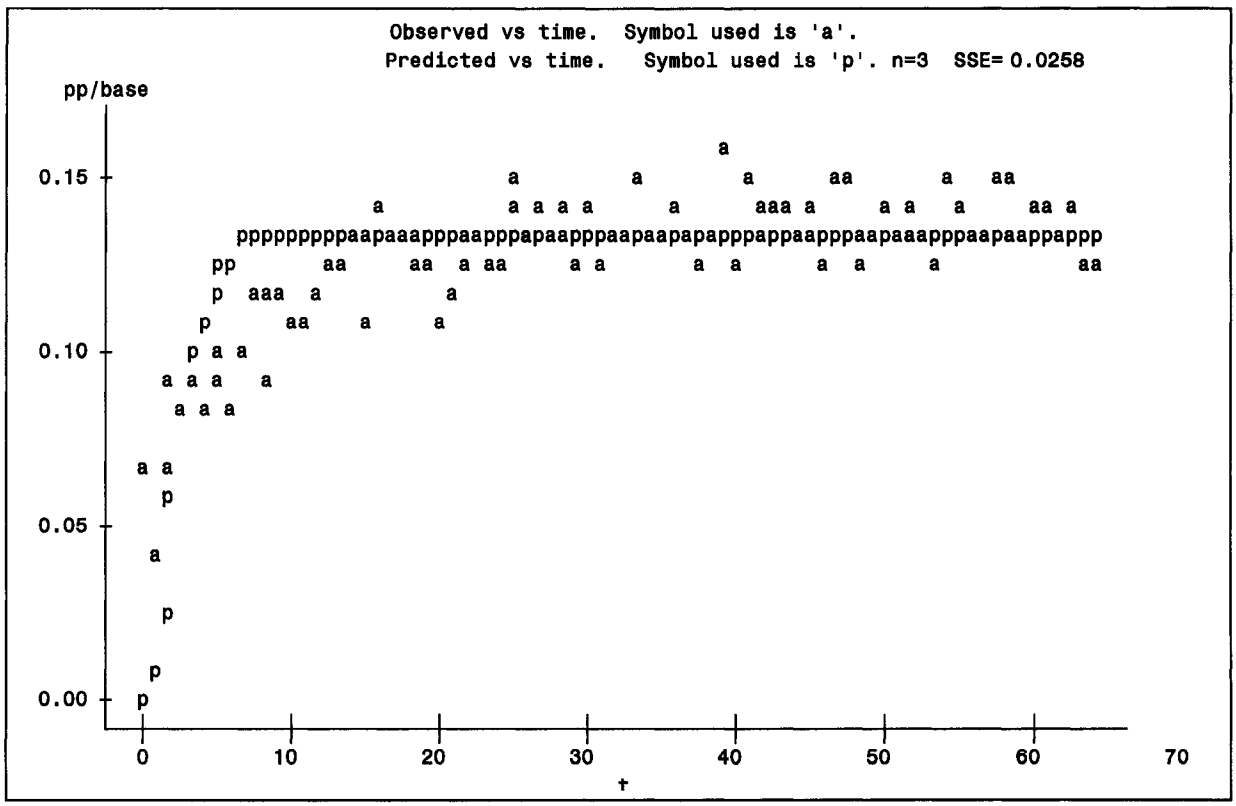

Figure 6.6 Plot of the observed PP/Base (for C_6H_{10}) and predicted value by fitting the data in Table 6.2 to Eq. (6.4).

The reaction rate μ is the rate at which C_6H_{10} reacts with hydrogen to give the cyclohexane by-product. It is known that this rate is a function of temperature, best described by the Arrhenius equation

$$\mu = k_0 e^{-\frac{E_a}{RT}} \quad . \tag{6.8}$$

This relationship allows us to estimate the activation energy (E_a) of the reaction from knowledge of estimates of μ at different temperatures. By solving the following system

$$\begin{aligned} \mu_1 &= k_0 e^{-\frac{E_a}{RT_1}} \\ \mu_2 &= k_0 e^{-\frac{E_a}{RT_2}}, \end{aligned} \tag{6.9}$$

the activation energy (E_a) of the cyclohexene hydrogenation reaction can be calculated as

$$E_a = \frac{\ln \frac{\mu_1}{\mu_2}}{(-\frac{1}{RT_1} + \frac{1}{RT_2})} \tag{6.10}$$

where $R = 8.314 J/mol \cdot K$ and temperature has K as the unit. Applying the estimated values $\mu_1 = 0.0793/M \cdot \min$, $\mu_2 = 0.2935/M \cdot \min$, T_1=56.37°C, and T_2=102.5°C to Eq. (6.10), the activation energy (E_a) of the cyclohexene hydrogenation reaction is calculated to be 29195.22 J/mol. Using this E_a value in Eq. (6.8), the k_0 value for the cyclohexene hydrogenation reaction is 3368.14.

6.1.2 Cyclohexene Dehydrogenation Reaction

In the case of the cyclohexene dehydrogenation experiment, the probability in Eq. (3.11) is the same as that for the cyclohexene hydrogenation experiment. It is the conversion rate of C_6H_{10} at time T for the case of an open flow involving C_6H_{10} and H_2. The probability as a function of time was compared to the observed C_6H_{10} conversion, from the cyclohexene dehydrogenation experiments, in order to estimate model parameters.

The data in Table 6.3 were used for estimating λ, μ, and n for a cyclohexene dehydrogenation experiment under the operating condition, temperature = 186.67°C, flow rate of hydrogen = 0.28 sccm, and flow rate of Argon = 0.82 sccm.

Table 6.3: Cyclohexene dehydrogenation experimental data, under the operating condition (temp = 186.67°C, flow rate of H_2 = 0.28 sccm, and flow rate of Ar = 0.82 sccm), used to estimate λ, μ, and n.

Time(min)	p.pc6h10/base	Time(min)	p.pc6h10/base	Time(min)	p.pc6h10/base
0.0000	0.0130	26.0044	0.0446	52.0095	0.0442
0.6667	0.0152	26.6710	0.0519	52.6764	0.0384
1.3335	0.0130	27.3380	0.0340	53.3432	0.0464
1.9997	0.0145	28.0046	0.0497	54.0102	0.0464
2.6667	0.0219	28.6714	0.0439	54.6764	0.0584
3.3339	0.0161	29.3385	0.0504	55.3432	0.0533
4.0016	0.0238	30.0055	0.0464	56.0100	0.0453
4.6675	0.0256	30.6721	0.0475	56.6770	0.0544
5.3343	0.0166	31.3391	0.0432	57.3440	0.0508
6.0011	0.0275	32.0058	0.0417	58.0114	0.0504
6.6682	0.0283	32.6723	0.0410	58.6770	0.0555
7.3357	0.0319	33.3391	0.0609	59.3438	0.0464
8.0011	0.0176	34.0059	0.0457	60.0108	0.0395
8.6680	0.0343	34.6727	0.0435	60.6777	0.0508
9.3349	0.0220	35.3397	0.0482	61.3447	0.0471
10.0015	0.0276	36.0066	0.0453	62.0115	0.0468
10.6695	0.0347	36.6729	0.0464	62.6785	0.0406
11.3351	0.0281	37.3404	0.0529	63.3447	0.0515
12.0022	0.0388	38.0082	0.0471	64.0119	0.0584
12.6684	0.0360	38.6736	0.0446	64.6781	0.0537
13.3353	0.0304	39.3402	0.0511	65.3449	0.0493
14.0024	0.0326	40.0069	0.0504	66.0117	0.0435
14.6689	0.0403	40.6736	0.0424	66.6792	0.0421
15.3359	0.0406	41.3408	0.0479	67.3462	0.0569
16.0030	0.0435	42.0076	0.0573	68.0133	0.0519
16.6693	0.0370	42.6745	0.0410	68.6792	0.0558
17.3371	0.0417	43.3415	0.0457	69.3458	0.0558
18.0027	0.0345	44.0084	0.0544	70.0130	0.0490
18.6697	0.0428	44.6744	0.0475	70.6800	0.0504
19.3366	0.0515	45.3412	0.0421	71.3474	0.0526
20.0033	0.0381	46.0080	0.0508	72.0136	0.0475
20.6701	0.0522	46.6751	0.0606	72.6800	0.0511
21.3367	0.0334	47.3421	0.0584	73.3466	0.0504
22.0039	0.0388	48.0090	0.0573	74.0136	0.0363
22.6708	0.0442	48.6751	0.0555	74.6811	0.0439
23.3382	0.0439	49.3428	0.0617	75.3468	0.0551
24.0040	0.0428	50.0102	0.0519	76.0136	0.0617
24.6711	0.0580	50.6757	0.0439	76.6807	0.0457
25.3376	0.0526	51.3429	0.0457	77.3473	0.0573

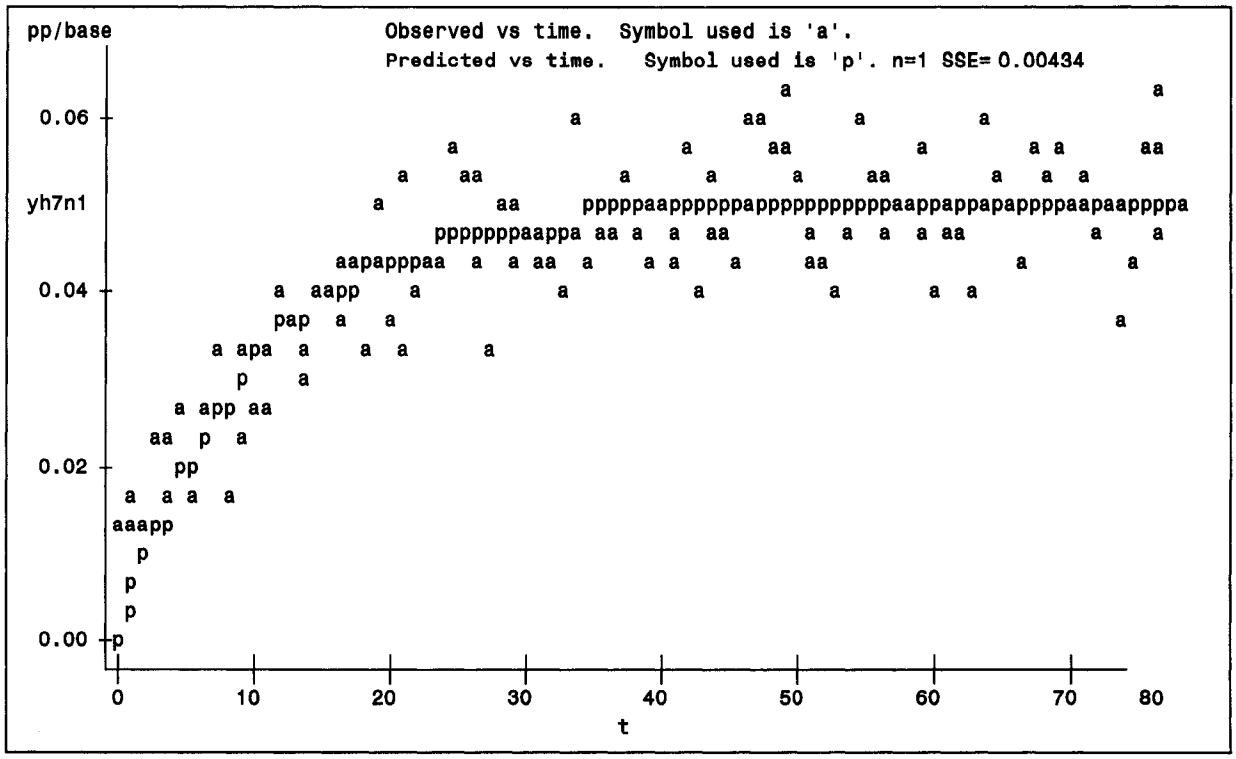

Figure 6.7 Plot of the observed PP/Base (for C_6H_{10}) and predicted value by fitting the data in Table 6.3 to Eq. (6.2).

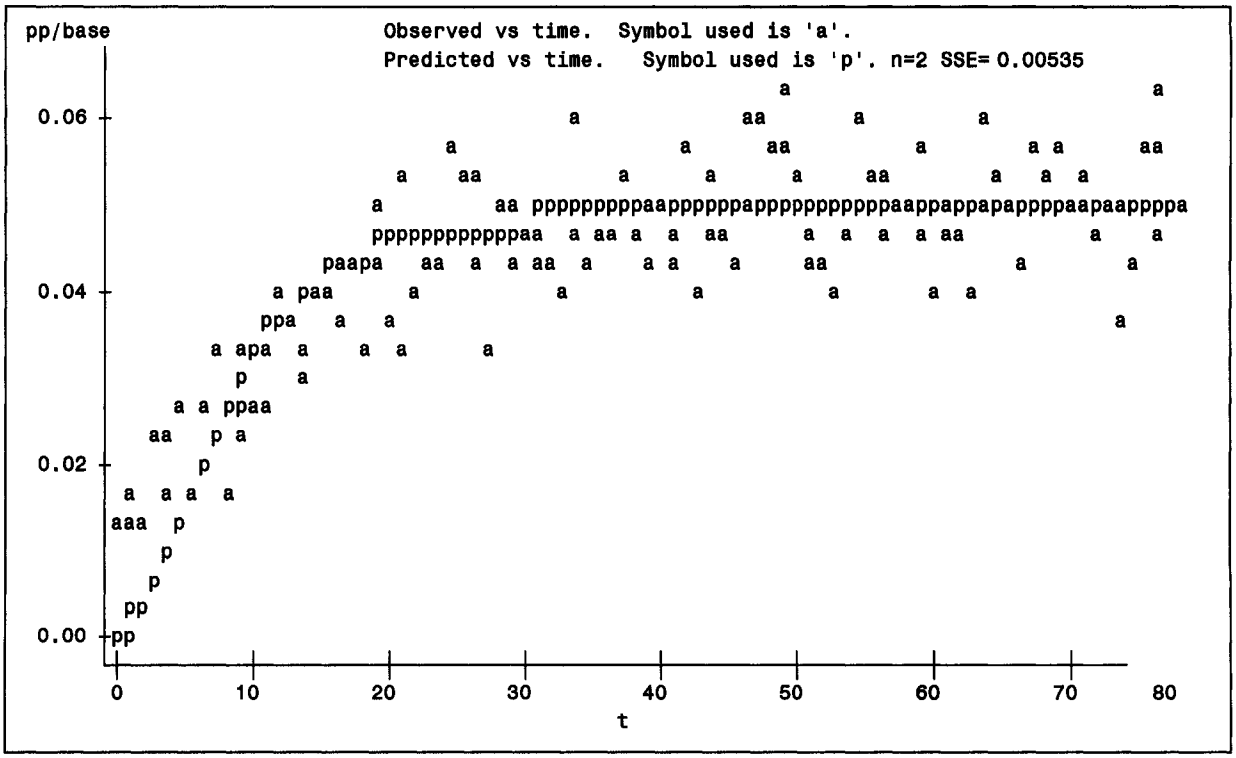

Figure 6.8 Plot of the observed PP/Base (for C_6H_{10}) and predicted value by fitting the data in Table 6.3 to Eq. (6.3).

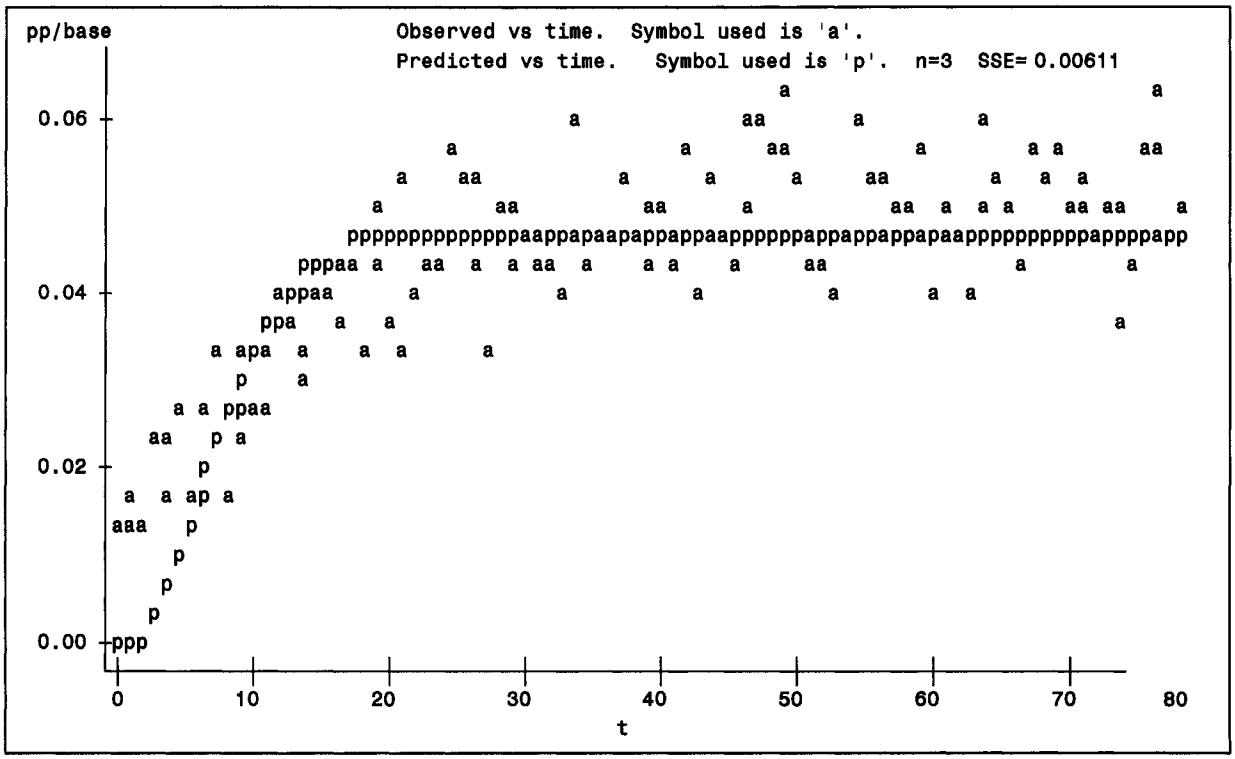

Figure 6.9 Plot of the observed PP/Base (for C_6H_{10}) and predicted value by fitting the data in Table 6.3 to Eq. (6.4).

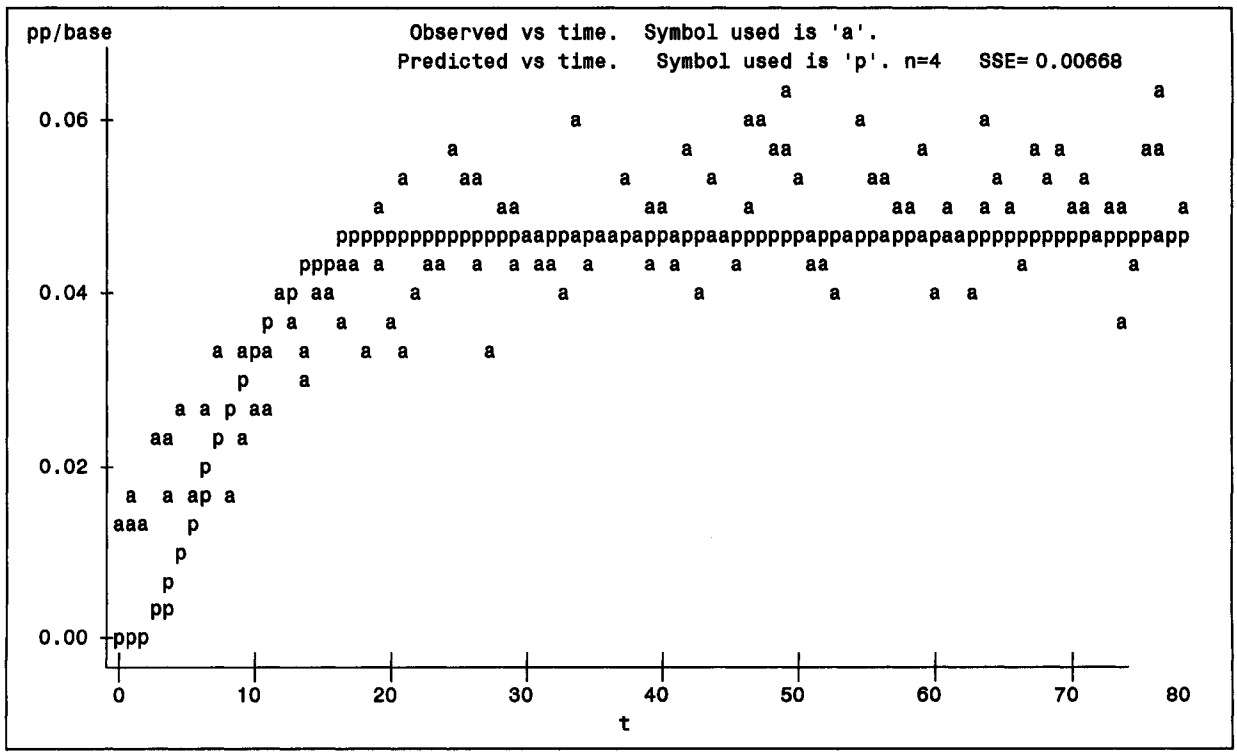

Figure 6.10 Plot of the observed PP/Base (for C_6H_{10}) and predicted value by fitting the data in Table 6.3 to Eq. (6.5).

The SAS software was used to fit the data in Table 6.3 to the model Eqs. (6.2)-(6.4) for different n values. Figures 6.7 to 6.10 show the observed values of PP/Base for C_6H_{10} over time and the predicted values from Eqs. (6.2) - (6.5). It is clear that the predicted values give the best fit to the observed values when n = 1 (Fig. 6.7). The SSE (sum of squared errors) of 0.00434 is minimal for n = 1. The lack-of-fit was even worse for higher n values. This result indicates that the microchannel behaves as one compartment, implying that the flow is well mixed and is time homogeneous, in which case, each molecule in the reactor has the same exit intensity (or rate) λ. The estimated values for λ and μ were 0.00506 /min and 0.0966/min, respectively.

The data in Table 6.4 were used for estimating λ, μ and n for a cyclohexene dehydrogenation experiment under the operating condition, temperature = 353.33°C, flow rate of hydrogen = 0.28 sccm, and flow rate of Argon = 0.82 sccm.

The SAS software was then used to fit the data in Table 6.4 to the model Eqs. (6.2)-(6.4) for different n values. Figures 6.11 to 6.13 show the observed values of PP/Base for C_6H_{10} over time and the predicted values from Eqs. (6.2) to (6.4). It is clear that the predicted values give the best fit to the observed values when n = 1 (Fig. 6.11). The SSE (sum of squared errors) of 0.00539 is minimal for n = 1. The lack-of-fit was worse for higher n values. This result indicates that the microchannel behaves as one compartment, implying that the flow is well mixed and is time homogeneous, in which case each molecule in the reactor has the same exit intensity (or rate) λ. The estimated values for λ and μ were 0.00569 /min and 0.0996/min, respectively.

Table 6.4: Cyclohexene dehydrogenation experimental data, under the operating condition (temp = 353.33°C, flow rate of H_2 = 0.28 sccm, and flow rate of Ar = 0.82 sccm), used to estimate λ, μ, and n.

Time(min)	C_6H_{10}:p.p/base	Time(min)	C_6H_{10}:p.p/base	Time(min)	C_6H_{10}:p.p/base
0.0000	0.0156	23.3384	0.0477	46.6755	0.0592
0.6668	0.0225	24.0047	0.0432	47.3426	0.0505
1.3337	0.0323	24.6722	0.0509	48.0094	0.0592
2.0005	0.0284	25.3391	0.0550	48.6770	0.0573
2.6673	0.0264	26.0052	0.0566	49.3427	0.0566
3.3341	0.0279	26.6723	0.0518	50.0095	0.0576
4.0013	0.0243	27.3393	0.0397	50.6762	0.0614
4.6677	0.0267	28.0063	0.0502	51.3432	0.0422
5.3344	0.0276	28.6722	0.0473	52.0100	0.0528
6.0013	0.0296	29.3391	0.0438	52.6768	0.0477
6.6681	0.0293	30.0058	0.0553	53.3441	0.0454
7.3350	0.0333	30.6729	0.0473	54.0110	0.0637
8.0026	0.0365	31.3399	0.0378	54.6772	0.0486
8.6688	0.0352	32.0067	0.0537	55.3440	0.0646
9.3365	0.0426	32.6736	0.0457	56.0114	0.0592
10.0020	0.0249	33.3406	0.0438	56.6782	0.0566
10.6690	0.0339	34.0067	0.0528	57.3448	0.0595
11.3355	0.0400	34.6734	0.0515	58.0111	0.0573
12.0023	0.0336	35.3402	0.0515	58.6777	0.0496
12.6695	0.0429	36.0073	0.0528	59.3457	0.0627
13.3367	0.0358	36.6746	0.0454	60.0115	0.0525
14.0039	0.0346	37.3406	0.0553	60.6783	0.0518
14.6696	0.0416	38.0080	0.0470	61.3453	0.0515
15.3365	0.0330	38.6745	0.0585	62.0122	0.0521
16.0033	0.0336	39.3414	0.0493	62.6791	0.0569
16.6705	0.0384	40.0082	0.0566	63.3463	0.0537
17.3368	0.0309	40.6755	0.0563	64.0126	0.0560
18.0036	0.0509	41.3412	0.0630	64.6789	0.0585
18.6704	0.0461	42.0080	0.0512	65.3457	0.0534
19.3373	0.0438	42.6747	0.0483	66.0124	0.0710
20.0039	0.0448	43.3420	0.0461	66.6792	0.0531
20.6707	0.0585	44.0085	0.0582	67.3460	0.0573
21.3377	0.0422	44.6754	0.0547	68.0135	0.0592
22.0048	0.0413	45.3427	0.0528	68.6804	0.0576
22.6713	0.0515	46.0097	0.0499	69.3471	0.0617

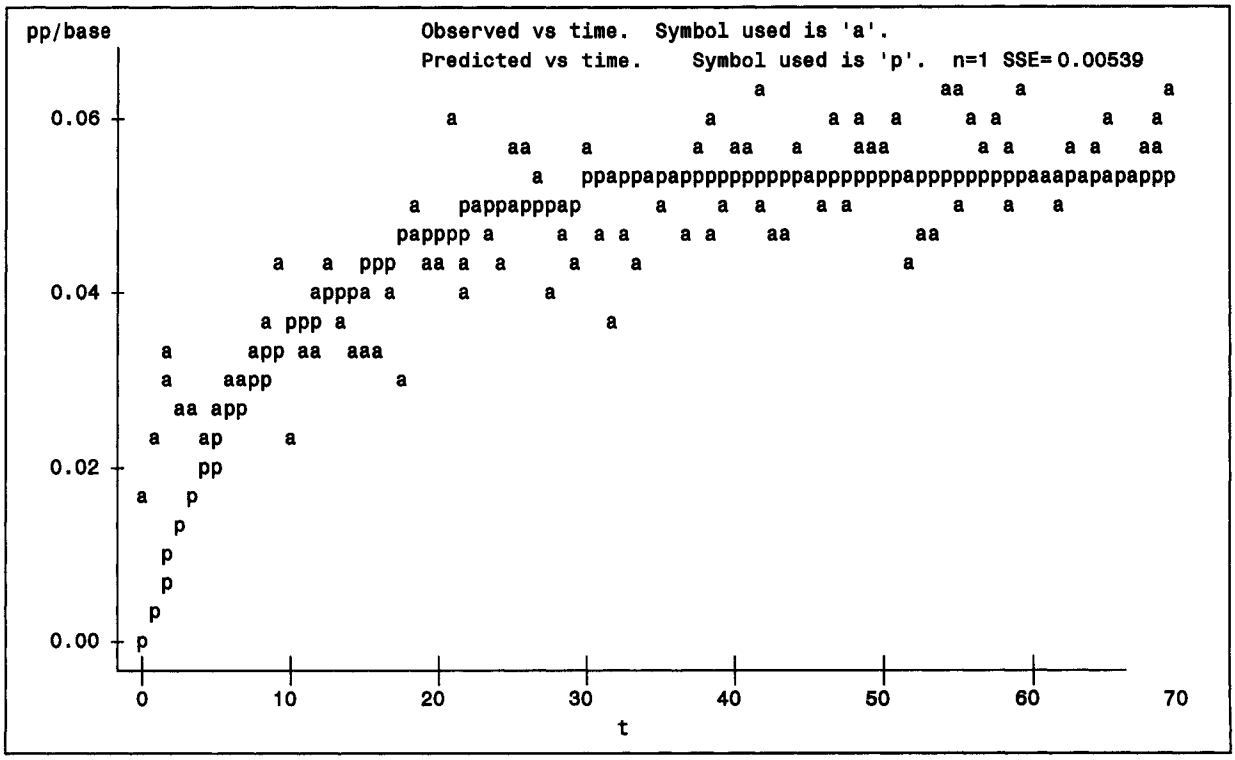

Figure 6.11 Plot of the observed PP/Base (for C_6H_{10}) and predicted value by fitting the data in Table 6.4 to Eq. (6.2).

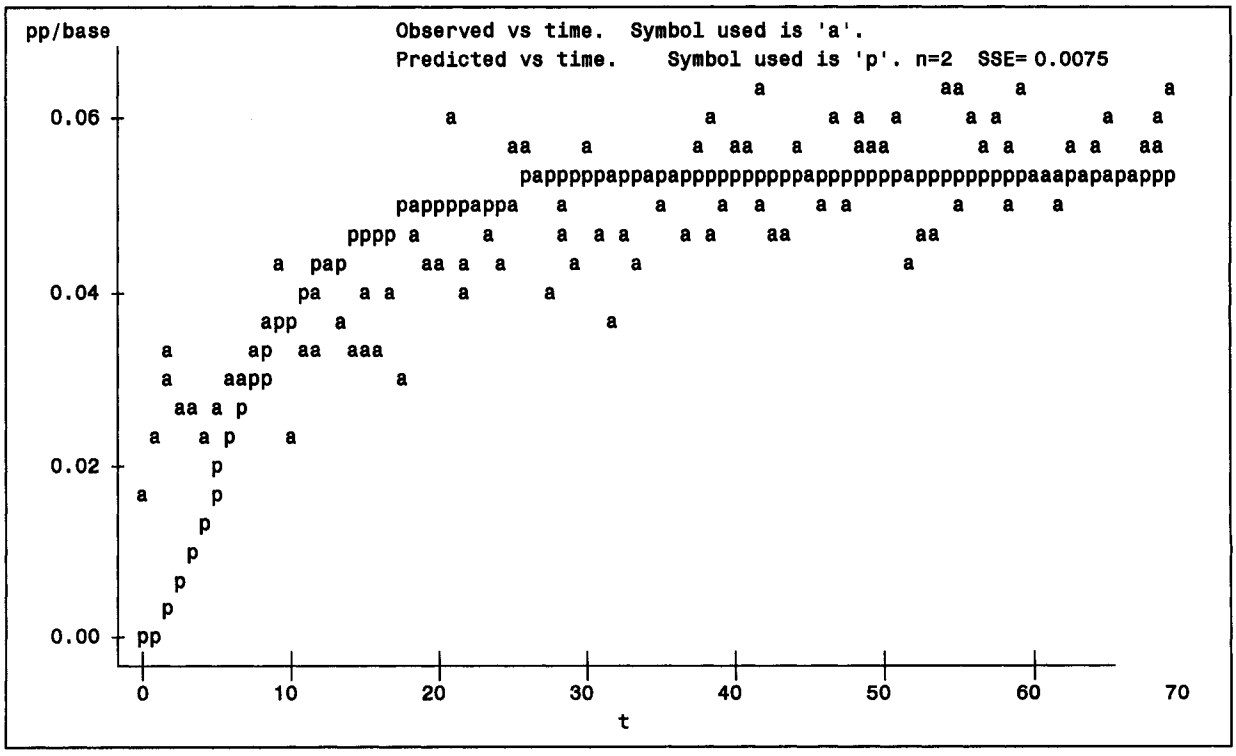

Figure 6.12 Plot of the observed PP/Base (for C_6H_{10}) and predicted value by fitting the data in Table 6.4 to Eq. (6.3).

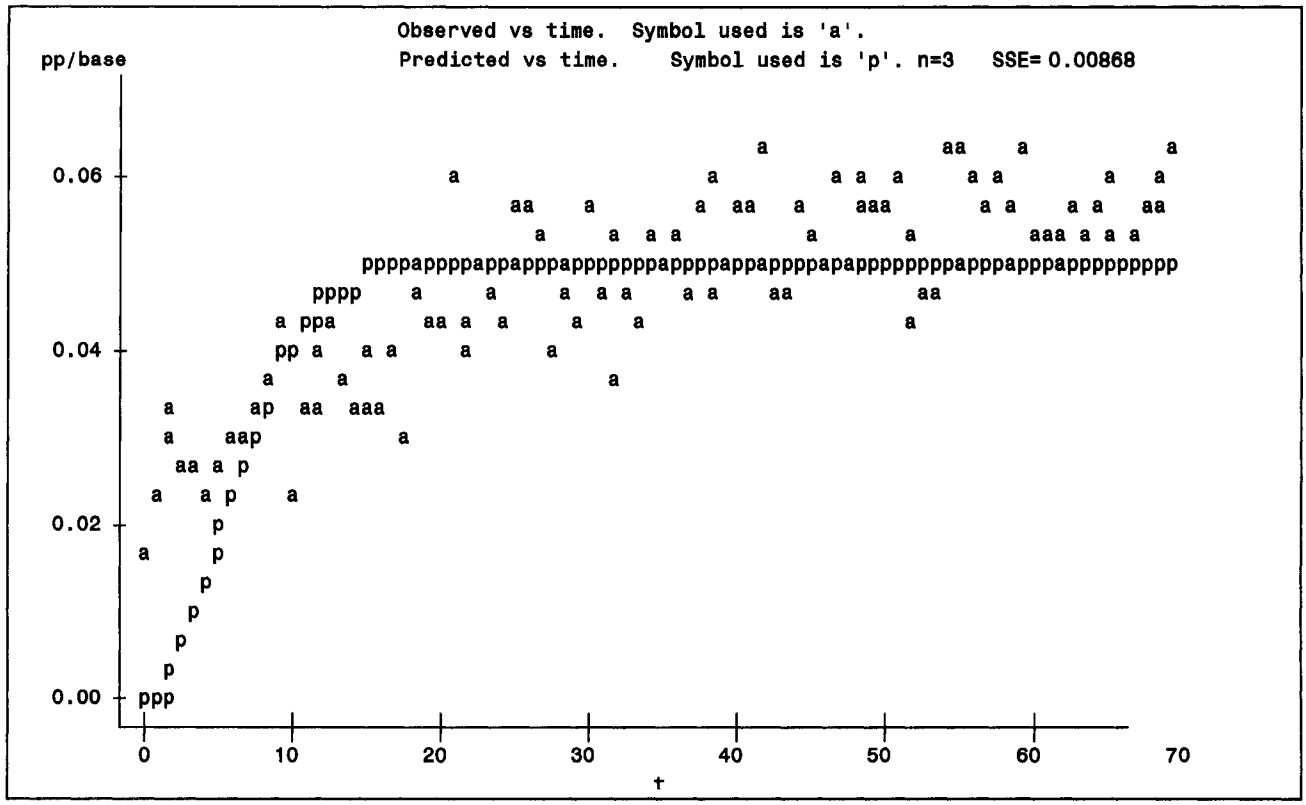

Figure 6.13 Plot of the observed PP/Base (for C_6H_{10}) and predicted value by fitting the data in Table 6.4 to Eq. (6.4).

The reaction rate μ for cyclohexene dehydrogenation reaction is the rate at which C_6h_{10} reacts to give the benzene by-product. Appling the estimated value $\mu_1 = 0.0966/\min$, $\mu_2 = 0.0996/\min$, T_1=186.67°C, and T_2=353.33°C to Eq. (6.10), the activation energy (E_a) of the cyclohexene dehydrogenation reaction was calculated to be $439.5\,J/mol$. Using this E_a value in Eq. (6.8), the k_0 value for the cyclohexene dehydrogenation reaction is found to be 0.108.

6.1.3 Syn-Gas Experiment

In the case of the syn-gas experiment, the probability in Eq. (6.1) gives the conversion rate of CO at time T for the case of an open flow involving CO and H_2. The

probability as a function of time was compared to observed *CO* conversion from syn-gas experiments in order to estimate model parameters. From these parameters, we estimated the reaction rate (and hence the activation energy of the reaction) and characterized the flow behavior from the residence time distribution.

The data in Table 6.5 were used for estimating λ, μ and n for a Syn-gas experiment under the operating condition, temperature = 250°C, total flow rate = 0.8 sccm, and H_2:*CO* ratio = 3:1 (where the flow rate of H2 is 0.6 sccm, and the flow rate of *CO* is 0.2 sccm).

Table 6.5: Syn-gas experimental data used to estimate λ, μ and n.

time(min)	CO:PP/Base	time(min)	CO:PP/Base	time(min)	PPCO/BaseCO
0.0000	0.0363	14.6667	0.3579	29.3333	0.4888
0.6667	0.0531	15.3333	0.3351	30.0000	0.5213
1.3333	0.0436	16.0000	0.3819	30.6667	0.4912
2.0000	0.0680	16.6667	0.2955	31.3333	0.4732
2.6667	0.1345	17.3333	0.2798	32.0000	0.4984
3.3333	0.1125	18.0000	0.3555	32.6667	0.4564
4.0000	0.1050	18.6667	0.3639	33.3333	0.4432
4.6667	0.1297	19.3333	0.3663	34.0000	0.5201
5.3333	0.1417	20.0000	0.3423	34.6667	0.5068
6.0000	0.1249	20.6667	0.3723	35.3333	0.4828
6.6667	0.1597	21.3333	0.4192	36.0000	0.4396
7.3333	0.2222	22.0000	0.4348	36.6667	0.5537
8.0000	0.2270	22.6667	0.4396	37.3333	0.4864
8.6667	0.1850	23.3333	0.4192	38.0000	0.4936
9.3333	0.1525	24.0000	0.4108	38.6667	0.5141
10.0000	0.2570	24.6667	0.4456	39.3333	0.5080
10.6667	0.2270	25.3333	0.4180	40.0000	0.5777
11.3333	0.2991	26.0000	0.4108	40.6667	0.4816
12.0000	0.2402	26.6667	0.4204	41.3333	0.4492
12.6667	0.2606	27.3333	0.4768	42.0000	0.5333
13.3333	0.2750	28.0000	0.4432	42.6667	0.4912
14.0000	0.2883	28.6667	0.5261	43.3333	0.5297

The SAS software was used to fit the data in Table 6.5 to the model Eqs. (6.2)-(6.7) for different n values. Figures 6.14 to 6.19 show the observed values of PP/Base for

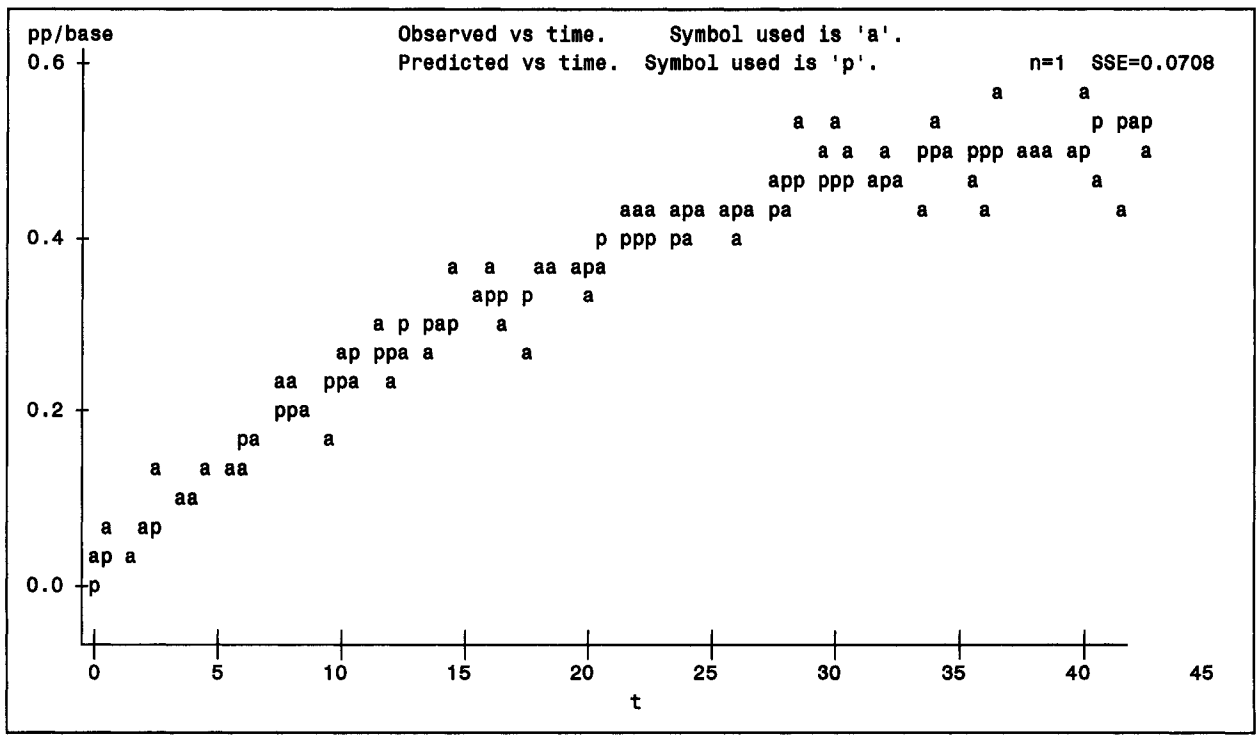

Figure 6.14 Plot of the observed PP/Base (for *CO*) and predicted value by fitting the data in Table 6.5 to Eq. (6.2).

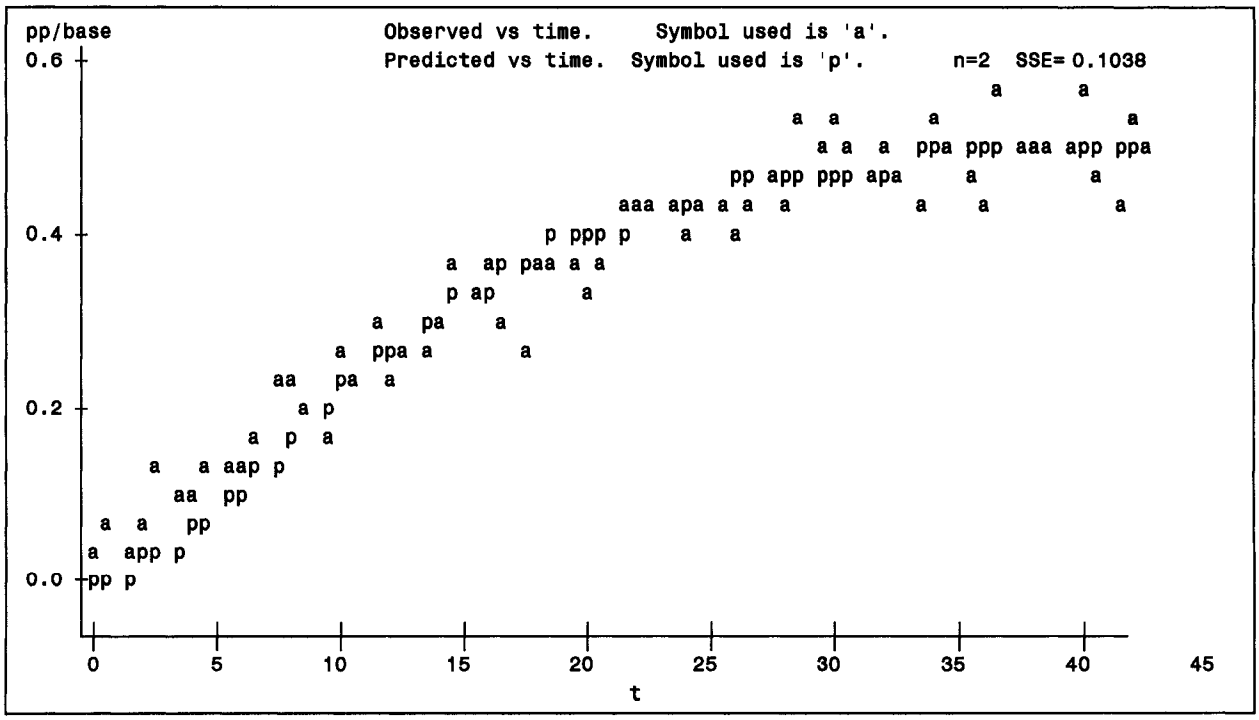

Figure 6.15 Plot of the observed PP/Base (for *CO*) and predicted value by fitting the data in Table 6.5 to Eq. (6.3).

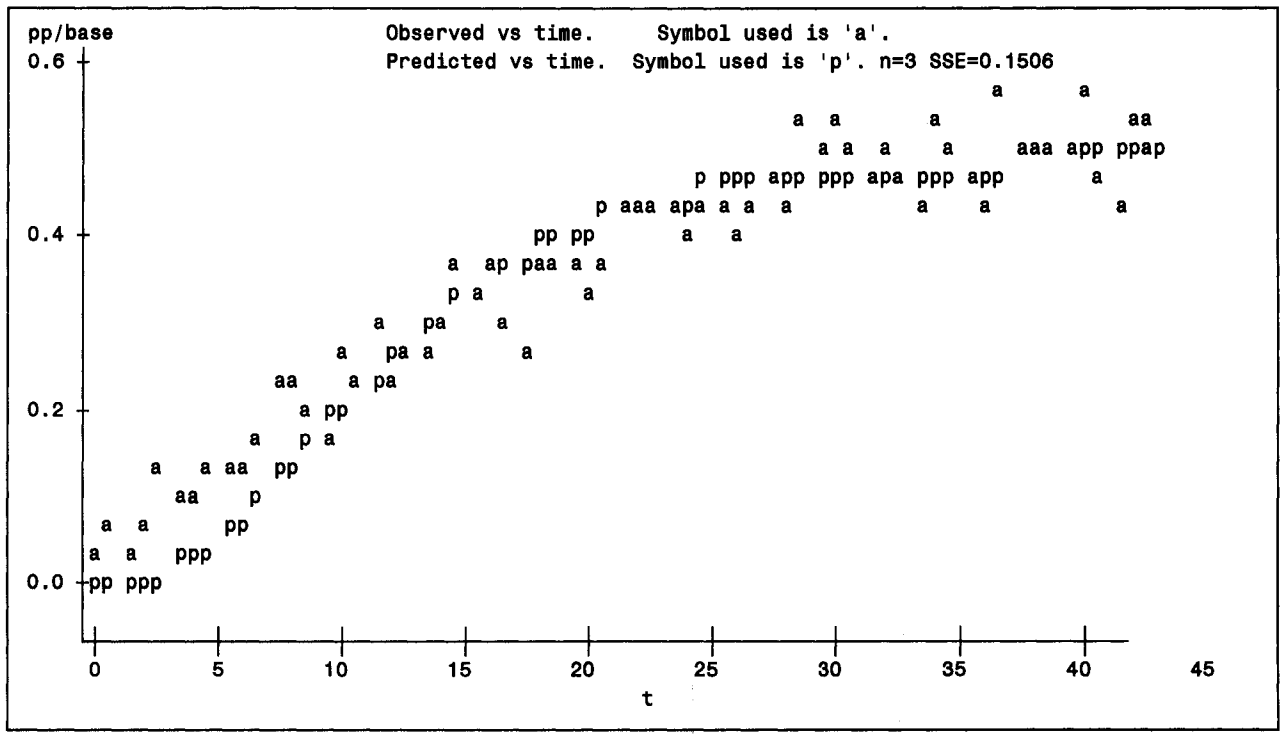

Figure 6.16 Plot of the observed PP/Base (for *CO*) and predicted value by fitting the data in Table 6.5 to Eq. (6.4).

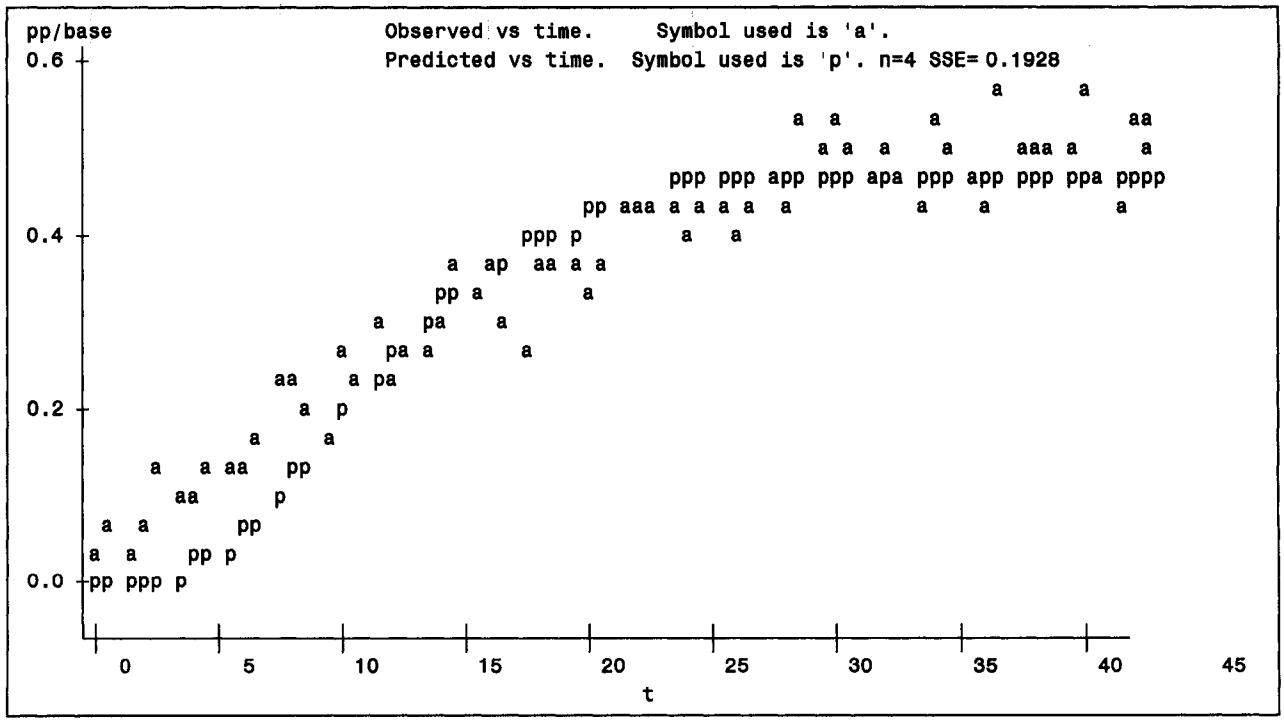

Figure 6.17 Plot of the observed PP/Base (for *CO*) and predicted value by fitting the data in Table 6.5 to Eq. (6.5).

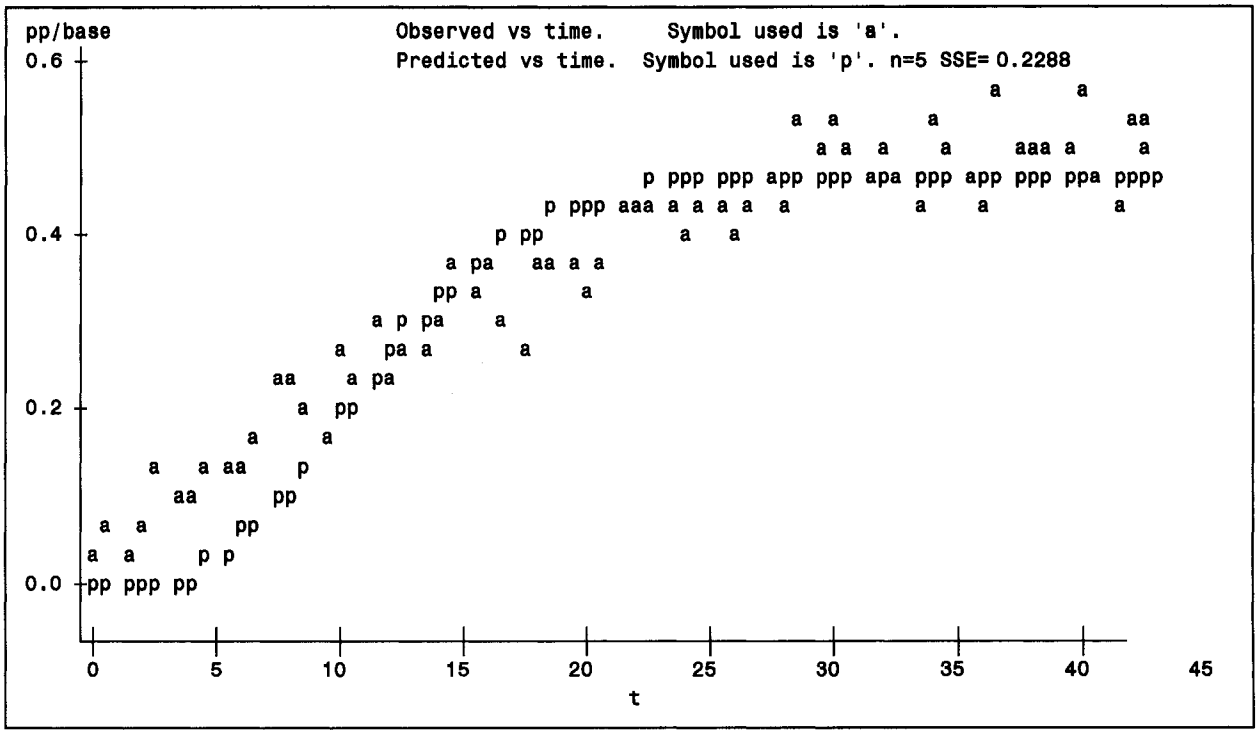

Figure 6.18 Plot of the observed PP/Base (for *CO*) and predicted value by fitting the data in Table 6.5 to Eq. (6.6).

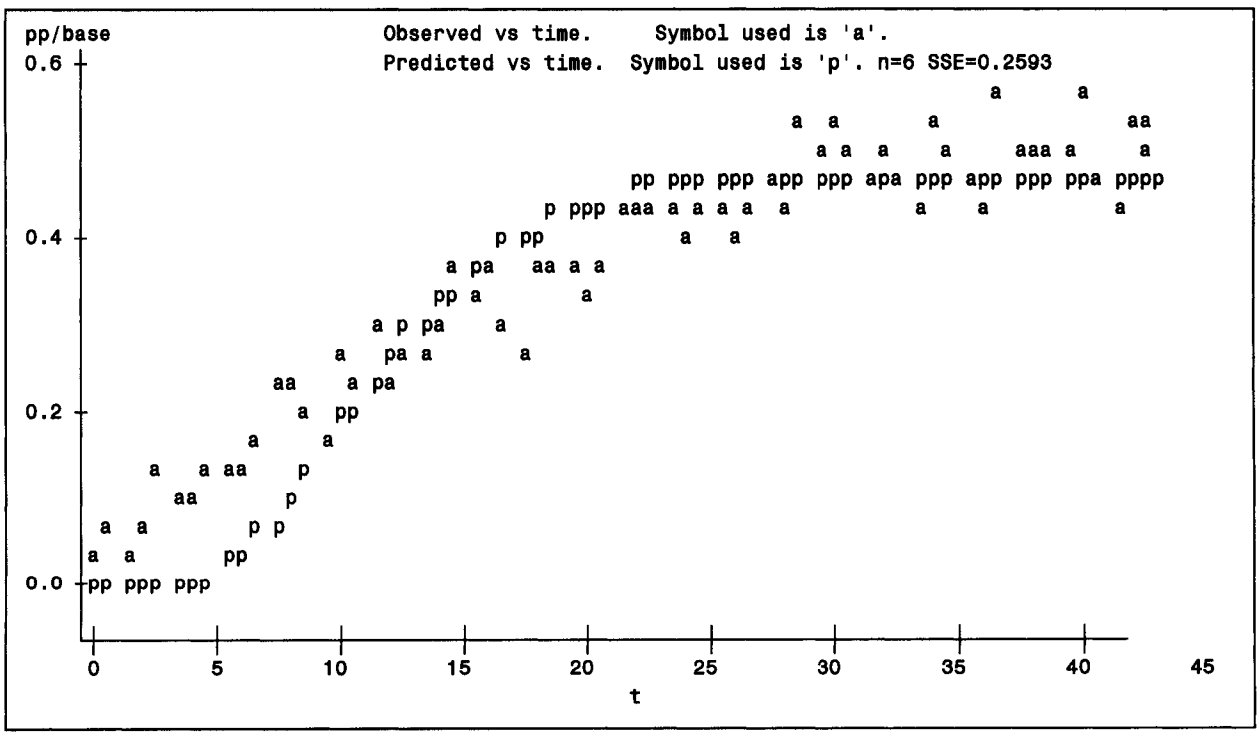

Figure 6.19 Plot of the observed PP/Base (for *CO*) and predicted value by fitting the data in Table 6.5 to Eq. (6.7).

CO over time and the predicted values from Eqs. (6.2) to (6.7). It is clear that the predicted values give the best fit to the observed values when n = 1 (Fig. 6.14). The SSE (sum of squared errors) of 0.0708 is minimal for n = 1. The lack-of-fit was worse for higher n values, not presented here. This result indicates again that the microchannel behaves as one compartment, implying that the flow is well mixed and is time homogeneous, in which case each molecule in the reactor has the same exit intensity (or rate) λ. The estimated values for λ and μ were 0.0305/min and 0.0213/min, respectively.

The above analysis demonstrates how the model may be used to characterize the flow and kinetic of the chemical reaction. The inference obtained from such a model is of course influenced by experimental conditions. In this case, for instance, one is not certain that the microreactor flow is well mixed, as represented by one compartment, without further experimentation. This is so since in the experimental setup, the volume of the space between the exit to the microreactor and the mass spectrometer reading was large as compared to that of the microreactor. As such, in fitting the model to the experimental data (measured by the mass spectrometer), one may be characterizing the flow in the exit stream (between microreactor and mass spectrometer) and not in the microreactor. Further data should be gathered at the exit to the microreactor in order to clarify this problem.

6.2 Stochastic Modeling: A Markov Chain Approach

6.2.1 Model Formulation

In this section, we extend the modeling approaches of Too et al. [Too 1983] and

Chou et al. [Chou 1988] to model cyclohexene hydrogenation and dehydrogenation reactions and the Fischer-Tropsch (F-T) synthesis reaction by considering the microreactor as composed of two phases, the solid phase and the flow or gas phase.

For the cyclohexene hydrogenation, the reaction scheme is

$$A_1 + A_2 \xrightarrow{k_1} A_3 \quad . \tag{6.11}$$

For the cyclohexene dehydrogenation, the reaction scheme is

$$A_1 \xrightarrow{k_2} A_4 + 2A_2 \quad . \tag{6.12}$$

Here, A_1, A_2, A_3, and A_4 represent cyclohexene (C_6H_{10}), hydrogen (H_2), cyclohexane (C_6H_{12}), and benzene (C_6H_6) on the catalyst (solid phase), respectively. Let A_1^*, A_2^*, A_3^*, and A_4^* represent cyclohexene (C_6H_{10}), hydrogen (H_2), cyclohexane (C_6H_{12}), and benzene (C_6H_6) in the gas phase, respectively. k_1 is the rate constant for the cyclohexene hydrogenation reaction, and k_2 is the rate constant for the cyclohexene dehydrogenation reaction. Let $n_i(m)\,(i=1,2,3,4)$ be the number of molecules of type A_i $(i=1,2,3,4)$ in the microreactor at time *m*. The stochastic model of these reactions is then completely defined under the following assumptions.

(1) The probability that a molecule in state A_1 at time *m* will be in state A_3 caused by the first reaction at time (*m*+1) is

$$p_{13}(m+1) = \varepsilon_1 n_2(m) \,, \tag{6.13}$$

where

$$\varepsilon_1 = k_1 \Delta t \tag{6.14}$$

(2) The probability that a molecule in state A_1 at time m will be in state A_2 and state A_4 caused by the second reaction at time (m+1) is

$$p_{12}(m+1)=\frac{2}{3}\varepsilon_2;\quad p_{14}(m+1)=\frac{1}{3}\varepsilon_2\,, \tag{6.15}$$

where

$$\varepsilon_2 = k_2\Delta t \tag{6.16}$$

(3) Any molecule of type $A_i(i=1,2,3,4)$ cannot exit from the microreactor unless it transfers to the gas phase $A_i^*(i=1,2,3,4)$. Thus, the probability that a molecule in state $A_i(i=1,2,3,4)$ at time m will be in the absorbing state D at time (m+1) is

$$p_{id}(m+1)=0 \tag{6.17}$$

(4) The probability that a molecule of type $A_i^*(i=1,2,3,4)$ in the microreactor at time m, will exit from it at time(m+1) is

$$p_{i^*d}(m+1)=\mu \qquad i=1,2,3,4 \tag{6.18}$$

(5) The probability that a molecule in state A_2 at time m will be in state A_3 caused by the first reaction at time (m+1) is

$$p_{23}(m+1)=\varepsilon_1 n_1(m) \tag{6.19}$$

(6) Let α be the adsorption rate, which is the probability that a gas type molecule $A_i^*(i=1,2,3,4)$ at time m will be in the solid phase state $A_i(i=1,2,3,4)$ at time (step) $m+1$, and β be the desorption rate, which

is the probability that a solid type molecules $A_i (i = 1,2,3,4)$ at time m will be in gas phase state $A_i^* (i = 1,2,3,4)$ at time $m+1$.

(7) Once a molecule enters state D at time m, it will not be able to return to the microreactor. Therefore, the probability that a molecule in state D at time m will be in any state of $A_i (i = 1,2,3,4)$ and $A_i^* (i = 1,2,3,4)$ in the microreactor at time $(m+1)$ is

$$p_{di}(m+1) = 0 \qquad i = 1,2,3,4,1^*,2^*,3^*,4^* \tag{6.20}$$

and

$$p_{dd}(m+1) = 1 \tag{6.21}$$

Assumptions (1)-(3) and (6), (7) imply that the probability for a molecule of type A_1 to remain in the same state during the transition is

$$p_{11}(m+1) = 1 - \beta - \varepsilon_2 - \varepsilon_1 n_2(m). \tag{6.22}$$

Similarly, assumptions (5), (6), (7), and (8) imply that

$$p_{22}(m+1) = 1 - \beta - \varepsilon_1 n_1(m) \tag{6.23}$$

$$p_{33}(m+1) = p_{44}(m+1) = 1 - \beta \tag{6.24}$$

$$p_{1^*1^*}(m+1) = p_{2^*2^*}(m+1) = p_{3^*3^*}(m+1) = p_{4^*4^*}(m+1) = 1 - \alpha - \mu \tag{6.25}$$

Therefore, the transition probability matrix for the cyclohexene hydrogenation and dehydrogenation in a CSTR can be expressed as

$$
\mathrm{P}(m+1)=\begin{array}{c} \\ A_1 \\ A_2 \\ A_3 \\ A_4 \\ A_1^* \\ A_2^* \\ A_3^* \\ A_4^* \\ D \end{array}
\begin{array}{c}
\begin{array}{ccccccccc} A_1 & A_2 & A_3 & A_4 & A_1^* & A_2^* & A_3^* & A_4^* & D \end{array} \\
\begin{pmatrix}
1-\beta-\varepsilon_1 n_2(m) & 2/3\varepsilon_2 & \varepsilon_1 n_2(m) & 1/3\varepsilon_2 & \beta & 0 & 0 & 0 & 0 \\
-\varepsilon_2 & & & & & & & & \\
0 & 1-\beta-\varepsilon_1 n_1(m) & \varepsilon_1 n_1(m) & 0 & 0 & \beta & 0 & 0 & 0 \\
0 & 0 & 1-\beta & 0 & 0 & 0 & \beta & 0 & 0 \\
0 & 0 & 0 & 1-\beta & 0 & 0 & 0 & \beta & 0 \\
\alpha & 0 & 0 & 0 & 1-\alpha-\mu & 0 & 0 & 0 & \mu \\
0 & \alpha & 0 & 0 & 0 & 1-\alpha-\mu & 0 & 0 & \mu \\
0 & 0 & \alpha & 0 & 0 & 0 & 1-\alpha-\mu & 0 & \mu \\
0 & 0 & 0 & \alpha & 0 & 0 & 0 & 1-\alpha-\mu & \mu \\
0 & 0 & 0 & 0 & 0 & 0 & 0 & 0 & 1
\end{pmatrix}
\end{array}
\tag{6.26}
$$

Let q be the volumetric flow rate of the feed and out-flow stream and V be the volume of the microreactor. Because the microreactor is completely mixed, we have

$$\mu = \frac{q}{V}\Delta t\,, \tag{6.27}$$

and

$$n_i(m+1) = \sum_j^4 n_j(m)p_{ji}(m+1) + x_i(m+1), \qquad i=1,2,3,4;\ m=0,1,2... \tag{6.28}$$

where k_1 is expressed per (time)$^{-1}$(molecule)$^{-1}$, k_2 is per (time)$^{-1}$, and $x_i(m+1)$ is the number of molecules of type A_i entering the microreactor in the time interval $(m, m+1)$.

Similarly, applying the same modeling approach to the following preferential oxidation for carbon monoxide in hydrogen fuel cell experiments

$$
\begin{aligned}
2A_1 + A_2 &\xrightarrow{k_1} 2A_3 \\
2A_4 + A_2 &\xrightarrow{k_2} 2A_5\,,
\end{aligned}
\tag{6.29}
$$

occurring in a CSTR, one obtains the transition probability matrix

$$
\mathrm{P}(m+1)=
\begin{array}{c}
\\ A_1 \\ A_2 \\ A_3 \\ A_4 \\ A_5 \\ A_1^* \\ A_2^* \\ A_3^* \\ A_4^* \\ A_5^* \\ D
\end{array}
\begin{array}{c}
\begin{array}{ccccccccccc} A_1 & A_2 & A_3 & A_4 & A_5 & A_1^* & A_2^* & A_3^* & A_4^* & A_5^* & D \end{array} \\
\begin{pmatrix}
1-\beta-\varepsilon_1 n_2(m) & 0 & \varepsilon_1 n_2(m) & 0 & 0 & \beta & 0 & 0 & 0 & 0 & 0 \\
0 & \begin{matrix}1-\beta-\varepsilon_1 n_1(m)\\ -\varepsilon_2 n_4(m)\end{matrix} & \varepsilon_1 n_1(m) & 0 & \varepsilon_2 n_4(m) & 0 & \beta & 0 & 0 & 0 & 0 \\
0 & 0 & 1-\beta & 0 & 0 & 0 & 0 & \beta & 0 & 0 & 0 \\
0 & 0 & 0 & 1-\beta-\varepsilon_2 n_2(m) & \varepsilon_2 n_2(m) & 0 & 0 & 0 & \beta & 0 & 0 \\
0 & 0 & 0 & 0 & 1-\beta & 0 & 0 & 0 & 0 & \beta & 0 \\
\alpha & 0 & 0 & 0 & 0 & 1-\alpha-\mu & 0 & 0 & 0 & 0 & \mu \\
0 & \alpha & 0 & 0 & 0 & 0 & 1-\alpha-\mu & 0 & 0 & 0 & \mu \\
0 & 0 & \alpha & 0 & 0 & 0 & 0 & 1-\alpha-\mu & 0 & 0 & \mu \\
0 & 0 & 0 & \alpha & 0 & 0 & 0 & 0 & 1-\alpha-\mu & 0 & \mu \\
0 & 0 & 0 & 0 & \alpha & 0 & 0 & 0 & 0 & 1-\alpha-\mu & \mu \\
0 & 0 & 0 & 0 & 0 & 0 & 0 & 0 & 0 & 0 & 1
\end{pmatrix}
\end{array}
\tag{6.30}
$$

where A_1, A_2, A_3, A_4, and A_5 represent carbon monoxide, oxygen, carbon dioxide, hydrogen, and water in the solid phase, respectively, and $A_i^*(i=1^*,2^*,3^*,4^*,5^*)$ represents carbon monoxide, oxygen, carbon dioxide, hydrogen, and water in the gas phase.

Here,

$$\varepsilon_i = k_i \Delta t \qquad i=1,2. \tag{6.31}$$

Thus, the number of molecules of type $A_i(i=1,2,...,5)$ in the CSTR can be obtained by iterating the following sequence.

$$
\begin{gathered}
n_i(m+1)=\sum_{j=1}^{5} k n_j(m) p_{ji}(m+1)+x_i(m+1) \qquad i=1,2,...,5;\ m=0,1,2,... \\
k=1 \text{ or } 2 \quad \textit{depending on the initial state.}
\end{gathered}
\tag{6.32}
$$

Next, we extend the modeling approach of Chou et al. [Chou 1988] to model cyclohexene hydrogenation and dehydrogenation reactions and the preferential oxidation of carbon monoxide in hydrogen fuel cell experiments in a microreactor. Both reaction systems are completely mixed and contain initially $n_i(0)$ molecules of type A_i. Let the number of molecules of this type entering the microreactor during the time interval

$[m\Delta t,(m+1)\Delta t]$ be $x_i(m)$, and the intensity of each molecule of any type exiting from it at any time be μ.

Therefore, for the cyclohexene hydrogenation and dehydrogenation reaction system in Eq. (6.11), the transition probability matrix in Eq. (6.27) with $n_i(m)$ "entities" at level i, i.e., $n_i(m)$ molecules of type A_i existing in the reactor at time $m\Delta t$, is expressed as

$$\mathrm{P}(m,m+1)=\begin{array}{c} \\ A_1 \\ A_3 \\ A_4 \\ A_1^* \\ A_3^* \\ A_4^* \\ D \end{array}\begin{array}{c} \begin{array}{ccccccc} A_1 & A_3 & A_4 & A_1^* & A_3^* & A_4^* & D \end{array} \\ \begin{pmatrix} 1-\beta\Delta t-\varepsilon_1 n_2(m)\Delta t-\varepsilon_2\Delta t & \varepsilon_1 n_2(m)\Delta t & \varepsilon_2\Delta t & \beta\Delta t & 0 & 0 & 0 \\ 0 & 1-\beta\Delta t & 0 & 0 & \beta\Delta t & 0 & 0 \\ 0 & 0 & 1-\beta\Delta t & 0 & 0 & \beta\Delta t & 0 \\ \alpha\Delta t & 0 & 0 & 1-\alpha\Delta t-\mu\Delta t & 0 & 0 & \mu\Delta t \\ 0 & \alpha\Delta t & 0 & 0 & 1-\alpha\Delta t-\mu\Delta t & 0 & \mu\Delta t \\ 0 & 0 & \alpha\Delta t & 0 & 0 & 1-\alpha\Delta t-\mu\Delta t & \mu\Delta t \\ 0 & 0 & 0 & 0 & 0 & 0 & 1 \end{pmatrix} \end{array} \tag{6.33}$$

Thus, we have

$$\begin{aligned} &E[N_j(m+1)\mid N_i(m)=n_i(m),X_i(m)=x_i(m),i=1,3,4,1^*,3^*,4^*] \\ &=\sum_{\substack{i=1,3,4\\1^*,3^*,4^*}} n_i(m)p_{ij}(m,m+1)+x_j(m+1),\quad j=1,3,4,1^*,3^*,4^*. \end{aligned} \tag{6.34}$$

Provided that $n_i(m)$ molecules of type $A_i(i=1,3,4,1^*,3^*,4^*)$ exist inside the microreactor at time $m\Delta t$ and $x_j(m+1)$ molecules of type A_i enter the microreactor during the time interval $[m\Delta t,(m+1)\Delta t]$, the conditional mean number of chemical species A_2 inside the microreactor at time $(m+1)\Delta t$ is obtained through the stoichiometric constraint as

$$\begin{aligned} &E[N_2(m+1)\mid N_i(m)=n_i(m),X_i(m)=x_i(m),i=1,3,4,1^*,3^*,4^*] \\ &=n_2(m)(1-\beta\Delta t)-n_1(m)p_{13}(m,m+1)+2n_1(m)p_{14}(m,m+1)+n_2^*(m)\alpha\Delta t, \end{aligned} \tag{6.35}$$

and

$$E[N_{2^*}(m+1) \mid N_i(m) = n_i(m), X_i(m) = x_i(m), i = 1,3,4,1^*,3^*,4^*]$$
$$= n_2^*(m)(1-\alpha\Delta t - \mu\Delta t) + n_2(m)\beta\Delta t + x_{2^*}(m). \tag{6.36}$$

Since the microreactor initially contains $n_i(0)$ molecules of type $A_i (i = 1,3,4,1^*,3^*,4^*)$, where $n_1(0) = n_3(0) = n_4(0) = 0$, the mean number of molecules of any type A_i in the CSTR at time $(m+1)\Delta t$ can be obtained by iterating the sequence in Eqs. (6.33)-(6.35).

Applying the same method to the preferential oxidation of carbon monoxide in hydrogen fuel cell experiments in a microreactor, the transition probability matrix in Eq. (6.29) with $n_i(m)$ "entities" at level i, i.e., $n_i(m)$ molecules of type A_i existing in the reactor at time $m\Delta t$, is expressed as

$$\mathrm{P}(m,m+1) = \begin{array}{c} \\ A_2 \\ A_3 \\ A_5 \\ A_2^* \\ A_3^* \\ A_5^* \\ D \end{array} \begin{array}{c} \begin{array}{ccccccc} A_2 & A_3 & A_5 & A_2^* & A_3^* & A_5^* & D \end{array} \\ \begin{pmatrix} 1-\beta\Delta t-\varepsilon_1 n_2(m)\Delta t \\ -\varepsilon_2 n_4(m)\Delta t \end{pmatrix} & \varepsilon_1 n_2(m)\Delta t & \varepsilon_2 n_4(m)\Delta t & \beta\Delta t & 0 & 0 & 0 \\ 0 & 1-\beta\Delta t & 0 & 0 & \beta\Delta t & 0 & 0 \\ 0 & 0 & 1-\beta\Delta t & 0 & 0 & \beta\Delta t & 0 \\ \alpha\Delta t & 0 & 0 & 1-\alpha\Delta t-\mu\Delta t & 0 & 0 & \mu\Delta t \\ 0 & \alpha\Delta t & 0 & 0 & 1-\alpha\Delta t-\mu\Delta t & 0 & \mu\Delta t \\ 0 & 0 & \alpha\Delta t & 0 & 0 & 1-\alpha\Delta t-\mu\Delta t & \mu\Delta t \\ 0 & 0 & 0 & 0 & 0 & 0 & 1 \end{array} \tag{6.37}$$

Thus, we have

$$E[N_j(m+1) \mid N_i(m) = n_i(m), X_i(m) = x_i(m), i = 2,3,5,2^*,3^*,5^*]$$
$$= \sum_{\substack{i=2,3,5 \\ 2^*,3^*,5^*}} k n_i(m) p_{ij}(m,m+1) + x_j(m), \quad j = 2,3,5,2^*,3^*,5^*; \tag{6.38}$$
$$k = 1 \text{ or } 2 \text{ depending on the initial state.}$$

Provided that $n_i(m)$ molecules of type $A_i (i = 2,3,5,2^*,3^*,5^*)$ exist inside the microreactor at time $m\Delta t$ and $x_i(m)$ molecules of type A_i enter the microreactor during the time

interval $[m\Delta t,(m+1)\Delta t]$, the conditional mean number of chemical species A_1. inside the microreactor at time $(m+1)\Delta t$ is obtained through the stoichiometric constraint as

$$\begin{aligned} &E[N_1.(m+1)\mid N_i(m)=n_i(m),X_i(m)=x_i(m),i=2,3,5,2^*,3^*,5^*] \\ &=n_1.(m)(1-\alpha\Delta t-\mu\Delta t)+x_1.(m) \end{aligned} \tag{6.39}$$

Similarly, for chemical species $A_4.$, A_1, and A_4 we have

$$\begin{aligned} &E[N_4.(m+1)\mid N_i(m)=n_i(m),X_i(m)=x_i(m),i=2,3,5,2^*,3^*,5^*] \\ &=n_4.(m)(1-\alpha\Delta t-\mu\Delta t)+x_4.(m) \end{aligned} \tag{6.40}$$

$$\begin{aligned} &E[N_1(m+1)\mid N_i(m)=n_i(m),X_i(m)=x_i(m),i=2,3,5,2^*,3^*,5^*] \\ &=n_1(m)(1-\beta\Delta t)-2n_2(m)p_{23}(m,m+1)+n_1^*(m)\alpha\Delta t \end{aligned} \tag{6.41}$$

and

$$\begin{aligned} &E[N_4(m+1)\mid N_i(m)=n_i(m),X_i(m)=x_i(m),i=2,3,5,2^*,3^*,5^*] \\ &=n_4(m)(1-\beta\Delta t)-2n_2(m)p_{25}(m,m+1)+n_4^*(m)\alpha\Delta t \end{aligned} \tag{6.42}$$

Since the microreactor initially contains $n_i(0)$ molecules of type $A_i(i=2,3,5,2^*,3^*,5^*)$, where $n_2(0)=n_3(0)=n_5(0)=0$, the mean number of molecules of any type A_i in the CSTR at time $(m+1)\Delta t$ can be obtained by iterating the sequence in Eqs. (6.37)-(6.41).

6.2.2 Markov Chain Simulation Results

Cyclohexene hydrogenation and dehydrogenation reactions are simulated in terms of temporal variation of concentrations of the reactants and products. As an example, we considered three situations ($(\alpha=\beta=k,\alpha=\beta=0.1k,\alpha=\beta=10k)$. The results obtained with the present approach (with Δt =0.1 min) are presented in Figs (6.20) – (6.26).

Coefficients used in the simulation of results in Figs (6.20)-(6.26) are presented in Table 6.6.

Table 6.6 Coefficients used in the simulation of results in Figs. (6.20)-(6.26).

coefficients	Figs (6.20)-(6.22)	Figs (6.23-6.26)
C_{i0} $(i=1,2,3,4)$	0	0
$C_1^*{}_f$(M)	0.00304	0.008064
$C_2^*{}_f$(M)	0.00218	0.0062
$C_3^*{}_f$(M)	0	0
$C_4^*{}_f$(M)	0	0
q (L/min)	0.00011	0.00011
V (L)	4.01	4.01
k_1^* (/M • min)	0.0793	0
k_2^* (/min)	0	0.0966
N_0	6.02×10^{23}	6.02×10^{23}
Δt (min)	1	1

In this table, C_{i0} represents the initial molar concentration of chemical species A_i in the microreactor, C_{if} represents molar concentration of chemical species A_i in the feed stream, q is the volumetric flow rate, V is the volume of the reacting mixture in the microreactor, k_i^* is the reaction rate constant, and N_0 is the Avogadro number. Because the cyclohexene hydrogenation reaction is a second-order reaction, the value of k_1 in Eq. (6.11) is obtained by dividing k_1^* by the product of the volume of the reacting mixture, V, and the Avogadro number, N_0. k_2 in Eq. (6.12) is equal to k_2^* as the cyclohexene dehydrogenation is a first-order reaction.

Figures (6.20)-(6.22) present the simulation results of the cyclohexene hydrogenation reaction for different values of the absorption (α) and desorption (β) rates. There are six different lines in every plot. Form top to bottom, in Fig. (6.20), these six lines present the molar concentration of A_2^*, A_1^*, A_2, A_1, A_3, and A_3^* in a microreactor, respectively. In Fig (6.21) and Fig (6.22), the six lines represent the molar concentration of A_2^*, A_2, A_1^*, A_1, A_3, and A_3^* in a microreactor, respectively. The molar concentration of

cyclohexene (A_1^*) is almost the same in these three plots. The concentration difference between the solid phase (A_i) and the gas phase (A_i^*) of a chemical species decreases with an increase in the absorption rate and the desorption rate. As expected, the molar concentration of any species increases with time until it reaches steady state.

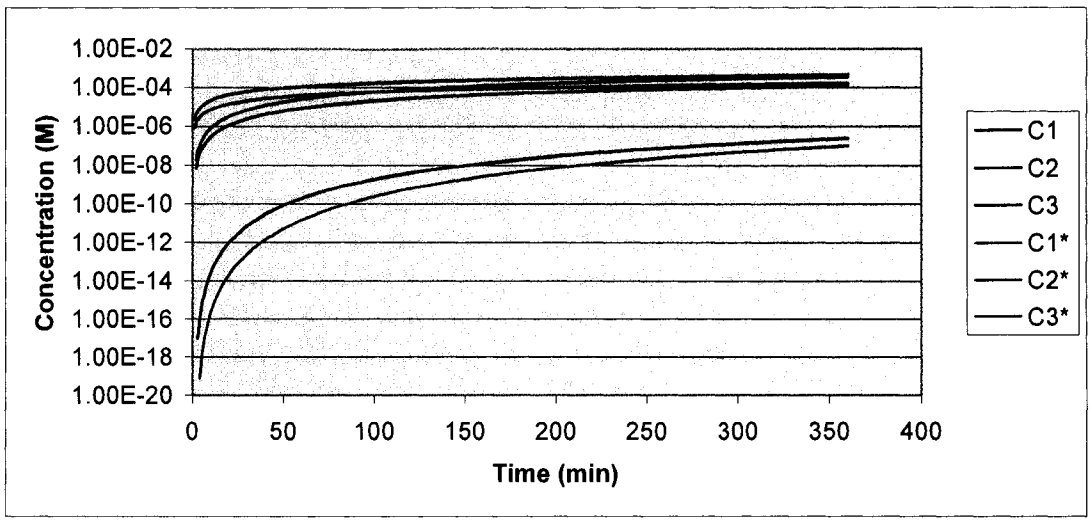

Figure 6.20 Temporal variations of concentrations of the reactants and products as functions of time for the cyclohexene hydrogenation reaction in a microreactor with initial condition C_{i0}=0, (i=1*, 2*, 3*, 4*), and $\alpha = \beta = 0.1k_1$.

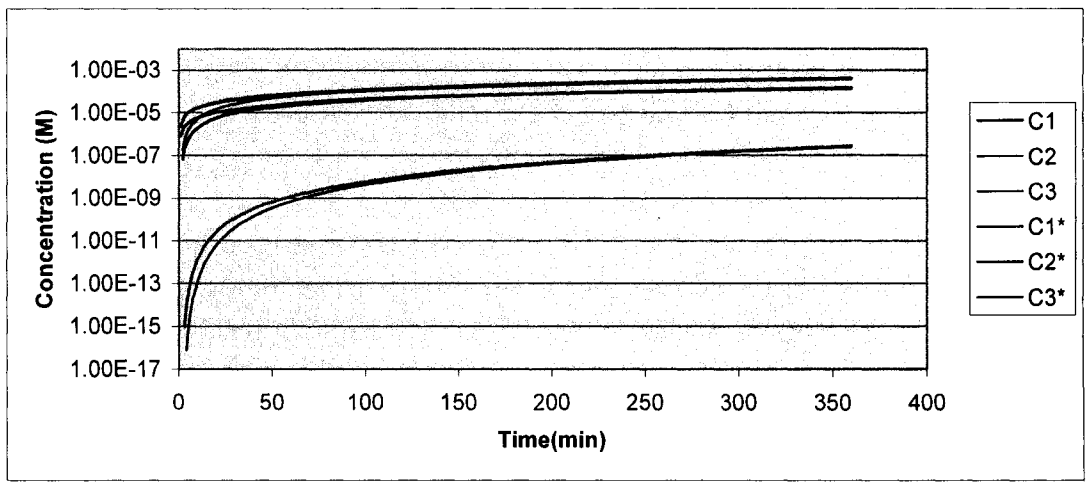

Figure 6.21 Temporal variations of concentrations of the reactants and products as functions of time for the cyclohexene hydrogenation reaction in a microreactor with initial condition C_{i0}=0, (i=1*, 2*, 3*, 4*), and $\alpha = \beta = k_1$.

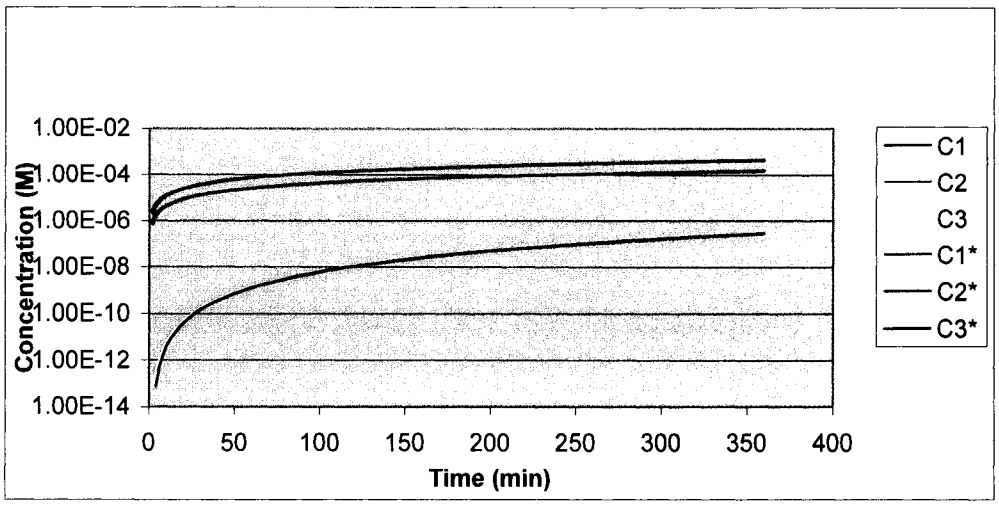

Figure 6.22 Temporal variations of concentrations of the reactants and products as functions of time for the cyclohexene hydrogenation reaction in a microreactor with initial condition C_{i0}=0, (i=1*, 2*, 3*, 4*), and $\alpha = \beta = 10k_1$.

Figures (6.23)-(6.25) present the simulation results of the cyclohexene dehydrogenation reaction for different values of absorption (α) and desorption (β) rates. From top to bottom, in Fig. (6.23), the six lines represent the molar concentration of A_2^*, A_1^*, A_2, A_1, A_4, and A_4^* in a microreactor, respectively. In Fig. (6.24) and Fig. (6.25), the six lines present the molar concentration of A_2^*, A_2, A_1^*, A_1, A_4, and A_4^* in a microreactor, respectively. From these three figures, the concentration difference between the solid phase (A_i) and the gas phase (A_i^*) of a chemical species decreased with an increase in the values of the absorption and desorption rates. The molar concentration of cyclohexene (A_1^*) also decreased with an increase in the absorption and the desorption rates.

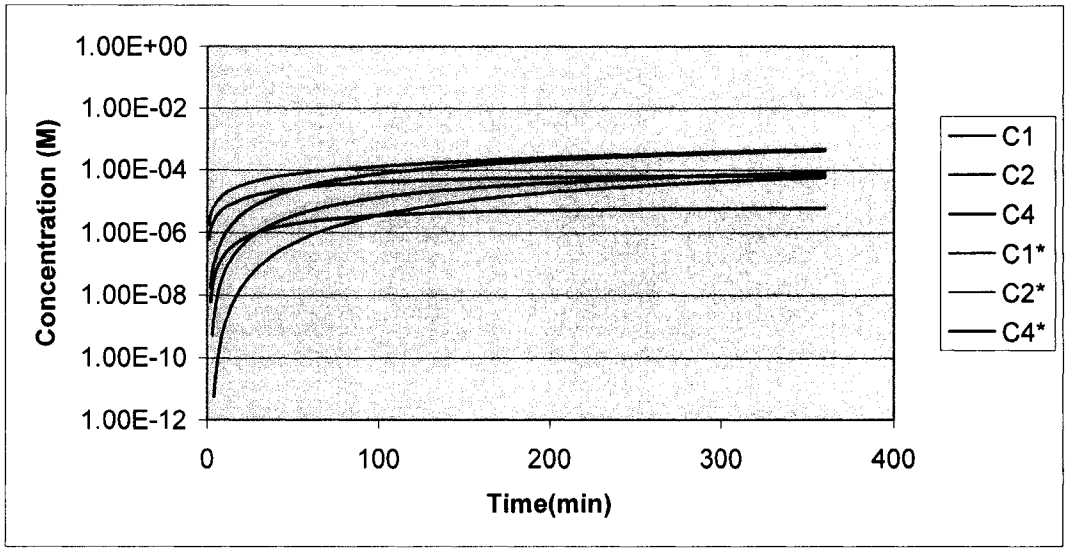

Figure 6.23 Temporal variations of concentrations of the reactants and products as functions of time for the cyclohexene dehydrogenation reaction in a microreactor with initial condition C_{i0}=0, (i=1*, 2*, 3*, 4*), and $\alpha = \beta = 0.1k_2$.

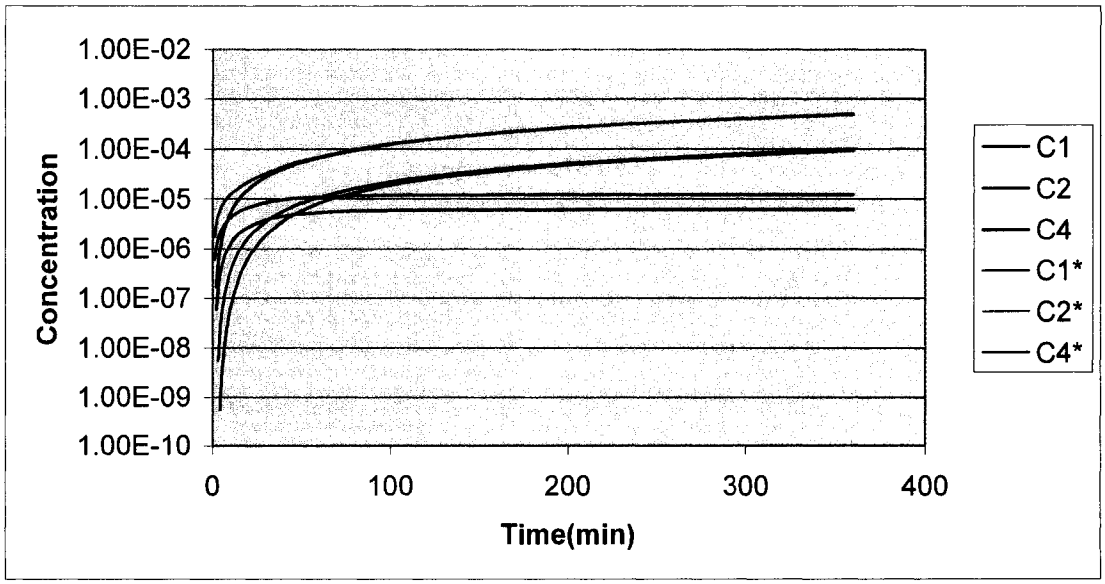

Figure 6.24 Temporal variations of concentrations of the reactants and products as functions of time for the cyclohexene dehydrogenation reaction in a microreactor with initial condition C_{i0}=0, (i=1*, 2*, 3*, 4*), and $\alpha = \beta = k_2$.

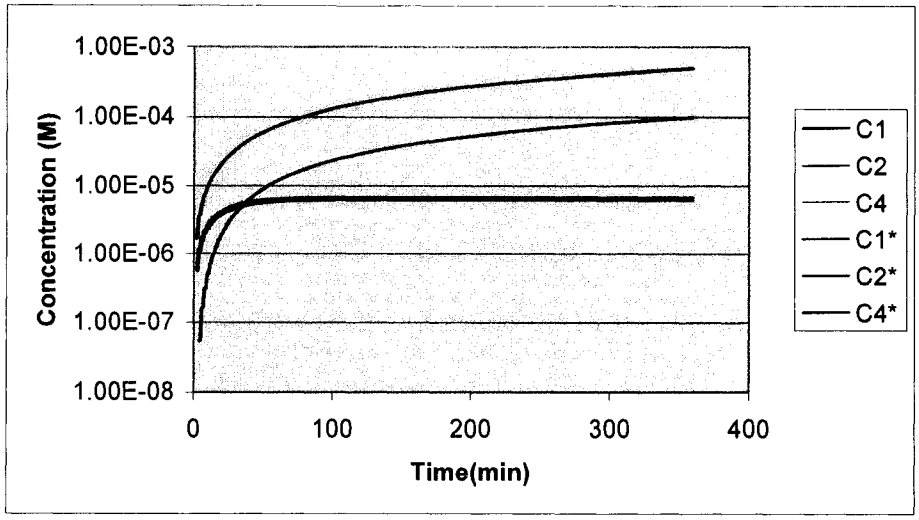

Figure 6.25 Temporal variations of concentrations of the reactants and products as functions of time for the cyclohexene dehydrogenation reaction in a microreactor with initial condition C_{i0}=0, (i=1*, 2*, 3*, 4*), and $\alpha = \beta = 10k_2$.

Figure (6.26) shows temporal variation of concentrations of the reactants and products as functions of time for the cyclohexene dehydrogenation reaction in the exit stream of a microreactor with initial condition C_{i0}=0, (i=1*, 2*, 3*, 4*) and $\alpha = \beta = k_2$. The three lines are the molar concentration of A_2^*, A_1^*, and A_4^*.

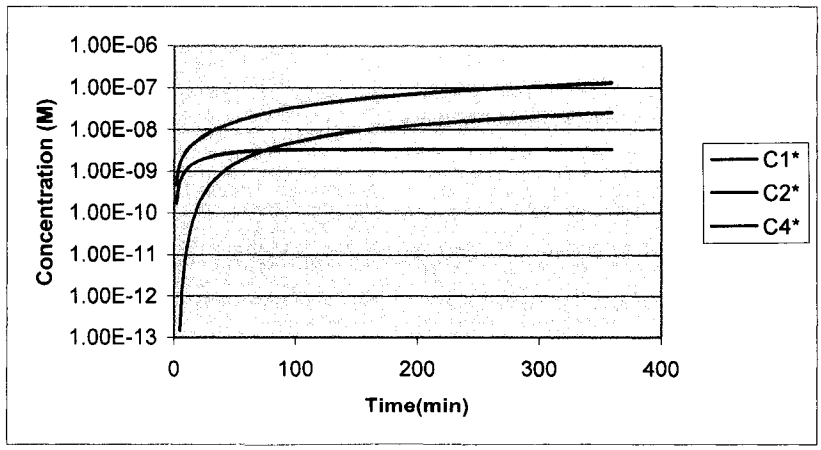

Figure 6.26 Temporal variations of concentrations of the reactants and products as functions of time for the cyclohexene dehydrogenation reaction in the exit stream of a microreactor with initial condition C_{i0}=0, (i=1*, 2*, 3*, 4*), and $\alpha = \beta = k_2$.

By considering the number of molecules in the exit stream with and without a catalyst, one may calculate the conversion rate. For instance, if we let $n_w(t)$ represent the predicted number of molecules of cyclohexene in the exit stream with a catalyst (or reaction) and $n_{wo}(t)$ the predicted number of molecules without a catalyst (no reaction), then the conversion rate (CR) is

$$CR = \frac{n_{wo}(t) - n_w(t)}{n_{wo}(t)} \tag{6.43}$$

Based on Eq. (6.43), the conversion rate (for $\alpha = \beta = k_2$ =0.0966/min) was 0.94 which is in qualitative agreement with the experimental results used to estimate the reaction rate, k_2, utilized in the simulation.

In reality, one may estimate the parameters (α, β, k) of the Markov chain model by fitting Eq. (6.43) to observed experimental data.

CHAPTER SEVEN

CONCLUSIONS AND FUTURE STUDIES

7.1 Conclusions

In this study, the box central composite design in conjunction with response surface methodology was used in order to determine the levels of the parameters of the chemical reactions that maximized reactant conversion and desired product selectivity for cyclohexene hydrogenation and dehydrogenation reactions, preferential oxidation of carbon monoxide reactions, and the Fischer-Tropsch synthesis reaction.

For cyclohexene hydrogenation and dehydrogenation reactions, the analysis showed that the response surface for conversion of C_6H_{10} was planar in both hydrogenation and dehydrogenation reactions. The conversion rate of C_6H_{10} is up to 93.6% in the hydrogenation reaction and 96.4% in the dehydrogenation reaction. For the preferential oxidation of carbon monoxide reactions, a temperature, $CO:O_2$ ratio, and total flow rate combination of 175.9°C, 1.31, and 0.2 sccm, respectively, was found to give the highest CO conversion (94%) and CO_2 selectivity (88%). For the Fischer-Tropsch synthesis reaction, a temperature, $H_2:CO$ ratio, and total flow rate combination of 218.2°C, 4.51, and 0.6 sccm, respectively, was found to give the highest propane

selectivity (88.25%). This study demonstrates how experimental design and response surface methodology can be used to efficiently optimize a process.

The probability modeling approach was applied to the cyclohexene hydrogenation and dehydrogenation experiments and to the Fischer-Tropsch synthesis experiment. Results from this approach indicate that the microchannel behaves as one compartment, implying that the flow is well mixed and is time homogeneous, in which case each molecule in the reactor has the same exit intensity (or rate) λ.

For the cyclohexene hydrogenation reaction, the estimated values for λ and μ were 0.0252/min and 0.0793/M•min, respectively, for the case where temperature = 56.37°C, flow rate of hydrogen = 0.28 sccm, and flow rate of argon = 0.82 sccm. Also, the estimated values for λ and μ were 0.0454/min and 0.2935/M•min for the case where temperature = 102.5°C, flow rate of hydrogen = 0.55 sccm, and flow rate of argon = 0.55 sccm. The activation energy (E_a) of the cyclohexene hydrogenation reaction is calculated to be $29195.22\,J/mol$, and the reaction constant k_0 for the cyclohexene hydrogenation reaction is found to be 3368.14.

For the cyclohexene dehydrogenation reaction, the estimated values for λ and μ were 0.00506 /min and 0.0966/min, respectively, under the operating condition of temperature = 186.67°C, flow rate of hydrogen = 0.28sccm, and flow rate of argon = 0.82 sccm. The estimated values for λ and μ were 0.00569/min and 0.0996/min, respectively under the condition that temperature = 353.33°C, flow rate of hydrogen = 0.28 sccm, and flow rate of argon = 0.82 sccm. The activation energy (E_a) of the cyclohexene

dehydrogenation reaction is found to be $439.5\,J/mol$, and the reaction constant k_0 for the cyclohexene dehydrogenation reaction is 0.108.

For the Fischer-Tropsch synthesis reaction, the estimated values for λ and μ were 0.0305/min and 0.0213/min, respectively when the temperature = 250°C, total flow rate = 0. 8 sccm, and $H_2:CO$ ratio = 3:1 (where flow rate of H_2 is 0.6 sccm, and flow rate of CO is 0.2 sccm).

In this study, a Markov chain approach was applied also to model cylohexene hydrogenation and dehydrogenation reactions and preferential oxidation of carbon monoxide in fuel cell reaction by considering the microreactor as composed of two phases, the solid phase and the flow or gas phase. Simulation results were in qualitative agreement with experimental results.

7.2 Future Studies

In future work, a Fischer-Tropsch synthesis reaction experiment needs to be run at a temperature, $H_2:CO$ ratio, and total flow rate combination of 218.2°C, 4.51, and 0.6 sccm to verify the predicted maxima from the quadratic model for propane selectivity. Furthermore, it would be useful to extend the Markov chain approach in order to predict the conversion rate for the Fischer-Tropsch synthesis reaction involving adsorption, surface reaction, desorption, and exit from the reactor, as well as shed light on the nature of the catalytic reaction scheme for each of the three reactions that were studied.

In addition, it would be useful to investigate an inverse problem solution to Eqs. (5.1)-(5.5) in order to predict the number of molecules of different chemical species from partial pressures.

APPENDIX

SOURCE CODES

1. 2nd-order regression model for base level partial pressure of C_6h_6, C_6H_{10}, C_6H_{12}, H_2, and He.

```
// EXEC SAS
//SAS.SYSIN DD *
OPTIONS NOCENTER;
DATA ONE;
INPUT  RUNNUM T N1 N2 N3 PC6H6;
TT=T*T;
N11=N1*N1;
N22=N2*N2;
N33=N3*N3;
TN1=T*N1;
TN2=T*N2;
TN3=T*N3;
N12=N1*N2;
N13=N1*N3;
N23=N2*N3;
CARDS;
(DATA)
...
;
PROC PRINT;
PROC REG;
MODEL PC6H6=T N1 N2 N3 TT N11 N22 N33 TN1 TN2 TN3  N12 N13 N23 /P R CLM CLI COVB;
PROC REG;
MODEL PC6H6=N2 N3 N22 TN3 N12 N23/P R CLM CLI COVB ;
PROC REG;
MODEL PC6H6=N3 TN1 N23/P R CLM CLI COVB;
```

2. Analysis of the cyclohexene hydrogenation reaction

```
*******************************************************************************
// EXEC SAS
//SAS.SYSIN DD *
OPTIONS NOCENTER;
DATA ONE;
INPUT RUNNUM T F1 F2 CONC6H10;
CARDS;
  3   56.36904762  0.817857143   0.282142857  0.88535443
  6   148.6309524  0.282142857   0.817857143  0.87063744
  1   56.36904762  0.282142857   0.282142857  0.90715219
 11         102.5         0.55          0.55  0.85997697
  5   148.6309524  0.282142857   0.282142857  0.92291718
  9         102.5         0.55          0.55  0.86028578
  2   56.36904762  0.282142857   0.817857143  0.74531682
  7   148.6309524  0.817857143   0.282142857   0.8558649
  4   56.36904762  0.817857143   0.817857143  0.74723613
 10         102.5         0.55          0.55  0.82075817
  8   148.6309524  0.817857143   0.817857143  0.82634915
 12         102.5         0.55          0.55  0.82371392
```

```
;
PROC PRINT;
PROC REG;
MODEL CONC6H10= F2/P R;
OUTPUT OUT=NEW PREDICTED=YHAT RESIDUAL=RS PRESS=PR STUDENT=SR;
PROC RANK DATA=NEW OUT=RANKS;
VAR RS;
RANKS RR;
DATA TWO;
SET RANKS;
I=(RR-0.5)/12;
PRO=PROBIT(I);
PROC PLOT DATA=TWO;
PLOT RS * PRO ='+';
PLOT RS * YHAT='*';
PLOT RS * RUNNUM='+';
DATA THREE;
INPUT X CONC6H10;
CARDS;
1 0.885354432
2 0.87063744
3 0.907152192
9 0.859976972
4 0.922917181
9 0.860285781
5 0.745316821
6 0.8558649
7 0.747236128
9 0.820758171
8 0.826349148
9 0.823713919
;
PROC GLM;
CLASSES X;
MODEL CONC6H10 = X;

**********************************************************************************
// EXEC SAS
//SAS.SYSIN DD *
OPTIONS NOCENTER;
TITLE 'LINEA PART OF LOWER TEMP RANGE';
DATA ONE;
INPUT RUNNUM T F1 F2 CONC6H10;
CARDS;
1       170     0.39    0.39    0.926348106
2       170     0.17    0.39    0.929566169
3       150     0.28    0.28    0.911149205
4       130     0.17    0.17    0.931023059
5       150     0.28    0.28    0.910726681
6       150     0.28    0.28    0.911994254
7       130     0.39    0.17    0.926500356
8       150     0.28    0.28    0.935456417
9       130     0.39    0.39    0.933056903
10      170     0.17    0.17    0.918004134
11      130     0.17    0.39    0.934319893
12      170     0.39    0.17    0.922954682
```

```
;
PROC PRINT;
RUN;
PROC REG;
MODEL CONC6H10= T F1 F2/P R;
OUTPUT OUT=NEW PREDICTED=YHAT RESIDUAL=RS PRESS=PR STUDENT=SR;
PROC RANK DATA=NEW OUT=RANKS;
VAR RS;
RANKS RR;
DATA TWO;
SET RANKS;
I=(RR-0.5)/12;
PRO=PROBIT(I);
PROC PLOT DATA=TWO;
PLOT RS * PRO ='+';
PLOT RS * YHAT='*';
PLOT RS * RUNNUM='+';
RUN;
DATA THREE;
INPUT X CONC6H10;
CARDS;
1       0.926348106
2       0.929566169
3       0.931023059
4       0.926500356
5       0.933056903
6       0.918004134
7       0.934319893
8       0.922954682
9       0.911149205
9       0.910726681
9       0.911994254
9       0.935456417
;
PROC GLM;
CLASSES X;
MODEL CONC6H10 = X;
RUN;
```

3. Analysis of the cyclohexene dehydrogenation reaction

```
**********************************************************************************
// EXEC SAS
//SAS.SYSIN DD *
OPTIONS NOCENTER;
TITLE 'LINEA PART OF HIGH TEMP RANGE11403(REPEAT2)';
DATA ONE;
INPUT RUNNUM T F1 F2 CONC6H10;
CARDS;
1       353.3333333     0.817857143     0.282142857     0.939960525
2       186.6666667     0.817857143     0.282142857     0.930450179
3       270             0.55            0.55            0.957027883
4       186.6666667     0.282142857     0.282142857     0.936934111
5       270             0.55            0.55            0.95648972
6       353.3333333     0.282142857     0.282142857     0.941705278
```

```
7       186.6666667     0.282142857     0.817857143     0.962133026
8       353.3333333     0.817857143     0.817857143     0.9631623
9       270             0.55            0.55            0.954927834
10      353.3333333     0.282142857     0.817857143     0.963650324
11      186.6666667     0.817857143     0.817857143     0.942565541
12      270             0.55            0.55            0.953005823
;
PROC PRINT;
RUN;
PROC REG;
MODEL CONC6H10= T F1 F2/P R;
OUTPUT OUT=NEW PREDICTED=YHAT RESIDUAL=RS PRESS=PR STUDENT=SR;
PROC RANK DATA=NEW OUT=RANKS;
VAR RS;
RANKS RR;
DATA TWO;
SET RANKS;
I=(RR-0.5)/12;
PRO=PROBIT(I);
PROC PLOT DATA=TWO;
PLOT RS * PRO ='+';
PLOT RS * YHAT='*';
PLOT RS * RUNNUM='+';
RUN;
DATA THREE;
INPUT X CONC6H10;
CARDS;
1       0.936934111
2       0.962133026
3       0.930450179
4       0.942565541
5       0.941705278
6       0.963650324
7       0.939960525
8       0.9631623
9       0.953005823
9       0.957027883
9       0.954927834
9       0.95648972
;
PROC GLM;
CLASSES X;
MODEL CONC6H10 = X;
RUN;
```

4. Randomization

```
*********************************************************************************
// EXEC SAS
//SAS.SYSIN DD *
OPTIONS NOCENTER;
DATA DESIGN;
INPUT TREATMENT @@;
RANNO=RANUNI(0);
LINES;
1 2 3 4 5 6 7 8 9 10 11 12 13 14 15 16 17 18
;
```

```
PROC PRINT;
RUN;
PROC SORT;
BY RANNO;
RUN;
PROC PRINT;
RUN;
```

5. Analysis of the Fuel Cell reaction

```
**********************************************************************************
// EXEC SAS
//SAS.SYSIN DD *
OPTIONS NOCENTER;
TITLE '1ST ORDER MODEL OF CO CONVERTION USING PURE O2';
DATA ONE;
INPUT RUNNUM X1 X2 X3 Y;
/* X1 IS TEMPERATURE, X2 IS THE CO:O2 RATIO, X3 IS THE TOTAL FLOW RATE
AND Y IS THE CONVERTION OF CO
*/
CARDS;
13      140.24  1.01    0.36    0.5956
18      140.24  1.01    0.84    0.3749
7       140.24  3.24    0.36    0.5346
2       140.24  3.24    0.84    0.3712
14      199.76  1.01    0.36    0.5765
8       199.76  1.01    0.84    0.3186
5       199.76  3.24    0.36    0.5068
11      199.76  3.24    0.84    0.3667
1       170.00  2.13    0.60    0.4010
16      170.00  2.13    0.60    0.3901
6       170.00  2.13    0.60    0.3923
9       170.00  2.13    0.60    0.4410
;
PROC PRINT;
PROC GLM;
CLASS X1 X2 X3;
MODEL Y=X1 X2 X3;
PROC REG;
MODEL Y= X1 X2 X3/P R;
OUTPUT OUT=NEW PREDICTED=YHAT RESIDUAL=RS PRESS=PR;
PROC RANK DATA=NEW OUT=RANKS;
VAR RS;
RANKS RR;
DATA TWO;
SET RANKS;
I=(RR-0.5)/12;
PRO=PROBIT(I);
PROC PLOT DATA=TWO;
PLOT RS * PRO ='+';
PLOT RS * YHAT='*';
PLOT RS * RUNNUM='+';
DATA THREE;
INPUT X Y;
CARDS;
1       0.5956
```

```
2       0.3749
3       0.5346
4       0.3712
5       0.5765
6       0.3186
7       0.5068
8       0.3667
9       0.4010
9       0.3901
9       0.3923
9       0.4410
;
PROC GLM;
CLASSES X;
MODEL Y = X;
RUN;

************************************************************
// EXEC SAS
//SAS.SYSIN DD *
OPTIONS NOCENTER;
TITLE '1ST ORDER MODEL OF CO2 SELECTIVITY USING PURE O2 (FUELCELL)';
DATA ONE;
INPUT RUNNUM X1 X2 X3 Y;
/* X1 IS TEMPERATURE, X2 IS THE CO:O2 RATIO, X3 IS THE TOTAL FLOW RATE
AND Y IS THE SELECTIVITY OF CO2.
*/
CARDS;
13      140.24  1.01    0.36    0.7265
18      140.24  1.01    0.84    0.3383
7       140.24  3.24    0.36    0.8569
2       140.24  3.24    0.84    0.5113
14      199.76  1.01    0.36    0.7477
8       199.76  1.01    0.84    0.3272
5       199.76  3.24    0.36    0.6348
11      199.76  3.24    0.84    0.4406
1       170.00  2.13    0.60    0.5338
16      170.00  2.13    0.60    0.3862
6       170.00  2.13    0.60    0.5594
9       170.00  2.13    0.60    0.4680
19      158.13  1.77    0.21    .
;
PROC PRINT;
PROC REG;
MODEL Y= X1 X2 X3/P R;
OUTPUT OUT=NEW PREDICTED=YHAT RESIDUAL=RS PRESS=PR;
PROC RANK DATA=NEW OUT=RANKS;
VAR RS;
RANKS RR;
DATA TWO;
SET RANKS;
I=(RR-0.5)/12;
PRO=PROBIT(I);
PROC PLOT DATA=TWO;
PLOT RS * PRO ='+';
PLOT RS * YHAT='*';
```

```
PLOT RS * RUNNUM='+';
DATA THREE;
INPUT X Y;
CARDS;
1       0.7265
2       0.3383
3       0.8569
4       0.5113
5       0.7477
6       0.3272
7       0.6348
8       0.4406
9       0.5338
9       0.3862
9       0.5594
9       0.4680
;
PROC GLM;
CLASSES X;
MODEL Y = X;
RUN;

************************************************************

// EXEC SAS
//SAS.SYSIN DD *
OPTIONS NOCENTER;
TITLE 'AGURMENT FUELCELL EXPRIMENT (PURE O2 42303) CO CONVERSION';
DATA ONE;
INPUT RUNNUM X1 X2 X3 Y;
/* X1 IS THE TEMPERATURE, X2 IS THE CO:O2 RATIO, X3 IS
THE TOTAL FLOW RATE. Y IS THE CONVERSION OF THE CO.
*/
X11=X1*X1;
X22=X2*X2;
X33=X3*X3;
X12=X1*X2;
X13=X1*X3;
X23=X2*X3;
CARDS;
13      140.24  1.01    0.36    0.5956
18      140.24  1.01    0.84    0.3749
7       140.24  3.24    0.36    0.5346
2       140.24  3.24    0.84    0.3712
14      199.76  1.01    0.36    0.5765
8       199.76  1.01    0.84    0.3186
5       199.76  3.24    0.36    0.5068
11      199.76  3.24    0.84    0.3667
1       170.00  2.13    0.60    0.4010
16      170.00  2.13    0.60    0.3901
6       170.00  2.13    0.60    0.3923
9       170.00  2.13    0.60    0.4410
12      120.00  2.13    0.60    0.4735
3       220     2.125   0.6     0.4225
4       170.00  0.25    0.60    0.4226
10      170.00  4.00    0.60    0.4512
```

```
15      170.00  2.13    0.20    0.7017
17      170.00  2.13    1.00    0.3375
19      158.13  1.77    0.21     .
;
PROC PRINT;
PROC REG;
MODEL Y=X1 X2 X3 X11 X22 X33 X12 X13 X23/P R;
PROC RSREG;
MODEL Y=X1 X2 X3/LACKFIT;
RUN;

**************************************************************************
// EXEC SAS
//SAS.SYSIN DD *
OPTIONS NOCENTER;
TITLE '1ST ORDER MODEL OF CO2 SELECTIVITY USING PURE O2(FUELCELL)';
DATA ONE;
INPUT RUNNUM X1 X2 X3 Y;
/* X1 IS TEMPERATURE, X2 IS THE CO:O2 RATIO, X3 IS THE TOTAL FLOW RATE
AND Y IS THE SELECTIVITY OF CO2.
*/
CARDS;
13      140.24  1.01    0.36    0.7265
18      140.24  1.01    0.84    0.3383
7       140.24  3.24    0.36    0.8569
2       140.24  3.24    0.84    0.5113
14      199.76  1.01    0.36    0.7477
8       199.76  1.01    0.84    0.3272
5       199.76  3.24    0.36    0.6348
11      199.76  3.24    0.84    0.4406
1       170.00  2.13    0.60    0.5338
16      170.00  2.13    0.60    0.3862
6       170.00  2.13    0.60    0.5594
9       170.00  2.13    0.60    0.4680
19      158.13  1.77    0.21     .
;
PROC PRINT;
PROC REG;
MODEL Y= X1 X2 X3/P R;
OUTPUT OUT=NEW PREDICTED=YHAT RESIDUAL=RS PRESS=PR;
PROC RANK DATA=NEW OUT=RANKS;
VAR RS;
RANKS RR;
DATA TWO;
SET RANKS;
I=(RR-0.5)/12;
PRO=PROBIT(I);
PROC PLOT DATA=TWO;
PLOT RS * PRO ='+';
PLOT RS * YHAT='*';
PLOT RS * RUNNUM='+';
DATA THREE;
INPUT X Y;
CARDS;
1       0.7265
2       0.3383
```

```
3       0.8569
4       0.5113
5       0.7477
6       0.3272
7       0.6348
8       0.4406
9       0.5338
9       0.3862
9       0.5594
9       0.4680
;
PROC GLM;
CLASSES X;
MODEL Y = X;
RUN;


*****************************************************************
// EXEC SAS
//SAS.SYSIN DD *
OPTIONS NOCENTER;
TITLE '1ST ORDER MODEL OF CO CONVERTION USING PURE O2 USING EXPERIMENT
RESULT 62603';
DATA ONE;
INPUT RUNNUM X1 X2 Y;
/* X1 IS TEMPERATURE, X2 IS THE CO:O2 RATIO, THE TOTAL FLOW RATE IS ALWAYS 0.2
SCCM
AND Y IS THE CONVERSION OF CO
*/
CARDS;
2       131.71  0.70    0.794
8       131.71  2.90    0.525
10      188.29  0.70    0.901
16      188.29  2.90    0.586
9       160.00  1.80    0.921
1       160.00  1.80    0.915
7       160.00  1.80    0.909
12      160.00  1.80    0.926
13      160.00  1.80    0.914
15      160.00  1.80    0.901
11      160.00  1.80    0.922
6       160.00  1.80    0.902
;
PROC PRINT;
PROC GLM;
CLASS X1 X2 ;
MODEL Y=X1 X2 ;
PROC REG;
MODEL Y= X1 X2 /P R;
OUTPUT OUT=NEW PREDICTED=YHAT RESIDUAL=RS PRESS=PR;
PROC RANK DATA=NEW OUT=RANKS;
VAR RS;
RANKS RR;
DATA TWO;
SET RANKS;
I=(RR-0.5)/12;
```

```
PRO=PROBIT(I);
PROC PLOT DATA=TWO;
PLOT RS * PRO ='+';
PLOT RS * YHAT='*';
PLOT RS * RUNNUM='+';
DATA THREE;
INPUT X Y;
CARDS;
1       0.794
2       0.525
3       0.901
4       0.586
5       0.921
5       0.915
5       0.909
5       0.926
5       0.914
5       0.901
5       0.922
5       0.902
;
PROC GLM;
CLASSES X;
MODEL Y = X;
RUN;

************************************************************
// EXEC SAS
//SAS.SYSIN DD *
OPTIONS NOCENTER;
TITLE '1ST ORDER MODEL OF CO2 SELECTIVITY USING PURE O2 USING EXPERIMENT
RESULT 62603';
DATA ONE;
INPUT RUNNUM X1 X2 Y;
/* X1 IS TEMPERATURE, X2 IS THE CO:O2 RATIO, THE TOTAL FLOW RATE IS ALWAYS 0.2
SCCM
AND Y IS THE SELECTIVITY OF CO2
*/
CARDS;
2       131.71  0.70    0.653
8       131.71  2.90    0.597
10      188.29  0.70    0.865
16      188.29  2.90    0.576
9       160.00  1.80    0.896
1       160.00  1.80    0.888
7       160.00  1.80    0.867
12      160.00  1.80    0.898
13      160.00  1.80    0.859
15      160.00  1.80    0.865
11      160.00  1.80    0.834
6       160.00  1.80    0.851
;
PROC PRINT;
PROC GLM;
CLASS X1 X2 ;
MODEL Y=X1 X2 ;
```

```
PROC REG;
MODEL Y= X1 X2 /P R;
OUTPUT OUT=NEW PREDICTED=YHAT RESIDUAL=RS PRESS=PR;
PROC RANK DATA=NEW OUT=RANKS;
VAR RS;
RANKS RR;
DATA TWO;
SET RANKS;
I=(RR-0.5)/12;
PRO=PROBIT(I);
PROC PLOT DATA=TWO;
PLOT RS * PRO ='+';
PLOT RS * YHAT='*';
PLOT RS * RUNNUM='+';
DATA THREE;
INPUT X Y;
CARDS;
1       0.653
2       0.597
3       0.865
4       0.576
5       0.896
5       0.888
5       0.867
5       0.898
5       0.859
5       0.865
5       0.834
5       0.851
;
PROC GLM;
CLASSES X;
MODEL Y = X;
RUN;

************************************************************
// EXEC SAS
//SAS.SYSIN DD *
OPTIONS NOCENTER;
TITLE 'AGURMENT FUELCELL EXPRIMENT(PURE O2 62603)CO CONVERSION';
DATA ONE;
INPUT RUNNUM X1 X2 Y;
/* X1 IS THE TEMPERATURE, X2 IS THE CO:O2 RATIO,
THE TOTAL FLOW RATE IS ALWAYS 0.2SCCM. Y IS THE CONVERSION OF THE CO.
*/
X11=X1*X1;
X22=X2*X2;
X12=X1*X2;
CARDS;
2       131.71  0.70    0.794
8       131.71  2.90    0.525
10      188.29  0.70    0.901
16      188.29  2.90    0.586
9       160.00  1.80    0.921
1       160.00  1.80    0.915
7       160.00  1.80    0.909
```

```
12      160.00  1.80    0.926
13      160.00  1.80    0.914
15      160.00  1.80    0.901
11      160.00  1.80    0.922
6       160.00  1.80    0.902
5       120.00  1.80    0.895
3       200.00  1.80    0.903
4       160.00  0.25    0.764
14      160.00  3.35    0.453
;
PROC PRINT;
PROC REG;
MODEL Y=X1 X2 X11 X22 X12 /P R;
PROC RSREG;
MODEL Y=X1 X2/LACKFIT;
RIDGE MAX;
RUN;

*******************************************************
// EXEC SAS
//SAS.SYSIN DD *
OPTIONS NOCENTER;
TITLE 'AGURMENT FUELCELL EXPRIMENT(PURE O2 62603)CO2 SELECTIVITY';
DATA ONE;
INPUT RUNNUM X1 X2 Y;
/* X1 IS THE TEMPERATURE, X2 IS THE CO:O2 RATIO,
THE TOTAL FLOW RATE IS ALWAYS 0.2SCCM. Y IS THE SELECTIVITY OF THE CO2.
*/
X11=X1*X1;
X22=X2*X2;
X12=X1*X2;
CARDS;
2       131.71  0.70    0.653
8       131.71  2.90    0.597
10      188.29  0.70    0.865
16      188.29  2.90    0.576
9       160.00  1.80    0.896
1       160.00  1.80    0.888
7       160.00  1.80    0.867
12      160.00  1.80    0.898
13      160.00  1.80    0.859
15      160.00  1.80    0.865
11      160.00  1.80    0.834
6       160.00  1.80    0.851
5       120.00  1.80    0.877
3       200.00  1.80    0.823
4       160.00  0.25    0.763
14      160.00  3.35    0.643
;
PROC PRINT;
PROC REG;
MODEL Y=X1 X2 X11 X22 X12 /P R;
PROC RSREG;
MODEL Y=X1 X2/LACKFIT;
RIDGE MAX;
RUN;
```

```
*******************************************************************************
```

6. Analysis of the syn-gas reaction

```
*******************************************************************************
// EXEC SAS
//SAS.SYSIN DD *
OPTIONS NOCENTER;
TITLE '1ST ORDER MODEL OF CO CONVERSION IN SYN-GAS 90203DATA';
DATA ONE;
INPUT BLOCK X1 X2 X3 Y;
/* X1 IS THE TOTAL FLOW RATE, X2 IS THE H2:CO RATIO, X3 IS THE TEMPERATURE
AND Y IS THE CONVERSION OF CO IN SYN-GAS EXPERIMENT
*/
CARDS;
0       0.5     2       180     0.5975
1       0.5     2       260     0.5454
1       0.5     4       180     0.6528
0       0.5     4       260     0.7097
1       1.1     2       180     0.6710
0       1.1     2       260     0.6132
0       1.1     4       180     0.6128
1       1.1     4       260     0.6139
0       0.8     3       220     0.6178
0       0.8     3       220     0.6264
0       0.8     3       220     0.6264
1       0.8     3       220     0.6121
1       0.8     3       220     0.6236
1       0.8     3       220     0.6264
;
PROC PRINT;
PROC REG;
MODEL Y= X1 X2 X3/P R;
OUTPUT OUT=NEW PREDICTED=YHAT RESIDUAL=RS PRESS=PR;
PROC RANK DATA=NEW OUT=RANKS;
VAR RS;
RANKS RR;
DATA TWO;
SET RANKS;
I=(RR-0.5)/14;
PRO=PROBIT(I);
PROC PLOT DATA=TWO;
PLOT RS * PRO ='+';
PLOT RS * YHAT='*';
PROC REG;
MODEL Y=BLOCK X1 X2 X3/P R;
OUTPUT OUT=NEW PREDICTED=YHAT RESIDUAL=RS PRESS=PR;
PROC RANK DATA=NEW OUT=RANKS;
VAR RS;
RANKS RR;
DATA THREE;
SET RANKS;
I=(RR-0.5)/14;
PRO=PROBIT(I);
PROC PLOT DATA=THREE;
```

```
PLOT RS * PRO ='+';
PLOT RS * YHAT='*';
RUN;

************************************************
// EXEC SAS
//SAS.SYSIN DD *
OPTIONS NOCENTER;
TITLE '1ST ORDER MODEL OF SELECTIVITY TO METHANE IN SYN-GAS 90203DATA';
DATA ONE;
INPUT BLOCK X1 X2 X3 Y;
/* X1 IS THE TOTAL FLOW RATE, X2 IS THE H2:CO RATIO, X3 IS THE TEMPERATURE
AND Y IS THE CONVERSION OF CO IN SYN-GAS EXPERIMENT
*/
CARDS;
0       0.5     2       180     0.1036
1       0.5     2       260     0.0506
1       0.5     4       180     0.0571
0       0.5     4       260     0.005
1       1.1     2       180     0.1052
0       1.1     2       260     0.0025
0       1.1     4       180     0.0399
1       1.1     4       260     0.0791
0       0.8     3       220     0.0704
0       0.8     3       220     0.0401
0       0.8     3       220     0.0524
1       0.8     3       220     0.0649
1       0.8     3       220     0.0582
1       0.8     3       220     0.0624
;
PROC PRINT;
PROC REG;
MODEL Y= X1 X2 X3/P R;
OUTPUT OUT=NEW PREDICTED=YHAT RESIDUAL=RS PRESS=PR;
PROC RANK DATA=NEW OUT=RANKS;
VAR RS;
RANKS RR;
DATA TWO;
SET RANKS;
I=(RR-0.5)/14;
PRO=PROBIT(I);
PROC PLOT DATA=TWO;
PLOT RS * PRO ='+';
PLOT RS * YHAT='*';
PROC REG;
MODEL Y=BLOCK X1 X2 X3/P R;
OUTPUT OUT=NEW PREDICTED=YHAT1 RESIDUAL=RS1 PRESS=PR1;
PROC RANK DATA=NEW OUT=RANKS;
VAR RS1;
RANKS RR;
DATA THREE;
SET RANKS;
I=(RR-0.5)/14;
PRO1=PROBIT(I);
PROC PLOT DATA=THREE;
PLOT RS1 * PRO1 ='+';
```

```
PLOT RS1 * YHAT1='*';
RUN;

************************************************************
// EXEC SAS
//SAS.SYSIN DD *
OPTIONS NOCENTER;
TITLE '1ST ORDER MODEL OF SELECTIVITY TO ETHANE IN SYN-GAS 90203DATA';
DATA ONE;
INPUT BLOCK X1 X2 X3 Y;
/* X1 IS THE TOTAL FLOW RATE, X2 IS THE H2:CO RATIO, X3 IS THE TEMPERATURE
AND Y IS THE CONVERSION OF CO IN SYN-GAS EXPERIMENT
*/
CARDS;
0       0.5     2       180     0.1149
1       0.5     2       260     0.1752
1       0.5     4       180     0.1272
0       0.5     4       260     0.0755
1       1.1     2       180     0.2273
0       1.1     2       260     0.2032
0       1.1     4       180     0.0862
1       1.1     4       260     0.1199
0       0.8     3       220     0.0835
0       0.8     3       220     0.09
0       0.8     3       220     0.0799
1       0.8     3       220     0.1
1       0.8     3       220     0.0787
1       0.8     3       220     0.0814
;
PROC PRINT;
PROC REG;
MODEL Y= X1 X2 X3/P R;
OUTPUT OUT=NEW PREDICTED=YHAT RESIDUAL=RS PRESS=PR;
PROC RANK DATA=NEW OUT=RANKS;
VAR RS;
RANKS RR;
DATA TWO;
SET RANKS;
I=(RR-0.5)/14;
PRO=PROBIT(I);
PROC PLOT DATA=TWO;
PLOT RS * PRO ='+';
PLOT RS * YHAT='*';
PROC REG;
MODEL Y=BLOCK X1 X2 X3/P R;
OUTPUT OUT=NEW PREDICTED=YHAT1 RESIDUAL=RS1 PRESS=PR1;
PROC RANK DATA=NEW OUT=RANKS;
VAR RS1;
RANKS RR;
DATA THREE;
SET RANKS;
I=(RR-0.5)/14;
PRO1=PROBIT(I);
PROC PLOT DATA=THREE;
PLOT RS1 * PRO1 ='+';
PLOT RS1 * YHAT1='*';
```

```
RUN;

*********************************************************************
// EXEC SAS
//SAS.SYSIN DD *
OPTIONS NOCENTER;
TITLE '1ST ORDER MODEL OF SELECTIVITY TO PROPANE IN SYN-GAS 90203DATA';
DATA ONE;
INPUT BLOCK X1 X2 X3 Y;
/* X1 IS THE TOTAL FLOW RATE, X2 IS THE H2:CO RATIO, X3 IS THE TEMPERATURE
AND Y IS THE CONVERSION OF CO IN SYN-GAS EXPERIMENT
*/
CARDS;
0       0.5     2       180     0.7815
1       0.5     2       260     0.7742
1       0.5     4       180     0.8157
0       0.5     4       260     0.9195
1       1.1     2       180     0.6675
0       1.1     2       260     0.7943
0       1.1     4       180     0.8739
1       1.1     4       260     0.801
0       0.8     3       220     0.8461
0       0.8     3       220     0.8699
0       0.8     3       220     0.8677
1       0.8     3       220     0.8351
1       0.8     3       220     0.8631
1       0.8     3       220     0.8562
;
PROC PRINT;
PROC REG;
MODEL Y= X1 X2 X3/P R;
OUTPUT OUT=NEW PREDICTED=YHAT RESIDUAL=RS PRESS=PR;
PROC RANK DATA=NEW OUT=RANKS;
VAR RS;
RANKS RR;
DATA TWO;
SET RANKS;
I=(RR-0.5)/14;
PRO=PROBIT(I);
PROC PLOT DATA=TWO;
PLOT RS * PRO ='+';
PLOT RS * YHAT='*';
PROC REG;
MODEL Y=BLOCK X1 X2 X3/P R;
OUTPUT OUT=NEW PREDICTED=YHAT1 RESIDUAL=RS1 PRESS=PR1;
PROC RANK DATA=NEW OUT=RANKS;
VAR RS1;
RANKS RR;
DATA THREE;
SET RANKS;
I=(RR-0.5)/14;
PRO1=PROBIT(I);
PROC PLOT DATA=THREE;
PLOT RS1 * PRO1 ='+';
PLOT RS1 * YHAT1='*';
RUN;
```

```
**********************************************
// EXEC SAS
//SAS.SYSIN DD *
OPTIONS NOCENTER;
TITLE 'AGURMENT SYNGAS EXPRIMENT90203 PROPANE SELECTIVITY WITH BLOCK';
DATA ONE;
INPUT B1 B2 X1 X2 X3 Y;
/* X1 IS THE TOTAL FLOW RATE, X2 IS THE H2:CO RATIO,
X3 IS TEMPERATURE. Y IS THE SELECTIVITY OF THE PROPANE.
*/
X11=X1*X1;
X22=X2*X2;
X33=X3*X3;
X12=X1*X2;
X13=X1*X3;
X23=X2*X3;
CARDS;
1       0       0.5     2       180     0.7815
0       1       0.5     2       260     0.7742
0       1       0.5     4       180     0.8157
1       0       0.5     4       260     0.9195
0       1       1.1     2       180     0.6675
1       0       1.1     2       260     0.7943
1       0       1.1     4       180     0.8739
0       1       1.1     4       260     0.8010
1       0       0.8     3       220     0.8461
1       0       0.8     3       220     0.8699
1       0       0.8     3       220     0.8677
0       1       0.8     3       220     0.8351
0       1       0.8     3       220     0.8631
0       1       0.8     3       220     0.8562
0       0       0.293   3       220     0.8405
0       0       1.307   3       220     0.8200
0       0       0.8     1.31    220     0.7632
0       0       0.8     4.69    220     0.8568
0       0       0.8     3       152.4   0.7676
0       0       0.8     3       287.6   0.7653
0       0       0.8     3       220     0.8455
0       0       0.8     3       220     0.8573
0       0       0.8     3       220     0.8131
0       0       0.8     3       220     0.8243
;
PROC PRINT;
PROC REG;
MODEL Y=B1 B2 X1 X2 X3 X11 X22 X33 X12 X13 X23 /P R;
PROC RSREG;
MODEL Y=B1 B2 X1 X2 X3/COVAR=2 LACKFIT;
RIDGE MAX;
RUN;

*******************************************************************************
```

7. Estimating λ μ and n for the cycohexene hydrogenation and dehydrogenation reactions and for the syn-gas reaction

```
*****************************************************************
// EXEC SAS
//SAS.SYSIN DD *
OPTIONS NOCENTER;
TITLE 'NWGATIVE EXPONENTIAL: Y=(R/(R+U))*(1-EXP(-(R+U)*T)) T IN MINITE';
DATA A;
INPUT T Y;
CARDS;
        0     0.0363
  0.66667     0.0531
  1.33333     0.0436
        2      0.068
  2.66667     0.1345
  3.33333     0.1125
        4      0.105
  4.66667     0.1297
  5.33333     0.1417
        6     0.1249
  6.66667     0.1597
  7.33333     0.2222
        8      0.227
  8.66667      0.185
  9.33333     0.1525
       10      0.257
  10.6667      0.227
  11.3333     0.2991
       12     0.2402
  12.6667     0.2606
  13.3333      0.275
       14     0.2883
  14.6667     0.3579
  15.3333     0.3351
       16     0.3819
  16.6667     0.2955
  17.3333     0.2798
       18     0.3555
  18.6667     0.3639
  19.3333     0.3663
       20     0.3423
  20.6667     0.3723
  21.3333     0.4192
       22     0.4348
  22.6667     0.4396
  23.3333     0.4192
       24     0.4108
  24.6667     0.4456
  25.3333      0.418
       26     0.4108
```

```
   26.6667     0.4204
   27.3333     0.4768
        28     0.4432
   28.6667     0.5261
   29.3333     0.4888
        30     0.5213
   30.6667     0.4912
   31.3333     0.4732
        32     0.4984
   32.6667     0.4564
   33.3333     0.4432
        34     0.5201
   34.6667     0.5068
   35.3333     0.4828
        36     0.4396
   36.6667     0.5537
   37.3333     0.4864
        38     0.4936
   38.6667     0.5141
   39.3333      0.508
        40     0.5777
   40.6667     0.4816
   41.3333     0.4492
        42     0.5333
   42.6667     0.4912
   43.3333     0.5297
;
PROC NLIN BEST=10 METHOD=DUD;
PARMS R=0 TO 2 BY .1 U=0 TO 3 BY .1;
BOUNDS R>0,U>0;
MODEL Y=(R/(R+U))*(1-EXP(-(R+U)*T));
OUTPUT OUT=B P=YHAT R=YRESID;
RUN;
PROC PLOT DATA=B;
PLOT Y*T='A' YHAT*T='P' /OVERLAY VPOS=20 HPOS=90;
PLOT YRESID*T / VREF=0 VPOS=25;
RUN;
**************************************************
// EXEC SAS
//SAS.SYSIN DD *
OPTIONS NOCENTER;
TITLE 'NWGATIVE EXPONENTIAL: Y=((-T*R**2)/(R+U))*EXP(-(R+U)*T)+((R*R)/(R+U)**2)*(1-
EXP(-(R+U)*T)) T IN MINITE';
DATA A;
INPUT T Y;
CARDS;
(DATA)
...
;
PROC NLIN BEST=10 METHOD=DUD;
PARMS R=0 TO 2 BY .1 U=0 TO 3 BY .1;
```

```
BOUNDS R>0,U>0;
MODEL Y=((-T*R**2)/(R+U))*EXP(-(R+U)*T)+((R*R)/(R+U)**2)*(1-EXP(-(R+U)*T));
OUTPUT OUT=B P=YHAT R=YRESID;
RUN;
PROC PLOT DATA=B;
PLOT Y*T='A' YHAT*T='P' /OVERLAY VPOS=25;
PLOT YRESID*T / VREF=0 VPOS=25;
RUN;

*********************************************************
// EXEC SAS
//SAS.SYSIN DD *
OPTIONS NOCENTER;
TITLE 'NWGATIVE EXPONENTIAL: Y=(-(R**3*T**2)/(2*(R+U))-(T*R**3)/(R+U)**2)*EXP(-
(R+U)*T)+(R/(R+U))**3*(1-EXP(-(R+U)*T)) T IN MINITE';
DATA A;
INPUT T Y;
CARDS;
(DATA)
...
;
PROC NLIN BEST=10 METHOD=DUD;
PARMS R=0 TO 2 BY .1 U=0 TO 3 BY .1;
BOUNDS R>0,U>0;
MODEL Y=(-(R**3*T**2)/(2*(R+U))-(T*R**3)/(R+U)**2)*EXP(-(R+U)*T)+(R/(R+U))**3*(1-EXP(-
(R+U)*T));
OUTPUT OUT=B P=YHAT R=YRESID;
RUN;
PROC PLOT DATA=B;
PLOT Y*T='A' YHAT*T='P' /OVERLAY VPOS=25;
PLOT YRESID*T / VREF=0 VPOS=25;
RUN;

*********************************************
// EXEC SAS
//SAS.SYSIN DD *
OPTIONS NOCENTER;
TITLE 'NWGATIVE EXPONENTIAL: Y=(-(R**4*T**3)/(6*(R+U))-(R**4*T**2)/(2*(R+U)**2)-
(R**4*T)/(R+U)**3)*EXP(-(R+U)*T)+(R/(R+U))**4*(1-EXP(-(R+U)*T))T IN MINITE';
DATA A;
INPUT T Y;
CARDS;
(DATA)
...
;
PROC NLIN BEST=10 METHOD=DUD;
PARMS R=0 TO 2 BY .1 U=0 TO 3 BY .1;
BOUNDS R>0,U>0;
MODEL Y=(-(R**4*T**3)/(6*(R+U))-(R**4*T**2)/(2*(R+U)**2)-(R**4*T)/(R+U)**3)*EXP(-
(R+U)*T)+(R/(R+U))**4*(1-EXP(-(R+U)*T));
OUTPUT OUT=B P=YHAT R=YRESID;
RUN;
PROC PLOT DATA=B;
PLOT Y*T='A' YHAT*T='P' /OVERLAY VPOS=25;
PLOT YRESID*T / VREF=0 VPOS=25;
RUN;
```

```
************************************************************
// EXEC SAS
//SAS.SYSIN DD *
OPTIONS NOCENTER;
TITLE 'NWGATIVE EXPONENTIAL: Y=(-(R**5*T**4)/(24*(R+U))-(R**5*T**3)/(6*(R+U)**2)-
(R**5*T**2)/(2*(R+U)**3)-(R**5*T)/(R+U)**4)*EXP(-(R+U)*T)+(R/(R+U))**5*(1-EXP(-(R+U)*T))T
IN MINITE';
DATA A;
INPUT T Y;
CARDS;
(DATA)
...
;
PROC NLIN BEST=10 METHOD=DUD;
PARMS R=0 TO 2 BY .1 U=0 TO 3 BY .1;
BOUNDS R>0,U>0;
MODEL Y=(-(R**5*T**4)/(24*(R+U))-(R**5*T**3)/(6*(R+U)**2)-(R**5*T**2)/(2*(R+U)**3)-
(R**5*T)/(R+U)**4)*EXP(-(R+U)*T)+(R/(R+U))**5*(1-EXP(-(R+U)*T));
OUTPUT OUT=B P=YHAT R=YRESID;
RUN;
PROC PLOT DATA=B;
PLOT Y*T='A' YHAT*T='P' /OVERLAY VPOS=25;
PLOT YRESID*T / VREF=0 VPOS=25;
RUN;

*********************************************
// EXEC SAS
//SAS.SYSIN DD *
OPTIONS NOCENTER;
TITLE 'NWGATIVE EXPONENTIAL: Y=(-(R**6*T**5)/(120*(R+U))-(R**6*T**4)/(24*(R+U)**2)-
(R**6*T**3)/(6*(R+U)**3)-(R**6*T**2)/(2*(R+U)**4)-(R**6*T)/(R+U)**5)*EXP(-
(R+U)*T)+(R/(R+U))**6*(1-EXP(-(R+U)*T))T IN MINITE';
DATA A;
INPUT T Y;
CARDS;
(DATA)
...
;
PROC NLIN BEST=10 METHOD=DUD;
PARMS R=0 TO 2 BY .1 U=0 TO 3 BY .1;
BOUNDS R>0,U>0;
MODEL Y=(-(R**6*T**5)/(120*(R+U))-(R**6*T**4)/(24*(R+U)**2)-(R**6*T**3)/(6*(R+U)**3)-
(R**6*T**2)/(2*(R+U)**4)-(R**6*T)/(R+U)**5)*EXP(-(R+U)*T)+(R/(R+U))**6*(1-EXP(-(R+U)*T));
OUTPUT OUT=B P=YHAT R=YRESID;
RUN;
PROC PLOT DATA=B;
PLOT Y*T='A' YHAT*T='P' /OVERLAY VPOS=25;
PLOT YRESID*T / VREF=0 VPOS=25;
RUN;
```

8. Source code for Markov chain apporach

```
************************************************************
// This program simulate a markov chain modeling approach for cyclohexene hydrogenation
// and dehydrogenation reaction in a microreactor.
```

```
// with Cio=0.i=1,2,...8. where Cio is initial molar concentration of chemical species i
// in the microreactor, i=1,2,3,4 represents the solide phase and i=5,6,7,8(where i=1*,2*,
// 3* and 4* in chapter 6) represents the liquid phase of chemical speciesA1,A2,A3 and A4.
// The operating condition is: temperature=186.67 C, FlowRateH2=0.28sccm, FlowrateAr=0.82sccm.

#include <iostream.h>
#include <fstream.h>

void main()
{

// Constants
const int T=361;          // 360 mins for simulation
const int Nr=9;           // Total 4 reactants and products both in solid phase and liquid phase
                  //, because 0 is not used for C here
const double N0 = 6.02E+23 ; // Arvgadro constant
const double V= 4.01;         // V is the volume of the microreactor

const double q = 0.0011;    // q is 0.0011 L/min for the velocity of feeding
const double deltaT=1.0;      // time interval 1 minute

const double k11=0.0;       // k1 is 0/min for the c6h10 hydrogenation reation rate
const double k22=0.0966;    // k2 is 0.0966/min for the c6h10 dehydrogenation reaction rate

//const double C10=0.5; // intial concentration of identity 1
//const double C40=1.0;
const double C5f=0.00218; //inital feed concentration
const double C6f=0.00620;

double x[Nr]; // xi  the number of molecule i feeding into the reactor
double n[Nr][T]; // n[i][t] the number of molecule i inside the reactor at time t
double C[Nr][T]; // C is concentration of molecule in mole/L
double P[Nr][Nr]; // markov chain matrix
double Conout[Nr][T]; // Conout is the concentration in the out stream of the reactor.

//double sumCon;  //sumCon is used for Calculating Concout

double  alpha, beta,k1,k2,mu ; //  mu is the probability of exiting the microreactor,
                  //  alpha is the absorption rate, beta is the desorption rate.
int i, j, k;

//sumCon=0.0;

//open a file
ofstream fout("dehyoutreactor-1Kc.txt",ios::out );

// intial calculations
mu= q/V;

k1=k11 ;
k2=k22 ;

alpha=k2;
beta=alpha;

//initilize the x, feeding matrix
```

```
for( i=0; i<Nr; i++ )
{
        x[i]=0;
        n[i][0]=0;
}
x[5]=C5f*q*N0; // calculate feeding number of molecule 1
x[6]=C6f*q*N0;


// initialization of the Makov Chain matrix
for( i=1; i<=Nr; i++)
{
        for(j=1; j<=Nr; j++)
        {
                P[i][j]=0;
        }
}
// Now iterate for T minutes and record the concentrations at each step

for( k=1; k<T; k++ ) //total 360 minutes
{

 // calculate P matrix first
 P[1][1]=1-beta*deltaT-k1*n[2][k-1]*deltaT-k2*deltaT;
 P[1][3]=k1*n[2][k-1]*deltaT;
 P[1][4]=k2*deltaT;
 P[1][5]=beta*deltaT;
 //3ed row
 P[3][3]=1-beta*deltaT;
 P[3][7]=beta*deltaT;

 //4th row
 P[4][4]=1-beta*deltaT;
 P[4][8]=beta*deltaT;

 //5th row
 P[5][1]=alpha*deltaT;
 P[5][5]=1-alpha*deltaT-mu*deltaT;
 P[5][9]=mu*deltaT;

 //7th row
 P[7][3]=alpha*deltaT;
 P[7][7]=1-alpha*deltaT-mu*deltaT;
 P[7][9]=mu*deltaT;

 //8th row
 P[8][4]=alpha*deltaT;
 P[8][8]=1-alpha*deltaT-mu*deltaT;
 P[8][9]=mu*deltaT;

 //9th row
 P[9][9]=1;

 //now calculate n[1][k] to n[8][k]
 for( j=1; j<=8; j++ )
 {
```

```
    double sum = 0;
    for( i=1;i<=8; i++ )
    {
     sum+=n[i][k-1]*P[i][j];
    }
    n[j][k]=sum+x[j];
  }

  //now calculate n[2][k], n[6][k]
  n[2][k]=n[2][k-1]*(1 - beta*deltaT)-n[1][k-1]*P[1][3]+2*n[1][k-1]*P[1][4]+n[6][k-1]*alpha*deltaT;
  n[6][k]=n[6][k-1]*(1-alpha*deltaT-mu*deltaT )+n[2][k-1]*beta*deltaT+x[6];

  cout<<k<<" ";
  fout<<k<<" ";

  // now calculate the molar concentration out of the reactor
  for(i=5; i<Nr; i++ )
  {      C[i][k]= n[i][k]/(N0*V );// molar concentration in the reactor
            Conout[i][k]=C[i][k]*mu*deltaT);// molar concentration in the out stream of the reactor

          cout<<Conout[i][k]<<" ";
      fout<<Conout[i][k]<<" ";
  }
  cout<<endl;
  fout<<endl;
}
   fout.close();
}
```

REFERENCES

[Angela 1999] Angela D., Voss D. "Design and Analysis of Experiments." Springer Texts in Statistics, Springer, ISBN 0-387-98561-1. 1999.

[Besser 2001] Besser, R.S., *Chemical Engineering Communications,* in press, 2001.

[Box and Draper 1987] Box, G.E.P. and N.R. Draper. Empirical Model-Building and Response Surfaces, John Wiley & Sons, New York, 1987.

[Box and Wilson 1951] Box, G. E. P. and Wilson, K. B., "On the experimental attainment of optimum conditions," *Journal of the Royal Statistical Society, Series B* 13, 1-45, 1951.

[Burstein 1998] Burstein G.T., "Fuel cells on the road to success," *Materials World*, v 6, n 7, Jul, pp. 412-413, ISSN: 0967-8638, 1998.

[Chen 1996] Chen, J.G. and Fruhberger, B., *Surf.Sci.* 367, L102-L110, 1996.

[Chiang 1975] Chiang, C. "An Introduction to Stochastic Processed and Their Applications." Published by Robert E. Krieger Publishing Co., Inc. 1975.

[Chou 1988] Chou, S.T., Fan, L. T. and Nassar, R., Modeling of complex chemical reactions in a continuous-flow reactor: a Markov chain approach, *Chemical Engineering Science*, Vol. 43, No. 10, pp. 2807-2815, 1988.

[Chung 1960] Chung, K. L. "Markov chains with stationary transition probabilities," Springer Verlag, Berlin, 1960.

[Cowan 1996] Cowan R., and Hulten S., *Technol Forecasting Social Change* 53:61-79, 1996.

[Davis 1980] Davis, S.M. and Somoriai, G.A., *J.Catal.* 65, 78-83, 1980.

[Dawson 1995] Dawson, P.H. Quadrupole Mass Spectrometry and Its Application, AIP Press, NY, 1995.

[Denis 1999] Denis, M.C., Lalande, G,; Guay, D.; Dodelet, J.P.; Schulz,R., "High energy ball-milled Pt and Pt-Ru catalysts for polymer electrolyte fuel cells and their tolerance to CO," *Journal of Applied Electrochemistry*, v 29, n 8, pp. 951-960 ISSN: 0021-891X, 1999.

[Dicks 1996] Dicks, Andrew L., "Hydrogen generation from natural gas for the fuel cells systems of tomorrow," *Journal of Power Sources*, v 61, n 1-2, ISSN: 0378-7753, Jul-Aug, 1996,

[Ehrfeld 2000] Ehrfeld, W., Hessel, V., and Lowe, H., *Microreactors, New Technology for Modern Chemistry*, 1st edition, 2000.

[Feller 1968] Feller, W. "An Introduction to Probability Theory and Its Applications,"(3rd edition), Wiley, New York, 1968.

[Fogler 1999] Fogler, H.S. Elements of Chemical Reaction Engineering, Third Edition, Prentice Hall, New Jersey. 1999.

[Gary 2001] Gary, J. H. and Handwerk, G.E., "Petroleum refining, technology and economics," *Marcel-Dekker*, New York, pp.175-214 , 2001.

[Gotz 1998] Gotz M., and Wendt H., *Electrochim*, Acta 43, 3847, 1998.

[Hassan 1995] Hassan, Salah A., Sadek, Salwa A, "Various characteristics of supported CoPc on Al_2O_3, SiO_2 and SiO_2-Al_2O_3 as selective catalysts in the oxidative dehydrogenation of cyclohexene," *Studies in Surface Science and Catalysis* (1996), 100 (Catalysts in Petroleum Refining and Petrochemical Industries), 407-18, ISSN: 0167-2991, 1995.

[Henn 1992] Henn F. C., Diaz A. L., Bussell M. E., Hugenschmidt M. B., Domagala M. E., and Campbell C. T., J. Phys. *Chem. 96*, 5965, and references therein, 1992

[Hunka 1997] Hunka, Deborah E., and Land, D. P., "Dehydrogenation of cyclohexene to benzene on Pd (111), " *Book of Abstracts, 214th ACS National Meeting*, Las Vegas, NV, September 7-11, 1997.

[Ito 1999] Ito, Takashi, "Technologies and catalysts of hydrogen generation for fuel cells," *Nihon Enerugi Gakkaishi/Journal of the Japan Institute of Energy*, v78, n11, pp 911-920, ISSN: 0916-8753, 1999.

[Jensen 2000] Jensen, K. F., *Technical Digest of the 2000 Solid-State Sensor and Actuator Worksho, Hilton Head Isl, SC*, 105-110, June 2000.

[Kovacs 1998] Kovacs, G.T., Maluf, N.I., and Petersen, K. E., *Proceedings of the IEEE, vol.* 86, No. 8, August 1998.

[Lichtman 1984] Lichtman, D., *J, Vac. Sci. Technol. A 2 (2),* PP.200-206. Apr-June, 1984.

[Linda 1993] Linda A., Bruce, Manh Hoang, "Ruthenium promotion of Fish-Tropsch synthesis over coprecipitated cobalt/ceria catalysts," *Applied Catalysis A*: General, 100, 51-67, 1993.

[Liu 2001] Liu, Ning, Chen, Jingguang G., "Synergistic effect in the dehydrogenation of cyclohexene on C/W(111) surfaces modified b submonolayer coverage Pt," *Catalysis Letter (2001)*, 77(1-3), 35-40. ISSN: 1011-372X, 2001.

[Liu 2001] Liu, Ning, Chen, Jingguang G., "A comparative surface science study of carbide and oxycarbide. The effect of oxygen modification of the surface reactivity of C/W (111)," Surface Science, 487(1-3), 107-117, ISSN; 0039-6028, 2001.

[Lloyd 2000] Lloyd A. J *Power Sources*, 86: 57-60, 2000.

[Lowe 1999] Lowe H., and Ehrfeld, W., *Electrochimica Acta, vol.* 44, 1999

[Manasilp 2002] Manasilp, Akkarat, and Gulari, Erdogan, "Selective CO oxidation over Pt/alumina catalysts for fuel cell applications," *Applied Catalysis B*: *Environmental*, v37, n1, Apr 8, pp. 17-25 ISSN: 0926-3373, 2002.

[Mao 1987] F. M. Mao et al., "The quadrupole mass spectrometer in practical operation," *Vacuum*, **37**, pp. 669-675, 1987.

[Okuzaki 2000] S. Okuzali, K. Okude, and T. Ohishi, "Photoluminescence behavior of SiO2 prepared by sol-gel processing," *Journal of Non-crystalline Solids*, vol. 265, pg 61-67, 2000.

[Ouyang 2003] Ouyang X., and Besser R. S., "Development of a microreactor-based parallel catalyst analysis system for synthesis gas conversion," *Catalysis Today* (2003), 84(1-2), 33-41, ISSN: 0920-5861, 2003.

[QMS 100] Stanford Research Systems, "User Manual: QMS 100 Series Gas Analyzer"

[Rase 2000] Rase H. F., "Handbook of Commercial Catalysts: Heterogeneous Catalysts," *CRC Press*, Boca Raton, pp. 105-204, 2000.

[Roberts 1990] Roberts Jeffrey T., and Madix Robert J., "Reactions of weak organic acids with oxygen atoms on silver (110): facile and selective conversion of cyclohexene to benzene," *Surface Science,* 226(3), L71-L78, ISSN: 0039-6028, 1990.

[Rohatgi 1976] Rohatgi, V.K., "An introduction to probability theory and mathematical statistics," pp.197-199. John Wiley, New York, 1976.

[Rohland 1999] Rohland B., and Plzak, J. V., *Power Sources* 84, 183, 1999.

[Sandestede 2000] Sandestede G., "Catalysis from A to Z, A concise encyclopedia," (B. Cornils, W. A. Herrmann, R. Schlogl, and C.-H. Wong, Eds.). *Wiley VCH, Weinheim*, pp. 228-229, 2000.

[SAS] SAS/STAT User's Guide, Version 6, Fourth Edition, Volume 2, SAS Institute Inc. Cary, NC.

[Segal 1978] Segal, E., Madon, R.J., and Boudart, M., *J. Catal.* 52, 45-49, 1978.

[Senkan 1999] Senkan, S., Krantz, K., Ozturk, S., Zengin, V., and Onal, I., Angewandte chemie-International Edition, 38, 2794-2799, 1999.

[Sossina 2003] Sossina M. Haile, *Materials for fuel cells*, Matreials today March, 2003

[Srinivasan 1997] Srinivasan, R., Hsing, I.M., Berger, P.E. and Jensen, K. F., "Micromachined reactors for catalytic partial oxidation reaction," *AICHE Journal 43*, No. 11, pp. 3059-3068, 1997.

[Su 1999] Su, K., Kung, K. Y., Lahtinen, J., Shen, Y.R., and Somorjai, G.A., *J.Molec. Catal. A: Chem.* 141, 9-19, 1999.

[Surangalikar 2003] Surangalikar H., Ouyang X., Besser R. S., "Experimental study of hydrocarbon hydrogenation and dehydrogenation reactions in silicon microfabricated reactors of two different geometries," *Chemical Engineering Journal* (Amsterdam, Netherlands), 93(3), 217-224, ISSN: 1385-8947, 2003.

[Too 1983] Too, J. R., Fan, L.T. and Nassar, R., "Markov chain models of complex chemical reactions in continuous flow reactors," *Comp.chem. Engng* 7, 1-12, 1983.

[Twigg 1989] Twigg M., Catalyst Handbook, Wolfe Publishers, London, UK, Chapters 4-7, 1989.

[van Kampen 1981] van Kampen, N. G., "Stochastic processes in physics and chemistry," pp. 180-208. Elsevier, New York, 1981.

[Venable 2000] J. D. Venable, J. A. Holcombe, "Signal enhancements produced from externally generated 'carrier' particles in electrothermal vaporization-inductively coupled plasma mass spectrometry," *Spectrochamica asta. Part B; Atomic spectroscopy*, 55, 753-766, 2000.

[Weissermel 1997] Weissermel K., and Arpe H,-J., "Industrial organic chemistry," *Wiley VCH, Weinheim*, pp. 314-317, 1997.

[Xu 1994] Xu, C. and Koel, B.E., "Adsorption and desorption behavior of n-butane and isobutene on Pt (111) and Sn/Pt (111) surface alloys," *Surf. Sci.* 304, 249-266, 1994.

[Zhao 2003] Zhao, S. "Nano-scale platinum and iron-cobalt catalysts deposited in microchannel microreactors for hydrogenation and dehydrogenation of cyclohexene, selective oxidation of carbon monoxide and Fischer-Tropsch process to higher alkanes," Ph.D. dissertation, Louisiana Tech University, Ruston, 2003.